SSD

SCIENCE FOR A SUSTAINABLE DEVELOPMENT

"ADVANCED EXPLOITATION OF GROUND-BASED MEASUREMENTS FOR ATMOSPHERIC CHEMISTRY AND CLIMATE APPLICATIONS"

«AGACC»

M. De Mazière, H. De Backer, M. Carleer, E. Mahieu, K. Clémer, B. Dils, M. Kruglanski, F. Hendrick, C. Hermans, M. Van Roozendael, C. Vigouroux, A. Cheymol, V. De Bock, A. Mangold, R. Van Malderen, P.-F. Coheur, S. Fally, J. Vander Auwera, J.-L. Lacour, P. Demoulin, P. Duchatelet

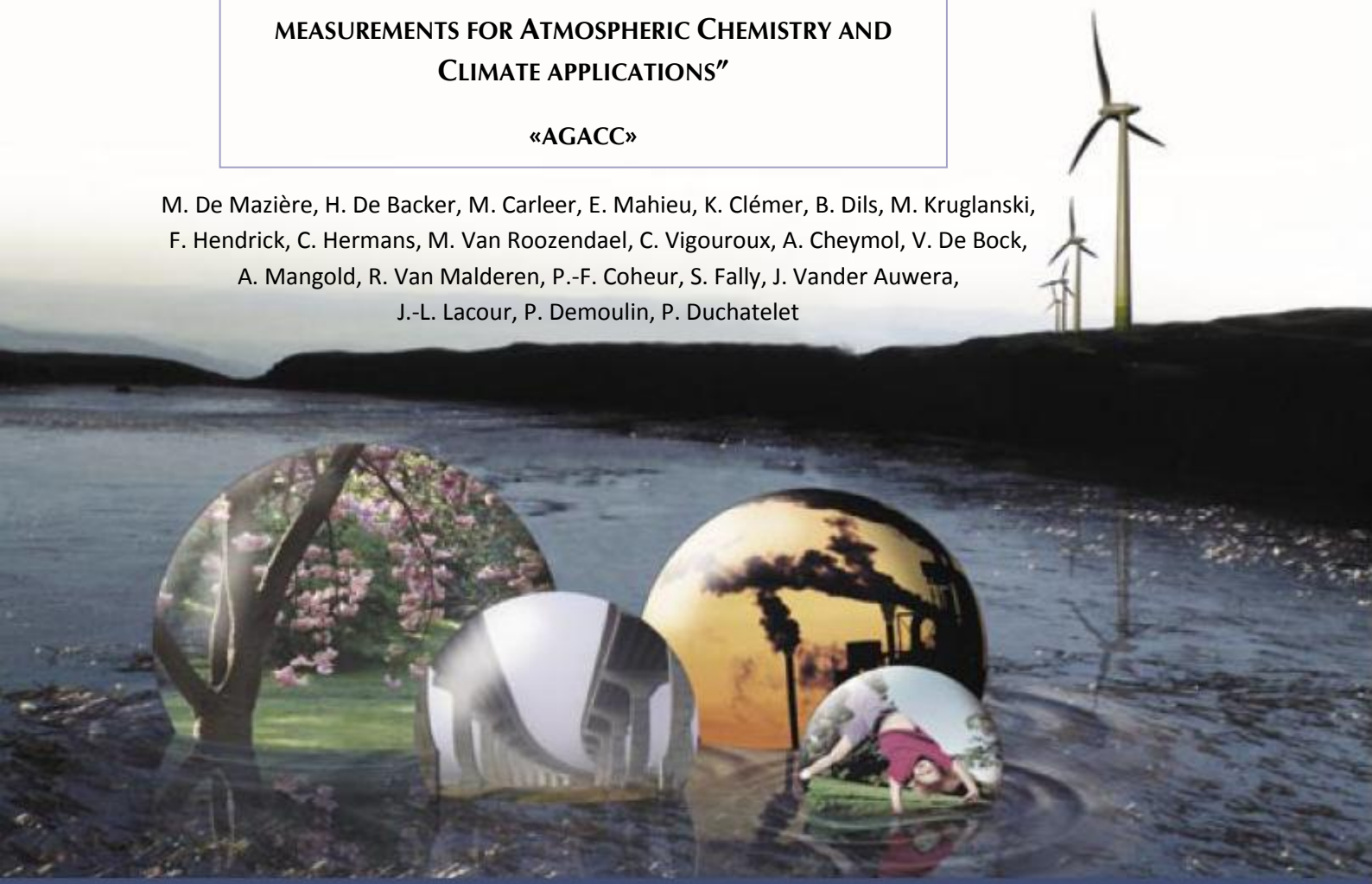

ENERGY

TRANSPORT AND MOBILITY

AGRO-FOOD

HEALTH AND ENVIRONMENT

ATMOSPHERE & CLIMATE

BIODIVERSITY

ATMOSPHERE AND TERRESTRIAL AND MARINE ECOSYSTEMS

TRANSVERSAL ACTIONS

.be

SCIENCE FOR A SUSTAINABLE DEVELOPMENT
(SSD)

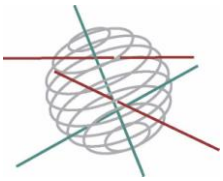

Atmosphere and Climate

FINAL REPORT

ADVANCED EXPLOITATION OF GROUND-BASED MEASUREMENTS FOR ATMOSPHERIC CHEMISTRY AND CLIMATE APPLICATIONS

«AGACC»

SD/AT/01

Promotors
Martine De Mazière (BIRA-IASB)
Hugo De Backer (KMI-IRM)
Michel Carleer (ULB)
Emmanuel Mahieu (ULg)

Authors
Martine De Mazière, Katrijn Clémer, Bart Dils, Michel Kruglanski, François Hendrick, Christian Hermans, Michel Van Roozendael, Corinne Vigouroux
(BIRA-IASB)

Hugo De Backer, Anne Cheymol, Veerle De Bock, Alexander Mangold, Roeland Van Malderen
(KMI-IRM)

Michel Carleer, Pierre-François Coheur, Jean-Lionel Lacour, Sophie Fally, Jean Vander Auwera
(ULB)

Emmanuel Mahieu, Pierre Duchatelet, Philippe Demoulin
(ULg)

Editorial support

Pauline Skarlas, Marielle Snellings

belspo

D/2011/1191/21
Published in 2011 by the Belgian Science Policy
Louizalaan 231
Avenue Louise 231
B-1050 Brussels
Belgium
Tel: +32 (0)2 238 34 11 – Fax: +32 (0)2 230 59 12
http://www.belspo.be

Contact person: Martine Vanderstraeten
+32 (0)2 238 36 10

Martine De Mazière, Hugo De Backer, Michel Carleer, Emmanuel Mahieu, Katrijn Clémer, Bart Dils, Michel Kruglanski, François Hendrick, Christian Hermans, Michel Van Roozendael, Corinne Vigouroux, Anne Cheymol, Alexander Mangold, Roeland Van Malderen, Pierre-François Coheur, Sophie Fally, Jean Vander Auwera, Jean-Lionel Lacour, Pierre Duchatelet, Philippe Demoulin. ***Advanced exploitation of Ground-based measurements for Atmospheric Chemistry and Climate applications "AGACC"***. Final Report. Brussels : Belgian Science Policy 2009 – 123 p. (Research Programme Science for a Sustainable Development)

TABLE OF CONTENT

SUMMARY

We live in an era in which human activities are causing significant changes to the atmospheric environment which result in local to global consequences on the ecosystems. Changes in the atmospheric composition impact our climate via chemical and dynamical feedback mechanisms; in many instances they also affect air quality, and the health of the biosphere. Monitoring and understanding those changes and their consequences is fundamental to establish adequate actions for adaptation to and mitigation of the environmental changes. Furthermore, after implementation of regulatory measures like the Montreal Protocol, it is necessary to verify whether the measures are effective. This can only be achieved if we have adequate detection methods and a reliable long record of a series of key geophysical parameters.

Thus the AGACC project contributes to the provision of basic new knowledge regarding the atmospheric composition and its changes, based on advanced ground-based monitoring, in combination with satellite and numerical modelling data. Its results are integrated in ongoing international research programmes.

The general objective of AGACC has been to improve and extend the ground-based detection capabilities for a number of climate-related target species and, based hereupon, analyse past and present observations to derive new information about the atmospheric composition, its variability and long-term changes. Despite the advent of a growing and more performant fleet of Earth Observation satellites, ground-based observations are still indispensable to (1) guarantee long-term continuity, homogeneity and high quality of the data, and (2) to underpin the satellite data for calibration and (long-term) validation.

A first target gas is atmospheric water vapour. It is the key trace gas controlling weather and climate. It is also the most important greenhouse gas in the Earth's atmosphere. Its amount and vertical distribution are changing, but how and why? Especially in the upper troposphere - lower stratosphere, the radiative effects of changes in the water vapour are significant and should be quantified. The measurement of water vapour is a hot topic since several years. It is a challenge, because water vapour exhibits a large gradient in its concentration when going from the ground to the stratosphere, and because it is highly variable in time and space. For example, we have found that the time scale of the variations of the total water vapour amount at Jungfraujoch is in the order of minutes.

In AGACC, we have therefore investigated various experimental techniques to measure the concentration of water vapour in the atmosphere, focusing on the total column as well as on the vertical distribution in the troposphere up to the lower stratosphere. The retrieval of water vapour vertical profiles and total columns from ground-based FTIR data has been initiated at three very different stations where correlative data for

verification are available, namely Ukkel (± sea level, mid-latitude), Ile de La Réunion (± sea level, tropical) and Jungfraujoch (high altitude, mid-latitude), with promising results. In particular, at Jungfraujoch, it has been demonstrated that the precision of the FTIR integrated water vapour (IWV) measurements is of order 2%. The capability to retrieve individual isotopologues of water vapour, and to monitor their daily and diurnal variations, has also been demonstrated. This could open new ways to study in the future the role of water vapour in the radiative balance, the global circulation, precipitation etc. We also started joint exploitation of ground-based FTIR and satellite IASI data for water vapour and its isotopologues, in order to exploit fully the potential of the existing instrumentation.

A correction method for the radiosoundings at Ukkel has been successfully implemented, resulting in a homogeneous and reliable time series from 1990 to 2008 from which trends in upper troposphere humidity (UTH) and tropopause characteristics have been derived. One observes a rising UTH until September 2001, followed by a decline, accompanied by a descent and heating of the tropopause up to the turning point and an ascent and cooling afterwards. The changes after September 2001 in the upper troposphere can be explained by surface heating and convective uplift. At Jungfraujoch, one does not observe any significant trend in the total water vapour abundance above the station over the 1988-2010 time period, although significant positive summer and negative winter trends have been detected.

We have made a quantitative statistical comparison between ground-based FTIR, CIMEL, GPS and integrated (corrected) radio sounding measurements of the IWV at Ukkel. This work is important to better characterize the different sensors in order to exploit together different observations made by different instruments.

A second target species is atmospheric aerosol. There is a very large variety of aerosol both from natural or anthropogenic origin. One of the reasons why they are so important is that they affect the optical properties of the atmosphere. In particular, it has been demonstrated in previous studies that the aerosols have a large impact on the quantity of harmful UV-B radiation received at the Earth's surface. The latest IPCC Report also stressed that the radiative forcing caused by atmospheric aerosols is one of the largest uncertainties in determining the total radiative forcing in the atmosphere. Better monitoring capabilities of aerosol properties can therefore improve our understanding and forecasting of the atmospheric processes and evolution, and in particular of UV-B and climate changes.

Several measurement techniques are now operational in the AGACC consortium for the ground-based monitoring of aerosol properties. These are the Brewer spectrometer and CIMEL observations at Ukkel, the latter contributing also to the AERONET network since July 2006, and the newly developed MAXDOAS observations. Unlike CIMEL and Brewer measurements, that provide the total Aerosol Optical Depth, it has been

demonstrated that the MAXDOAS measurements also provide additional information about the vertical distribution of the aerosol extinction in the lowest kilometres of the troposphere. A better understanding of the ultimate capabilities of MAXDOAS aerosol remote sensing has been gained through participation to the international CINDI campaign (Cabauw Intercomparison Campaign of Nitrogen Dioxide measuring Instruments) in summer 2009. The combination of Brewer, CIMEL and MAXDOAS instruments gives us a remote-sensing dataset that will enable a more comprehensive characterization of the tropospheric aerosol optical properties. The usefulness of these aerosol observations has already been demonstrated in the improvement of the UV-index predictions for the general public. Another application is their use as input data in the retrieval of vertical profiles of tropospheric pollutants from MAXDOAS measurements, like tropospheric NO_2 and formaldehyde.

Third we have focused on a few climate-related trace gases. Changing greenhouse gas and aerosol concentrations directly affect the radiative budget of the atmosphere, and therefore climate. But many species known as pollutants like carbon monoxide (CO), nitrogen oxides (NOx) and hydrocarbons, - often related to fossil fuel or biomass burning -, also affect climate through their role in chemical reactions that produce tropospheric ozone, which is a well-known greenhouse gas, or that modify the lifetime of gases like methane, or the oxidation capacity of the atmosphere.

Therefore in AGACC, we have focused on the measurement of a number of trace gases that are subject to changing concentrations, that directly or indirectly affect climate, and that are either difficult to monitor or that have not yet been measured from the ground. We have included attempts to observe distinctly some isotopologues, because the isotopic ratios observed in an airmass provide information on its history, and because the FTIR solar absorption measurements provide a rather unique capability hereto.

The investigated species are the isotopologues of CH_4 and CO, and hydrogen cyanide (HCN), as examples of biomass burning tracers, some hydrocarbons like formaldehyde (HCHO), ethylene (C_2H_4) and acetylene (C_2H_2), and HCFC-142b, a replacement product for CFCs and a greenhouse gas.

In many cases, retrieval strategies had to be adapted when going from one site to another with different atmospheric conditions, especially when the local humidity and abundances are very different as is the case between Jungfraujoch (dry, high altitude, mid-latitude) and Ile de La Réunion (humid, low altitude, low latitude). Still we have been able to show the feasibility of retrieving particular trace gas information even under difficult conditions. Many of our results have been compared to correlative data, to validate the approach and to gain complementary information. It is also important to note that the retrieval strategies developed in AGACC have regularly been presented to the global Network for the Detection of Atmospheric Composition Change (NDACC) UV-Vis and Infrared communities and have often been adopted by others or even

proposed for adoption as a standard in the community (e.g., for hydrogen cyanide (HCN)).

In particular:

We have been able to study the seasonal variations of *HCN* at the Jungfraujoch and at Ile de La Réunion, and to show the dominant impact of biomass burning.

Formaldehyde was studied in much detail at Ukkel, Jungfraujoch and Ile de la Réunion. The challenge for detection at Jungfraujoch is the small abundance (about 10 times smaller than at Ukkel and Ile de La Réunion); a particular observation strategy was developed successfully, resulting in a time series that already shows the day-to-day and seasonal variations. At Ile de La Réunion, comparisons of FTIR, MAXDOAS, satellite and model data have (1) shown the good agreement between the various data sets, but also, (2), the variability of HCHO (diurnal, seasonal, day-to-day), and (3), thanks to the complementarities of the various data sets, they have enabled us to learn more about the long-range transport of Non-methane Volatile Organic Compounds (NMVOCS, precursors of HCHO) and deficiencies in the models. It was shown that fast, direct transport of NMVOCS from Madagascar has a significant impact on the HCHO abundance and its variability at Ile de La Réunion, and that this is underestimated in the model.

Significant progress was made as to the detection of $^{13}CH_4$ *and* CH_3D from ground-based FTIR observations, both at Jungfraujoch and Ile de La Réunion. To our knowledge, it is the first time that a $\delta^{13}C$ data set is derived from ground-based FTIR observations. More work is needed to improve the CH_3D retrieval at Ile de La Réunion, and to interpret the results, in combination with models.

Also for the first time, ^{12}CO *and* ^{13}CO have been retrieved individually at Jungfraujoch. The $\delta^{13}C$ time series shows significant seasonal and interannual changes.

As to the hydrocarbon *ethylene*, it is shown that it can be detected at Jungfraujoch only in spectra at low solar elevation, given its small atmospheric abundance.

Regarding acetylene, the observed time series at Jungfraujoch and Ile de La Réunion show clear seasonal variations and enhancements due to the impact of biomass burning events, correlated with enhancements in CO, C_2H_6 and HCN.

It is not clear yet whether we can reliably retrieve the concentration of HCFC-142b, a replacement product that is increasing strongly in the troposphere. New line parameters for the interfering species HFC-134a are required to confirm/infirm the preliminary results. This highlights again the importance of the laboratory work for providing such parameters.

Improved line parameters have been obtained for water vapour and its isotopologues, ethylene and formic acid. These AGACC results have been integrated in the international spectroscopic databases. We also showed that line intensities available

around 2096 cm^{-1} for the $^{13}C^{16}O$ isotopologue of carbon monoxide in the HITRAN database seem to be accurate to 2%. We failed to improve line intensities for the 13.6 μm region of acetylene.

The new data sets that have been derived in AGACC from FTIR and MAXDOAS observations have been archived in the NDACC data centre, where they are available for users (generally modelers and satellite teams). In addition, they are stored locally and are available to users upon request.

AGACC results have been reported to the international scientific community, via the literature, via integration in geophysical or spectroscopic databases, and via participation to international research initiatives like the Atmospheric Water Vapour in the Climate System (WAVACS) Cost Action, the International Space Science Institute (ISSI) Working Group on Atmospheric Water Vapour, the International Union of Pure and Applied Chemistry (IUPAC) project, the International CINDI campaign, etc.

The results have already found important scientific applications. A few examples are worth mentioning: the re-evaluation of methane emissions in the tropics from SCIAMACHY based on the new H_2O spectroscopy, and the improved retrievals of HCOOH from the satellite experiments ACE-FTS and IASI, and from the ground.

In the longer-term, the AGACC results will no doubt benefit the research in atmospheric sciences –in particular in the monitoring of its composition changes–, which is the fundamental basis of environmental assessment reports for supporting policy makers.

Keywords:

Atmospheric composition change; trends; monitoring; remote-sensing; ground-based spectrometry; radio soundings; greenhouse gases; tropospheric chemistry; climate change

I INTRODUCTION

I.1 Focus on chemistry-climate interactions: rationale

Because of their environmental consequences, including their effects on the climate system and on living organisms, perturbations in the chemical composition of the stratosphere and the troposphere have drawn the attention of the scientists, the decision makers and the general public. Before any measures can be taken to counter harmful changes, one must (1) identify the changes, and (2) understand the chemical and physical processes that are involved, and (3) be able to predict the future evolution.
This project focuses on the first and second points, and particularly looks at a few atmospheric constituents that have a direct or indirect impact on the Earth climate. It is well understood that many changes in the chemical composition of the atmosphere not necessarily directly affect the radiative budget of the atmosphere, but often affect it via chemical processes that create tropospheric ozone, or change the lifetime of greenhouse gases, or – in case of the aerosol – create clouds and fog that alter the penetration of sunlight through the atmosphere. Often the changes go hand in hand with a degrading of the air quality and of the quality of life.

I.2 Objectives

The choice of the scientific objectives of the project have taken into account ongoing international research programmes, the specific observation capabilities and expertise in the consortium, as well as its collaborations with foreign research teams.
The general objective has therefore been to improve and extend the ground-based detection capabilities for a number of climate-related target species and, based on these new or improved capabilities, analyse past and present observations to derive new information about the atmospheric composition, its variability and long-term changes. Despite the advent of a growing and more performant fleet of Earth Observation satellites, ground-based observations are still indispensable to (1) guarantee long-term continuity, homogeneity and high quality of the data, and (2) to underpin the satellite data for calibration and (long-term) validation.

The more specific objectives have been:

- To gain a better understanding of the atmospheric water vapour, by (1) correcting and exploiting long-term radiosoundings of the atmospheric humidity up to the Upper Troposphere/Lower Stratosphere (UTLS) at Ukkel, (2) contributing to the development of retrieval strategies for water vapour and its isotopologues from ground-based Fourier transform infrared remote-sensing observations, at various

types of sites. A side objective has been to study the consistency between various observing systems for the integrated water vapour (IWV) content in the atmosphere.

- To develop new observation capabilities for operational monitoring of the aerosol optical depth and additional optical properties, and to improve UV-index forecasts and the retrieval of other trace gases based on the derived aerosol information.
- To develop observation and retrieval strategies for some atmospheric climate-related gases that have not yet or not yet sufficiently precisely been detected and that are important in the chemistry of the troposphere or stratosphere. The species considered are methane and carbon monoxide and their isotopologues, formaldehyde, hydrogen cyanide, HCFC-142b, ethylene, acetylene, and OH.
- To use all these developments to analyse past and present timeseries, to obtain new information about the atmospheric composition and variability.
- Our advantage is that we make observations at different sites under different atmospheric conditions, and that we are thus well placed to evaluate such strategies and, once operational, to derive interesting information;
- To provide improved spectroscopic data to support not only the above ground-based remote-sensing observations but also the satellite measurements, as well as radiative budget calculations.
- To prepare for satellite validation: many of the above targets are also measured from satellite but urgently need to be validated.

II METHODOLOGY AND RESULTS

Section II is structured as follows:
For each major research topic (sections II.N.n), we start with a rationale for the topic, then we give the more technical information about the research activities that have been carried out and we discuss detailed results, and we end with some major conclusions.
Some of the technical details that were discussed in intermediate reports have not been repeated here. We refer to them as AGACC2007, AGACC200806, and AGACC200812 for the Activity Report intended for the Intermediary Evaluation, the Final Report of Phase I and the Annual Report 2008, respectively.

II.1 Field observations

II.1.1 Water Vapour

II.1.1.1 Rationale

Water vapour in the atmosphere is the key trace gas controlling weather and climate. It also plays a central role in atmospheric chemistry, e.g., by influencing the heterogeneous chemical reactions that destroy stratospheric ozone. Water vapour is also the most important greenhouse gas in the Earth's atmosphere. Its amount is changing. Much research is ongoing to identify these changes and to understand their origin and consequences. There exist many in situ and remote sensing techniques – from ground, balloon, aircraft and space - to measure water vapour in the atmosphere. Some measure only the total amount, also called the Integrated Water Vapour amount or IWV. Some techniques are capable of determining the vertical distribution of water vapour in the atmosphere, in a limited altitude range. There is no technique available that can measure the water vapour vertical profile with sufficient precision over the whole altitude range of the atmosphere, mainly because of the large vertical gradient in the water vapour concentration. Therefore, different techniques are needed to get a complete picture. But an additional challenge is that the abundance of water vapour is highly variable in time and space. Therefore, it is more difficult to compare or to use in a synergistic way different observations that are not taken exactly in the same airmass.
The measurement of water vapour is a hot topic since several years, this can be demonstrated by the large number of coordinated investigations that have been and are still ongoing. We can mention the latest SPARC (Stratospheric Processes and their Role in Climate) Assessment of Upper Tropospheric and Stratospheric Water Vapour [SPARC, 2000], as well as the ongoing WAVACS Cost Action (Atmospheric Water Vapour in the Climate System; http://www.isac.cnr.it/~wavacs/), and the meetings and reports of the

ISSI (International Space Science Institute) Working Group on Atmospheric Water Vapour.
(http://www.iapmw.unibe.ch/research/projects/issi/index.html)

In the AGACC consortium, we have various techniques at our disposal to observe water vapour, especially the IWV and the vertical distribution in the troposphere up to lower stratosphere. In the Upper Troposphere/Lower Stratosphere (UTLS), the effects of water vapour are large and its long-term variation is not well known.
Our objectives have therefore been (1) to improve the quality of radiosonde measurements of upper troposphere humidity (UTH), (2) to investigate trends in UTH, (3) to investigate the capabilities of Fourier-transform infrared measurements from ground and space for the observation of the column and vertical distribution of water vapour, (4) to compare various observation techniques of the IWV, and (5) to contribute with this expertise to the international research forum via WAVACS and the ISSI Working Group on Atmospheric Water Vapour.
Recent studies have demonstrated the potential and the interest of the water vapour isotopologues for studying fine processes of the hydrological cycle ([Worden, 2007]; [Frankenberg, 2009]; [Risi, 2010]; [Sherwood, 2010]). The analysis of the water vapour isotopologic partioning is strongly influenced by evaporation sources and condensation conditions and it is therefore very useful to derive information on the water vapour sources, sinks and dynamics ([Herbin et al, 2009]; [Zahn et al.,2006]). In this perspective, an additional objective has been to investigate the potentiality of FTIR measurements to retrieve information on water vapour isotopes.

II.1.1.2 Exploitation of radiosondes measurements at Ukkel

Climate models predict that the concentration of water vapour in the upper troposphere could double by the end of the century as a result of increases in greenhouse gases [Soden et al., 2005]. Observations indicate that the height of the tropopause has increased by several hundred meters since 1979 [Santer et al., 2003]. We try to reconcile these two trends by using the rather uniform dataset of radiosonde vertical profiles we gathered at Ukkel since 1990. This dataset can form the basis for a time series analysis of the humidity field in the UTLS.

As the radiosonde humidity sensors suffer from several instrumental or calibration shortcomings (e.g. time lag of the response, inaccurate calibration model for the temperature dependence of the response at low temperatures, solar radiation dry bias, chemical contamination dry bias, icing during the ascent…) we compared 2 different

and independent (dry) bias correction methods suggested in the literature by Leiterer et al. [2005] and Miloshevich et al. [2004]. After comparison of the humidity profiles corrected by either method with simultaneous data measured by another radiosonde type on the same balloon, we conclude that the Miloshevich method tends to overcorrect the humidity profile in UT conditions (i.e. at low temperatures and high relative humidity). This finding is in agreement with studies based on the comparison of radiosonde data with data from independent and well-calibrated hygrometers [Suortti et al., 2008]. We therefore chosed to correct our database with the method developed by Leiterer et al. [2005].

Nevertheless, after correction, a dry bias persists in the humidity profiles of the RS80 type of sondes, even at the lower tropospheric layers. A supplementary indication for this dry bias is given by the comparison of the total integrated water vapour amount (IWV) calculated from or measured with four different instruments at Ukkel, as discussed hereafter in Section II.1.1.4.

The 1990-2007 time series of corrected relative humidity profiles was then further used for a trend analysis, where we first focus on the UTH. As can be seen in Figure 1, the upper tropospheric layers are moistening until ± September 2001, underwent a drop in humidity around this date, and are drying (not significantly, however) afterwards. The same change point occurs for the tropopause temperature/height/pressure: before Sept. 2001, the tropopause layer was descending, after this date, it is moving up.

So we conclude that the tropopause layer above Ukkel is going down from 1990 – September 2001, hence warming up, which results in a moistening. After September 2001, the tropopause layer is lifting, cooling down and (slightly) drying. The September 2001 change seems to have a physical origin, because this change point or trend turning point was detected in the time series of different observed variables. Moreover, Randel et al. [2006] also mentioned decreases in *stratospheric* water vapour after 2001 in both satellite (HALOE) and balloon (Boulder) observations. They related this feature to an enhanced tropical upwelling after 2001 – resulting also in lower tropical tropopause temperatures and a lower ozone amount near the tropical tropopause – and leading to a change in the Brewer-Dobson circulation.

However, we found indications that the movement of the upper tropospheric layers is rather due to the dynamics of the underlying troposphere, which in turn is governed by the temperature variation at the surface. Indeed, the surface temperature is correlated with the temperature at 500 hPa, which is anti-correlated with the tropopause temperature. As shown in Figure 2, the surface warming is responsible for the heating of the lower tropospheric layers. Due to convection, this heating will give rise to a lifting and hence a cooling of the upper tropospheric layers. A supplementary evidence for this scenario is given by the calculation of the thickness of the free troposphere (the

difference of the geopotential height at 300 hPa with the geopotential height at 700 hPa): its trend is clearly correlated with the lower tropospheric temperature trend and anti-correlated with the tropopause temperature trend, with also a change point around September 2001. Finally, we also calculated the trends of the tropopause temperature (i) from the Ukkel radiosonde time series starting in 1969 and (ii) for radiosonde databases gathered at other European stations. It turns out that the September 2001 change point is degraded in the longer times series (other, stronger, change points exist), but that it is nevertheless present in the time series at stations located close to Ukkel. We also conclude that the Ukkel monthly mean tropopause temperature anomaly trends are very typical for the 45°– 55° NB and 5°WL – 15°OL geographical range (correlation coefficients larger than 0.6). The scenario discussed in Figure 2 can also be applied to this geographical range to explain the observed temperature trends.

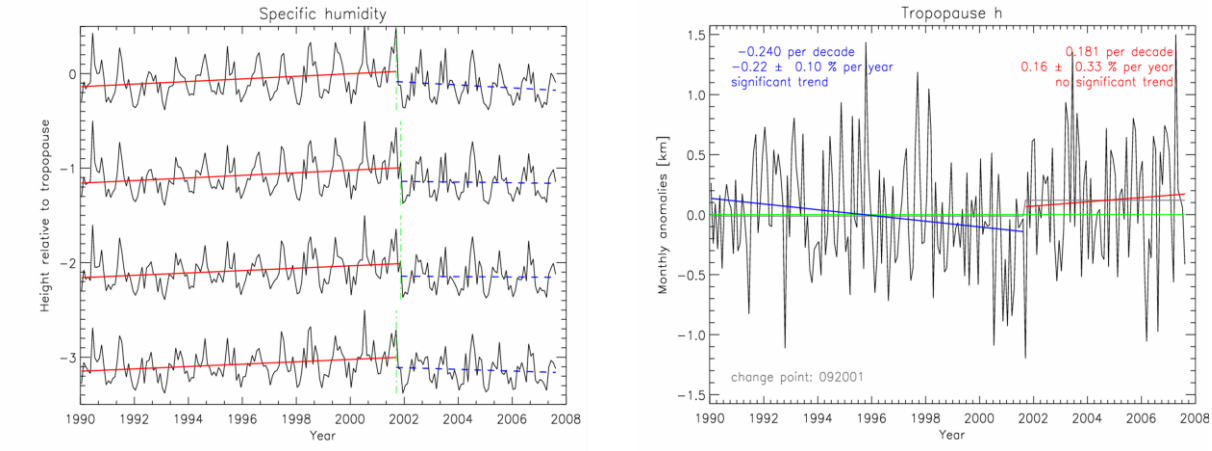

Figure 1 : Left panel: Ukkel trend analysis results for the monthly means of specific humidity calculated for layers of thickness 1 km and central height relative to the tropopause. The vertical green dash-dotted line marks the September 2001 change point, full lines represent statistically significant linear trends, dashed lines non-significant trends. Right panel: Ukkel trend analysis results for the monthly anomalies of tropopause height (in km). The time series is split in two parts: one before and one after the September 2001 change point and trends are calculated for the partial time series.

A new, very surprising result of our detailed analysis of the radiosonde time series at Ukkel is the presence of a correlation between the 11-years solar cycle and, for instance, the tropopause temperature (see Figure 3). It seems that the solar cycle influences the time series of the studied tropospheric variables and it might also partly be responsible for the September 2001 change in UTH and tropopause properties.

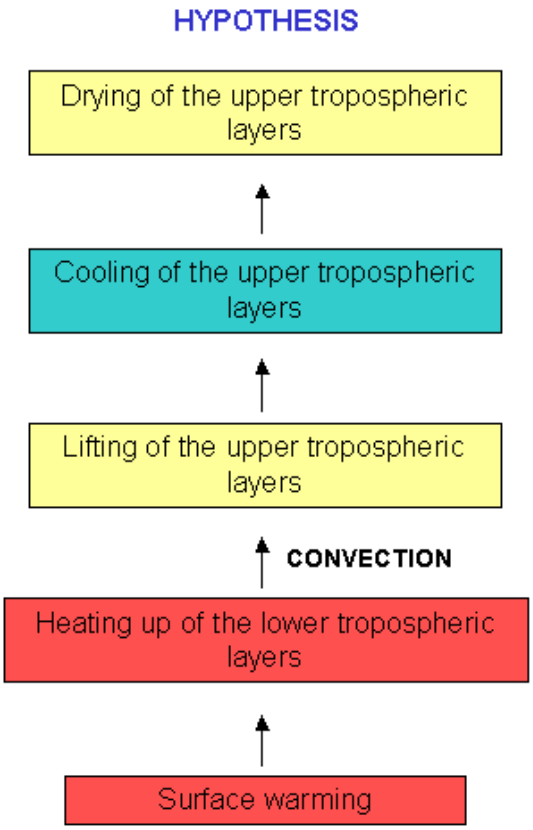

Figure 2 : Proposed scenario, which is able to explain the observed temperature and humidity trends at different heights at Ukkel.

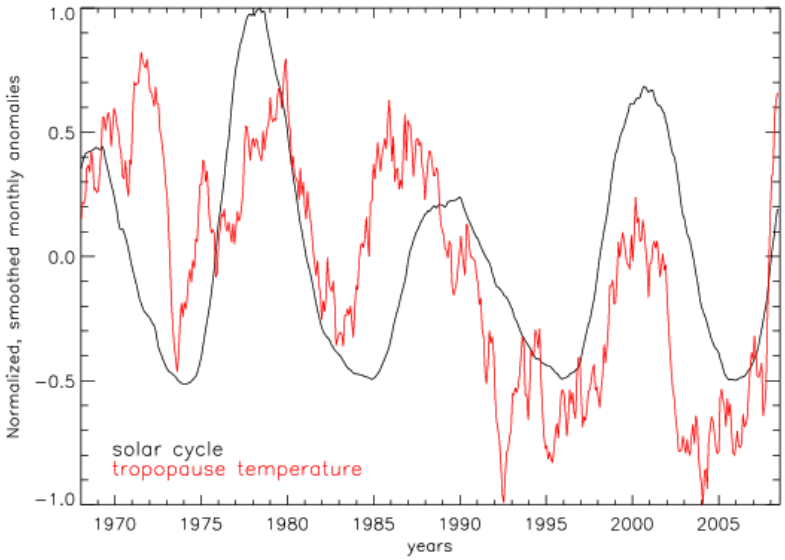

Figure 3 : Comparison of the normalized smoothed monthly anomalies of the time series of the solar (radio) flux at 10.7cm and the tropopause temperature.

II.1.1.3 Retrieval of water vapour from Fourier Transform Infrared observations

Retrieval of water vapour (total column and profile information) from ground-based FTIR observations is a relatively new activity which is still under development [e.g., Schneider et al., 2009a; 2009b]. One of the key issues in the development of the technique is to have coincident measurements available for comparison and validation of the FTIR results. This is problematic owing to the extreme temporal and spatial variability of water vapour in the troposphere. Therefore, we have initiated these developments at three stations where correlative data are available, namely Ukkel, Ile de La Réunion and Jungfraujoch. Details about the retrieval strategy at the three locations have been provided in the Annex to AGACC2007; updates since then at Jungfraujoch are discussed hereinafter (Section II.1.1.3.3).

II.1.1.3.1 At Ukkel

At Ukkel, we had a dedicated observations campaign with simultaneous FTIR, CIMEL, radiosonde and GPS measurements, between July 13, 2006 and April 22, 2007. Details about the experimental setup during this campaign have been decribed in the Annex to AGACC2007. During this period, about 900 spectra were recorded in the IR during 37 sunny days, and 20 noon PTU soundings were performed. Finally for only 11 IR spectra recorded on 4 different days the temporal noon coincidence with the sonde was achieved. The coincidence criteria have been set as: $\pm$ 75 minutes time difference between sonde launch and FTIR spectrum acquisition.

Much effort has been put on the retrieval of the main isotopologue $H_2{}^{16}O$ from the FTIR data for the purpose of intercomparison with the radiosonde data. The characterization of the information comprised in the measurements and error budgets computations have been performed. Typical averaging kernels show that the FTIR observations contain information about the vertical distribution from the surface up to 12 km. The best vertical resolution of the retrieval is observed between 0 and 6 km. The number of independent layers contained in the retrieved profile is 3 at best. On the basis of errors and averaging kernels, the sensitivity is max between 0 and 8 km, and the corresponding uncertainty is less than 50%.

Total columns (expressed as molec/cm^2) have been converted to Total Precipitable Water (TPW) or IWV (mm) and comparisons have been made with CIMEL, integrated sonde and GPS data, as further discussed in Section II.1.1.4. We observe a systematic dry bias of the FTIR with respect to the other data.

To compare the retrieved low-resolution vertical distribution from the ground-based FTIR data with the high-vertical-resolution radiosoundings, the latter profiles have been smoothed with the FTIR averaging kernels. Figure 4 shows a typical example comparison on Oct. 11, 2006. The agreement is good except for the lowest layers below

4 km, where the FTIR underestimates the concentration in water vapour, thus explaining the dry bias in the columns.

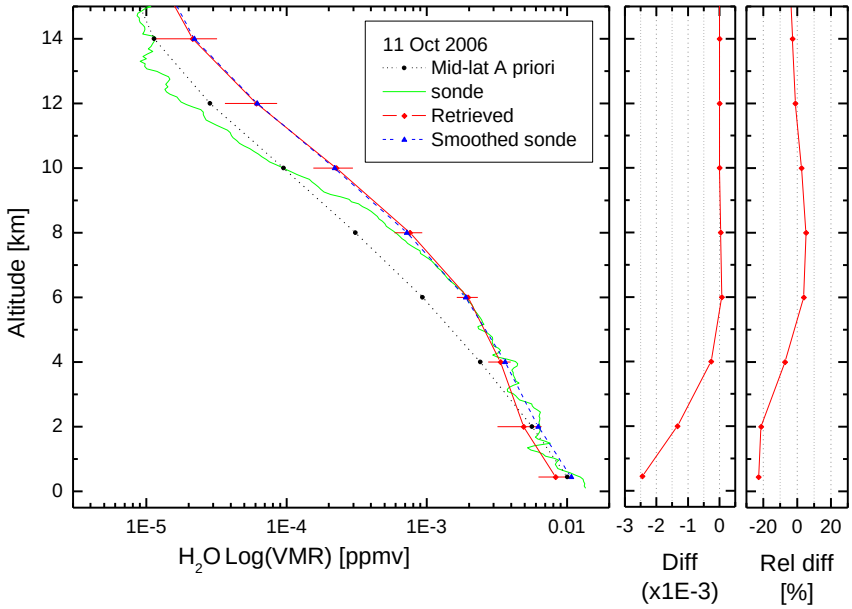

Figure 4: Retrieved $H_2{}^{16}O$ profile in log(vmr) on Oct. 11, 2006 (4 other coincident retrievals gave identical results but are not shown for clarity), and comparison with the coincident sonde profile. The a priori profile is also shown.

II.1.1.3.2 At Jungfraujoch

A validation campaign has been performed above the Zugspitze station (~250 km away from Jungfraujoch) in the second part of 2002, allowing to perform comparisons between radiosondes and FTIR integrated water vapor (IWV) measurements taken within ±1 hour and a few km apart. This offered the unique possibility to set up and tune the FTIR retrieval strategy for water vapour, to match IWV deduced from the radiosondes. The optimization was achieved by implementing a Tikhonov regularization scheme and tuning the corresponding parameters to get the best agreement between both data sets. Three domains completely free of telluric interferences were selected for the FTIR retrievals (839.5 – 840.5, 849.0 – 850.2 and 852.0 – 853.1 cm^{-1}), they include strong and weak absorption lines to maximize the information content and get optimum sensitivity in the whole troposphere.

This retrieval approach has been adopted also for Jungfraujoch, after proper adjustment of the retrieval parameters, e.g. taking into consideration the influence of the spectral point spacing on the regularization strength. Further harmonization was ensured by using, e.g., the same a priori H_2O vertical distribution for both Alpine sites, the same criterion for spectrum selection and similar "exponential" layering schemes. All

Jungfraujoch spectra encompassing the selected windows and recorded either with the Homemade or the Bruker instrument from 1988 onwards have been analyzed. After selection, results from more than 9000 spectra were included in the trend analysis; a mean Degree of Freedom for Signal (DOFS) of 1.87 was achieved.

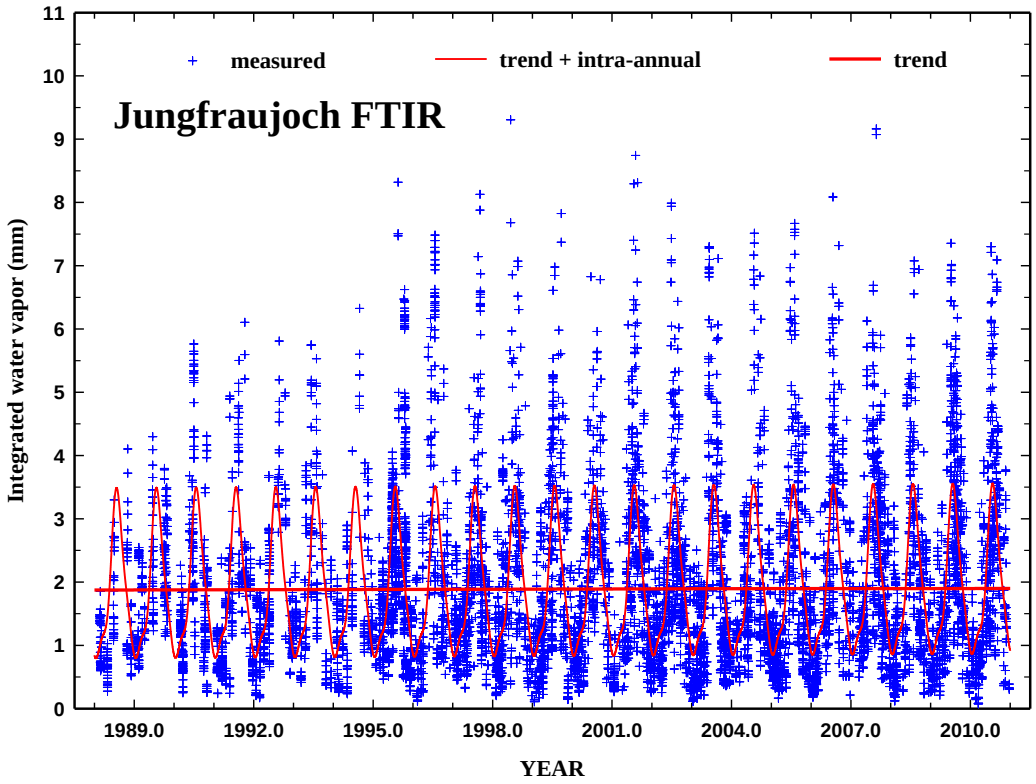

Figure 5 : Time series of IWV measurement derived from Jungfraujoch observations performed with the homemade and the Bruker FTIR instruments [updated from Sussmann et al., 2009].

Table I : Trend statistics for IWV above Jungfraujoch

	2.5th percentile	Trend	97.5th percentile	Trend
1988-2010	mm/decade			
Wintertime (Dec.-Feb.)	-0.168	-0.129	-0.093	-0.13 ± 0.04
Summertime (Jun-Aug)	0.256	0.360	0.459	0.36 ± 0.10
Year-round	-0.008	0.031	0.068	0.03 ± 0.04

Trends are given in mm/decade, for the time periods identified in the first column. The uncertainty intervals are provided at the 2.5th and 97.5th percentiles.

Figure 5 reproduces the Jungfraujoch IWV time series. The long-term trend was evaluated using the bootstrap resampling method described in Gardiner et al. [2008]. The derived trend (as well as its linear component) is reproduced as a thick red line in Figure 5. As expected, the seasonal modulation shows a very large amplitude, with

maximum IWV in August while the driest days are found in winter. Table I lists the trends derived over 1988 – 2010, together with associated uncertainties (95% interval), when considering year-round data or only the winter and summer seasons. If significant positive or negative trends are derived for summer and winter, respectively, the whole set does not show a statistically significant trend, in contrast with Zugspitze results. Identification of the causes for these uneven trend behaviors will require further investigations.

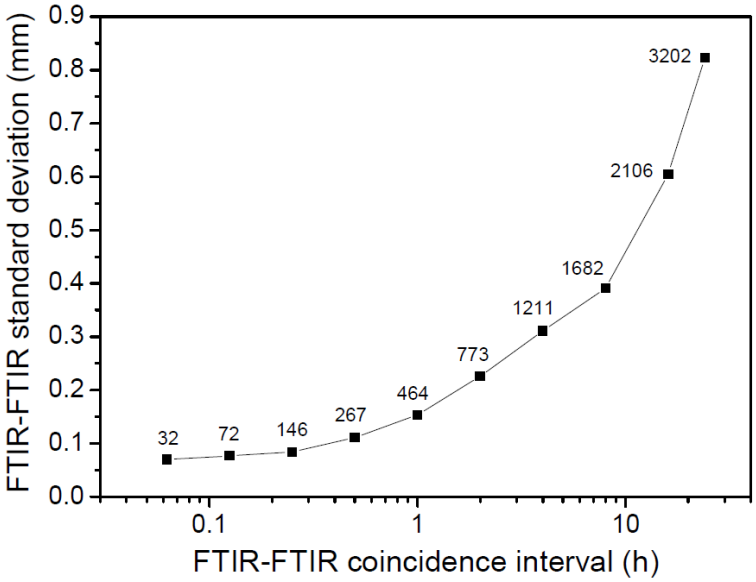

Figure 6 : Standard deviation of the IWV differences deduced from nearly coincident measurements performed at the Jungfraujoch with the homemade and the Bruker FTIR instruments. The rapid increase noted in the standard deviation reflects the very large intraday variability of water vapor [Sussmann et al., 2009].

In addition, we have taken advantage of the fact that two FTIR instruments are regularly operated simultaneously at the Jungfraujoch. Nearly coincident measurements have been compared to check the consistency between both instruments, but also to derive the precision of the IWV measurements. IWV data derived from the two FTIRs were compared, a series of subsets were generated, allowing progressively for an increasing time difference between the two measurements, from a few minutes to several hours. In a next step, the standard deviation was computed for each ensemble. All these values are reported in Figure 6 as a function of the maximum time difference allowed. The numbers of available coincidences per subset are provided in the figure. This allows (i) to determine a negligible bias between the two instruments of 0.02 ± 0.01 mm when considering the 32 coincidences within 3.75 min, the corresponding standard deviation amounts to 0.07 mm; (ii) to illustrate how rapidly the natural atmospheric variability impacts and dominates the statistics of the comparisons, and therefore that meaningful comparisons really require very close coincident measurements of water vapor, in space and time; (iii) to estimate the precision of the IWV measurement as stdv/sqrt(2), hence

lower than 0.05 mm, or 2.2% of the mean IWV. More details about these investigations can be found in Sussmann et al. [2009].

II.1.1.3.3 At Reunion Island

Because of the increasing interest of water vapour isotopologues for studying the physical processes underlying the hydrological cycle, the retrieval of vertical profiles of different isotopic species from the FTIR spectra has been initiated in the course of the project. We focused on the two isotopologues $H_2{}^{16}O$ and HDO because the accuracy needed to get variations of the HDO/H_2O ratio (5-10%), wich expresses the fractionation processes between the two species, is expected to be achieveable with FTIR measurements. However, the retrieval of accurate HDO/H_2O ratios is highly challenging. In the case of $H_2{}^{18}O$ and $H_2{}^{17}O$ the variations of their respective ratios with H_2O ($H_2{}^{18}O/H_2O$ and $H_2{}^{17}O/H_2O$) are smaller than the HDO/H_2O ratio and would require accuracies of 1% which are hardly reachable. Nevertheless, the retrievals of $H_2{}^{18}O$ and $H_2{}^{17}O$ were tested in order to fully exploit the measurements. The retrieval code was *Atmosphit* [Barret et al., 2005; Hurtmans et al., 2005].

It is the first time that retrievals of water isotopologues are attempted at sea level with high humidity level. For that reason a series of new narrow spectral windows, including lines of medium strength have been studied and selected.

For $H_2{}^{16}O$, 4 independent pieces of vertical information, mainly located between the ground and 7 km could be extracted. The retrieved profiles and total columns were compared to coincident CIMEL sunphotometer measurements and a good agreement was obtained (Figure 8 and Figure 9). For $H_2{}^{18}O$, vertical profiles are obtained for the first time. They also contain 4 independent pieces of information, with a vertical sensitivity similar to that of $H_2{}^{16}O$. For HDO, the coupling of 2 well-chosen micro-windows instead of a single micro-window gave improved results as to the quantitative information that could be extracted from the measurements as well as to the error budget. This approach allowed extracting 3 pieces of information with a vertical sensitivity again similar to that of $H_2{}^{16}O$ in the best cases. Finally, for $H_2{}^{17}O$ only total columns could be retrieved because the absorptions are very weak. For all, the retrieved information is mainly restricted to the low and the free troposphere (up to 14 km at best). An example timeseries for $H_2{}^{18}O$ is presented in Figure 7.

Figure 10Figure 10 shows the ∂D time series for the 2009 campaign of measurements at Ile de la Réunion. We only plot the results between 1 and 5 kilometers where the sensitivity is maximum for H_2O and HDO. Beyond these maximum sensitivity limits, the computation of the ∂D shows values quite far from reasonable expectations. The trend

of this time series shows low ∂D values for June and high values during the austral summer. This can be explained simply by the increase of the sea surface temperature and thus the increase of evaporation from ocean wich is the source of heavy molecules. However points are quite scattered around this seasonal trend. The scattering of the points can be explained for two reasons: the limited accuracy of the retrievals and a possible diurnal cycle for ∂D. Our measurements have provided evidence for the existence of this diurnal cycle (Figure 11).

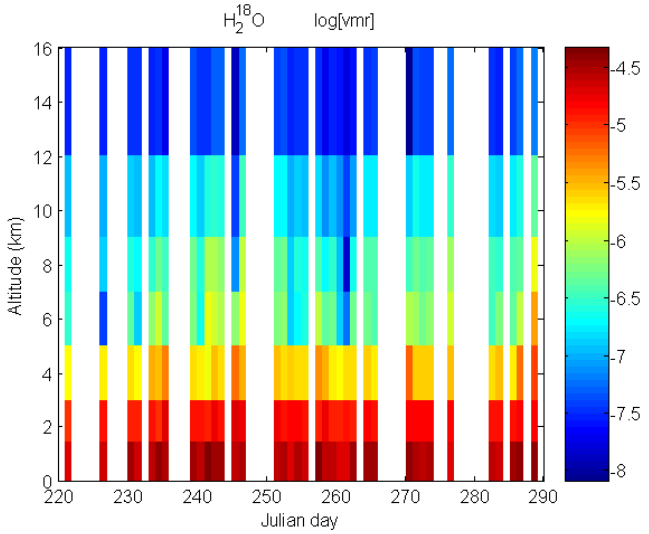

Figure 7 : Temporal evolution of the $H_2{}^{18}O$ vertical profiles during the 2004 campaign.

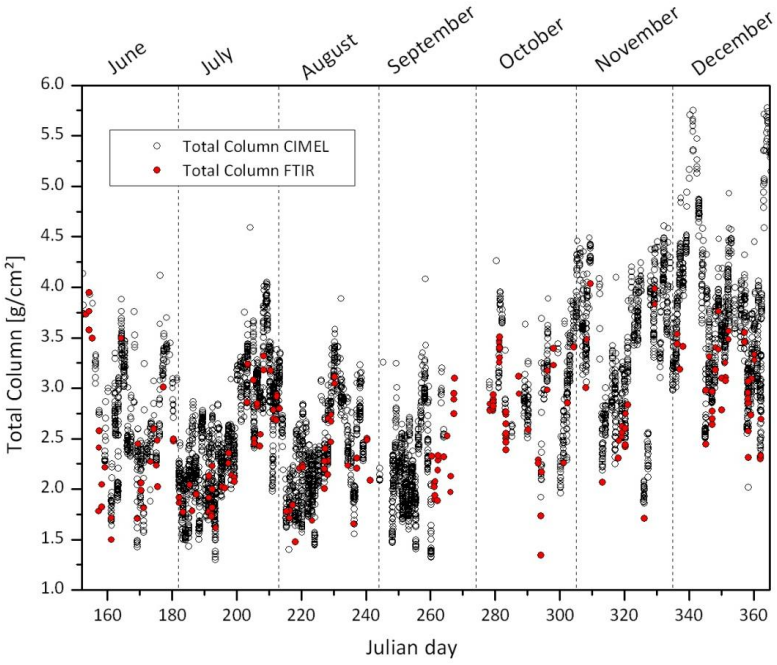

Figure 8 : Time series of IWP at Ile de la Reunion with CIMEL time series 2009 campaign.

As in situ measurements of ∂D require specific instruments, the validation of measurements of water vapour isotopologues is an issue. A first evaluation of the results

is provided through comparison to simple models. Figure 12 shows a delta-q diagram for the ∂D estimates of the 2009 campaign [Worden, 2007]. The Rayleigh distillation curve describes the depletion of air mass with respect to sea surface temperature. The evaporation line represents the enriching effect that arises from mixing moist marine with drier air parcel. If the air mass behaves exactly as the model predicts, the measurements should be located between the two curves. The pattern of our results follows well a Rayleigh distillation pattern with an increase of the depletion with drier air masses. However our measurements seem to be more depleted than predicted, which could indicate a bias in the retrievals. Worden (2006) has earlier suggested the existence of a 5% bias due to errors in HDO reference line intensities.

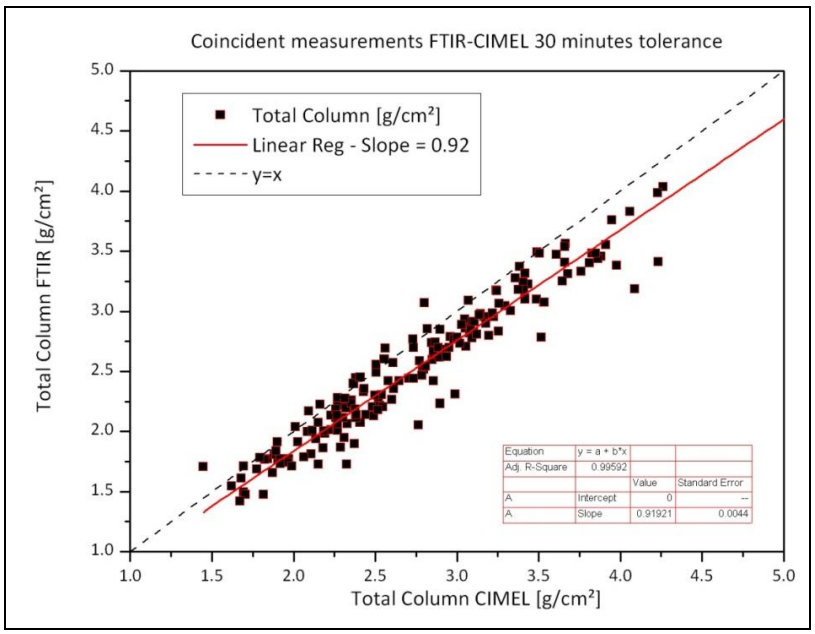

Figure 9 : Comparison of coincident FTIR and CIMEL measurements at Ile de la Réunion during the 2009 campaign.

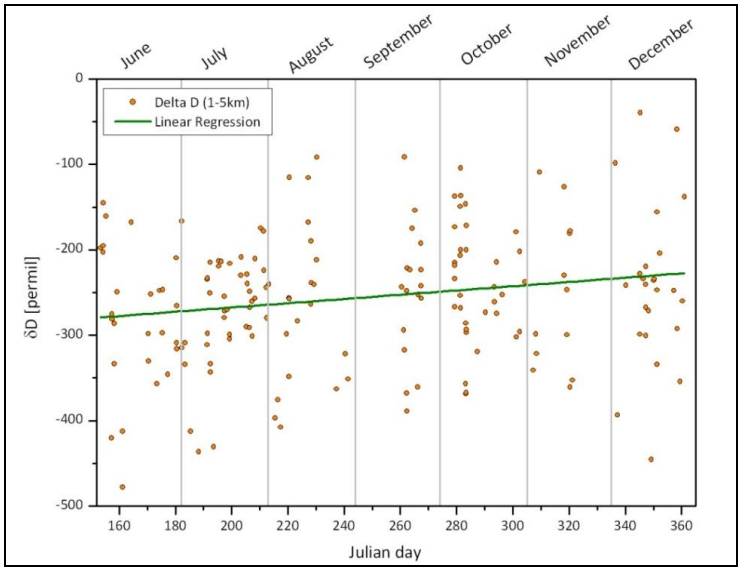

Figure 10 : ∂D time series for the 2009 campaign. ∂D = 1000*((HDO/H_2O)/VSMOW-1). VSMOW is the Vienna standard for the mean isotopic composition of ocean water.

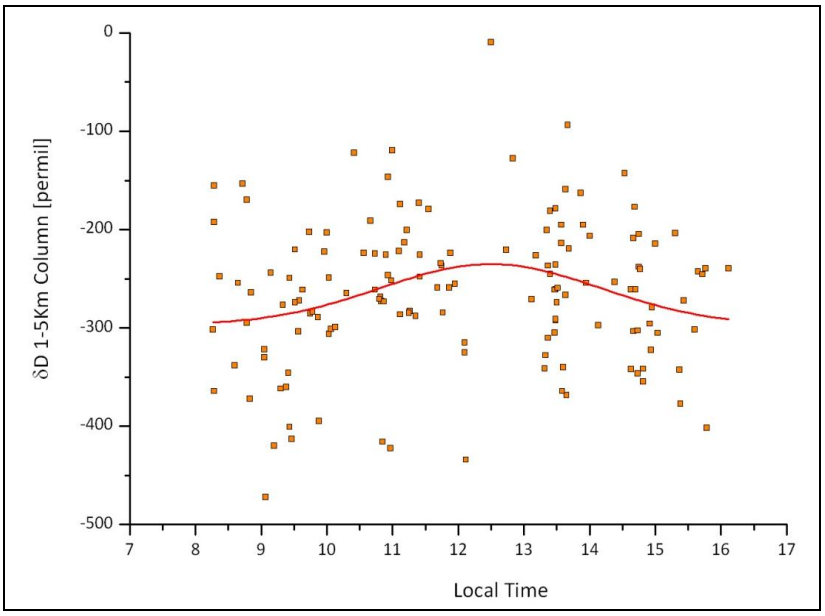

Figure 11 : ∂D plotted in function of the local time. The trend shows a diurnal cycle of the depletion with an increase of ∂D from 8 hr to 12 hr and a decrease from 12 hr to 16 hr.

The coupling of ground-based upward looking FTIR measurements with the IASI nadir infrared satellite measurements was attempted during the project. Retrievals of $H_2{}^{16}O$, HDO and $H_2{}^{18}O$ from ground based and IASI spectra were first compared and characterized. Ground-based retrievals show a better sensitivity in the planetary boundary layer (PBL, 0-1 km), but a loss of sensitivity and a significant increase of the uncertainties above 6km. On the other hand, IASI retrievals give a higher number of independent values and a uniform sensitivity throughout the troposphere above the PBL. Near the surface, IASI retrievals show less sensitivity as expected from nadir thermal IR soundings.

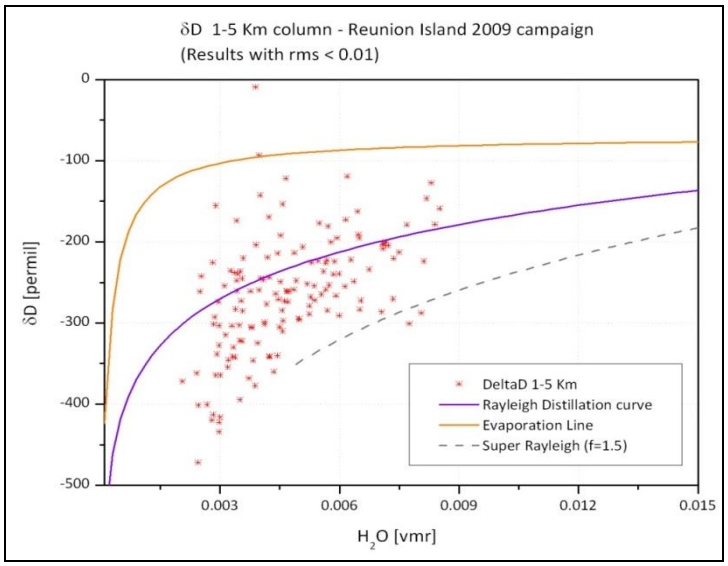

Figure 12 : Delta-q diagram of FTIR measurements at Ile de La Réunion

A joint retrieval was shown to improve the vertical sensitivity, mainly by adding to the satellite data information on the concentration of the heavier isotopologues in the boundary layer, as illustrated in Figure 13.

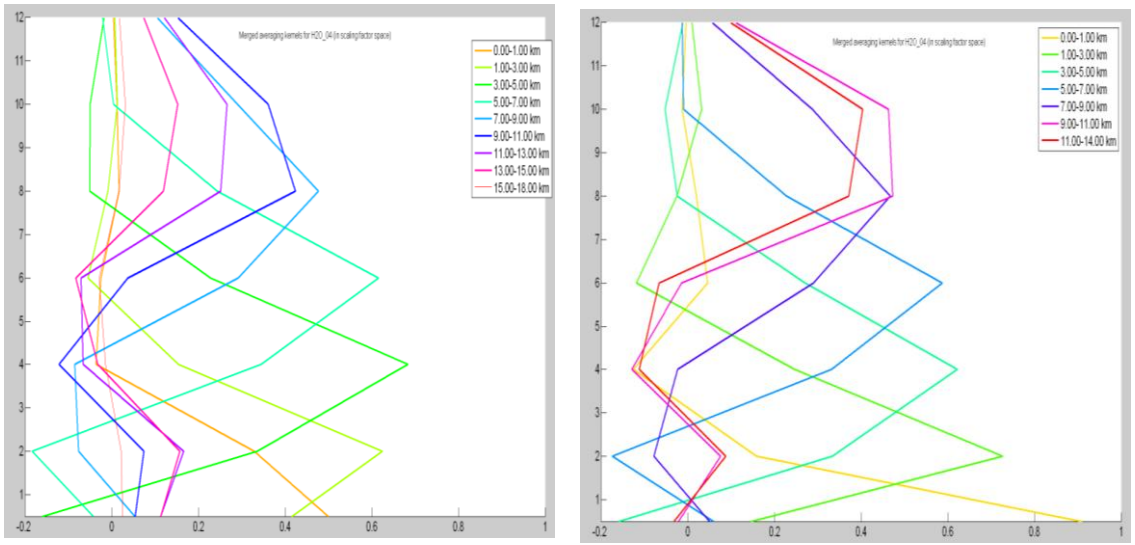

Figure 13: Averaging kernels for HDO obtained from an IASI retrieval alone (left) and a joint gb + IASI retrieval (right).

The maximal sensitivity which was located in the 4-6km altitude layer for IASI alone is extended to the 0-6 km altitude range. Also, the number of independent information on the vertical has slightly increased (degrees of freedom = 3.43 for IASI alone and 3.88 for the combination). The situation is a bit different for $H_2{}^{16}O$ because the sensitivity close to the ground is already good for the IASI retrieval. In fact, we find that the joint retrieval allows an increase of the vertical sensitivity in the upper troposphere, up to the tropopause. The errors remain, however, relatively large and this is likely to be a drawback in determining isotopic ratios. Considerable time and efforts were devoted to

improving the algorithm, notably by introducing a constrained retrieval of the isotopic ratio. The technique was tested on the IASI HDO/H_2O ratio but again with mitigated results, likely due to improper retrieval constraints (a priori variance-covariance matrix). The results gathered during this project with regard to the retrieval off the heavier isotopologues open promising research perspective for the future. However, we recommend that more work is carried out to build adapted covariance matrices and/or to assign the constrain during the retrieval process on the HDO/H_2O directly.

II.1.1.4 Comparisons of IWV measurements from FTIR, radiosoundings, CIMEL and GPS at Ukkel

The data collected during the campaign at Ukkel from July 2006 to April 2007 constitute a very useful set for comparing IWV measurements from ground-based FTIR, CIMEL, and GPS instruments and radiosoundings. Although the measurement principles for the various instruments are very different, one sees from Figure 14. a relatively good agreement between all data sets.

Nevertheless, if we look at the differences relative to the GPS measurement, we see a seasonal variation in the difference, especially of the CIMEL versus the GPS. Table II provides an overview of the statistical results of the comparisons.

Table II : Results of different intercomparisons between instruments measuring IWV (in mm) at Ukkel. RMS: root-mean-square standard deviation of the differences; N: number of measurements in the comparison data sets; Slope, Intercept and R2 define the correlation line and the correlation coefficient, respectively.

	Bias (mm)	RMS (mm)	N	$RMS/\sqrt{N}$	Comments (1→2)	Slope	Intercept	R^2
CIMEL-GPS	0.28	1.16	734	0.043	No bias	0.87	2.10	0.98
FTIR-GPS	-2.64	3.58	25	0.716	Dry bias	0.82	0.25	0.87
RS80-GPS	-1.22	2.21	123	0.199	Dry bias	0.88	0.74	0.94
RS9x-GPS	0.91	1.41	17	0.342	Wet bias	1.01	0.66	0.91

We can conclude that the FTIR data gives the driest results, followed (in order dry to wet) by the RS80, then the GPS, the CIMEL and finally the RS9x soundings that give the wettest results. We have not yet further investigated the reasons for the differences. Schneider et al. [2009b] have made a similar study at Izaña very recently.

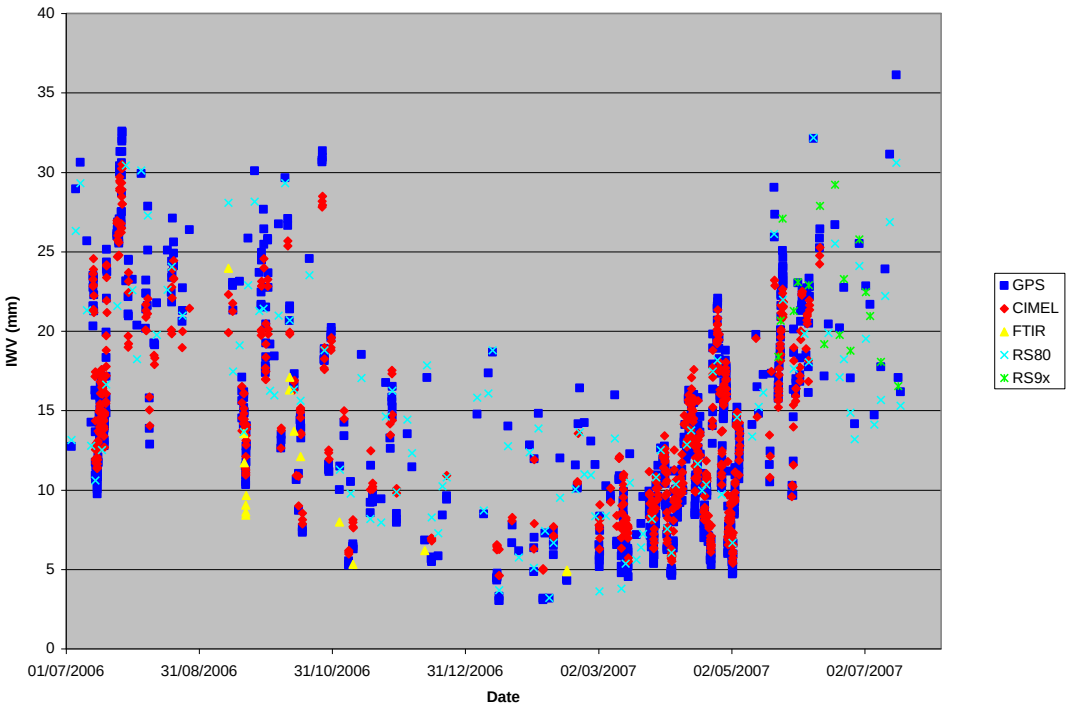

Figure 14 : Comparison of simultaneous integrated water vapour (IWV) amounts at Ukkel measured by 4 different techniques (5 instruments) for the period July 2006 to April 2007. The vertical humidity profiles measured by radiosondes were corrected with the Leiterer method (RS80) or the Miloshevich method (RS9x) before calculating the IWVs.

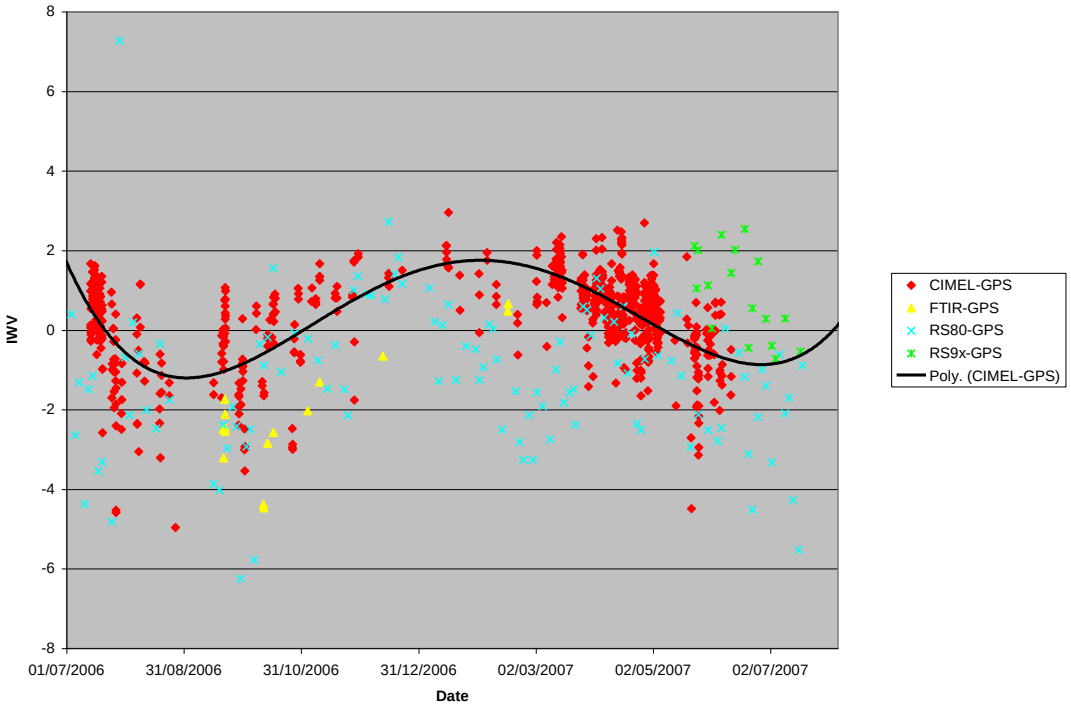

Figure 15 : Time series of differences between simultaneous hourly Integrated Water Vapour values recorded by different instruments at Ukkel (July 2006-April 2007). The black line shows a polynomial fit through the difference between the CIMEL and the GPS data.

II.1.1.5 Major conclusions

In AGACC, we have investigated various experimental techniques to measure the concentration of water vapour in the atmosphere, focusing on the total column as well as on the vertical distribution in the troposphere up to the lower stratosphere. The retrieval of water vapour profiles and total columns from ground-based FTIR data has been initiated at three very different stations where correlative data for verification are available, namely Ukkel (± sea level, mid-latitude), Ile de La Réunion (± sea level, tropical) and Jungfraujoch (high altitude, mid-latitude), with promising results. In particular, at Jungfraujoch, it has been demonstrated that the precision of the FTIR IWV measurements is of order 2%. The capability to retrieve from the FTIR measurements individual isotopologues of water vapour and to follow their day-to-day and even their diurnal cycle has been demonstrated. The comparison to models sheds light on some of the fine processes of the hydrological cycle. Joint retrievals of FTIR water vapour profiles with IASI have been attempted and look promising, but need further investigations.

A correction method for the radiosoundings at Ukkel has been successfully implemented, resulting in a homogeneous and reliable time series from 1990 to 2008 from which trends in UTH and tropopause characteristics have been derived. One observes a rising UTH until September 2001, followed by a decline. These trends are accompanied by a descent and heating of the tropopause up to the turning point and an ascent and cooling afterwards. The changes after September 2001 in the upper troposphere can be explained by surface heating and convective uplift. A new result is also the correlation between the 11-year solar cycle and the tropopause properties at Ukkel.

At Jungfraujoch, one does not observe any significant trends in the total water vapour abundance above the station for the last 23 years, although significant negative winter and positive summer trends have been detected. A study of the time variability of the total water vapour abundance has indicated that the time scale of the variations is in the order of minutes.

We have made a quantitative statistical comparison between ground-based FTIR, CIMEL, GPS and integrated (corrected) sonde measurements of IWV at Ukkel: we find very good correlations between all datasets, but also some wet and dry biases.

II.1.2 Aerosol detection and properties

II.1.2.1 Rationale

Atmospheric particulate matter is commonly referred to as aerosols. There is a very large variety of aerosol both from natural or anthropogenic origin. They are important

for various reasons. First they serve to transport nonvolatile material from one place to another on Earth. Second, they affect the optical properties of the atmosphere. In particular, it has been demonstrated in previous studies that the aerosols have a large impact on the quantity of harmful UV-B radiation received at the Earth's surface. This radiation has consequences on both climate and the health of the biosphere (including human health, crop growth, etc.). The latest IPCC Report also stressed that the radiative forcing caused by atmospheric aerosols is one of the largest uncertainties in determining the total radiative budget of the atmosphere. Part of the radiative forcing is indirect, because the aerosols act as nuclei for the formation of clouds or fog, which in turn affect the penetration of sunlight to the surface. And last but not least, aerosols affect the chemical reactions in the atmosphere; a well-known effect is their impact on the ozone depletion processes. Better monitoring capabilities of aerosol properties can therefore improve our understanding and forecasting of the atmospheric processes and evolution, and in particular of UV-B and climate changes.

In AGACC, we developed and implemented new observation techniques for monitoring aerosol properties. The focus is on the total aerosol optical depth (AOD), profiling in the boundary layer, and the derivation of some optical properties. These developments have already served to improve UV-B forecasting and the retrieval of other trace gases that are affected by the presence of aerosol.

That operational monitoring of aerosol is of current interest in the international atmospheric research community can be seen also in the efforts that have been deployed in this direction during the CINDI (Cabauw Intercomparison Campaign of Nitrogen Dioxide measuring Instruments; http://www.knmi.nl/samenw/cindi/index.php) campaign in June-July 2009 in Cabauw (the Netherlands), that is discussed briefly in Section II.1.2.3. This campaign was supported by CEOS (Committee on Earth Observation Satellites) and the EU Integrated Project GEOmon (http://www.geomon.eu). BIRA-IASB participated to this campaign and is currently working on the results.

II.1.2.2 CIMEL sunphotometer measurements of aerosol

A CIMEL sunphotometer was installed at Ukkel (50.5°N, 4°E) in July 2006 and has operated correctly from July 2006 to September 2007 and from March 2008 to April 2009. There have been 2 recalibration periods (standard intercalibration with an AERONET master instrument at Carpentras (44° N, 5° E)) during October 2007-February 2008 and May 2009. Since June 2009 the recalibrated instrument is back in operation.

The instrument is part of the AERONET network [Holben et al. (1998)] and its processed data (e.g., aerosol optical depth (AOD), aerosol size distribution, and integrated water vapor (IWV) are available on the associated website (http://aeronet.gsfc.nasa.gov/). They

have already been used in several studies – e.g., in the IWV comparisons discussed in Section II.1.1.4, and in Dewitte et al. [2007] to perform an analysis of the solar radiation at Ukkel from a climate change point of view. The AOD data have also been used in an intercomparison of AOD retrieved from the CIMEL measurements and from Brewer ozone measurements by Cheymol et al. [2008]. And they supported the validation of the AODs retrieved from MAXDOAS measurements in Ukkel – see Section II.1.2.3.4, and for intercomparison with the Brewer data, as described in Section II.1.2.4.

II.1.2.3 MAXDOAS measurements of aerosol

In the framework of the AGACC project a "new generation" of multi-axis differential optical absorption spectroscopy (MAXDOAS) instruments has been designed. These instruments are optimized for the retrieval of atmospheric absorbers, including aerosol and trace gases, present in the lower troposphere. They are able to measure the direct-sun and scattered light at various elevation and azimuth angles in the UV and visible (VIS) regions of the electromagnetic spectrum. To obtain near real time information on aerosol properties and trace gas profiles from the MAXDOAS measurements, a state-of-the-art retrieval algorithm was developed based on the radiative transfer code LIDORT and the optimal estimation method (OEM).

Currently two of these "new generation" MAXDOAS instruments are operational: A first one has been operated for a 10-month time period (June 2008 to April 2009) in Beijing (39°58'37"N; 116°22'51"E), China, where it was installed on the roof of the institute of atmospheric physics a few hundred meters from the Beijing Olympic stadium. Later on, this instrument was involved in the CINDI campaign in June-July 2009 in Cabauw, the Netherlands. During this campaign a large number of MAXDOAS instruments were brought together to evaluate the performance of the newly developed systems through intercomparison of the measured differential slant column densities (DSCDs) and relative intensities. As part of post-campaign activities, the aerosol extinction and trace gas vertical profiles retrieved by the different participating state-of-the-art algorithms will be intercompared. We will also have the opportunity to validate and uniformize the retrievals through comparison with additional aerosol and trace gas measurements (sunphotometer, LIDAR, and in-situ measurements) made in Cabauw. Such validations of both measurements and retrieved data products are essential milestones in the process of building reliable monitoring facilities for the near real time retrieval of aerosol and trace gas properties from MAXDOAS measurements.

A second MAXDOAS instrument was installed on the roof of the building of the Royal Meteorological Institute in Ukkel (50.5°N, 4°E). The instrument operated continuously from March until June 2009.

A short description of the MAXDOAS instruments designed and assembled at BIRA-IASB was already given in AGACC200806 and is not repeated here. The next section provides a short outline of how these systems were set up at the different observation sites and how the raw DSCDs measurements are obtained. The following section describes the algorithm developed for the retrieval of aerosol extinction vertical profiles and shows the results for two different sites: The heavily polluted Beijing site, and the relatively less polluted site Brussels.

II.1.2.3.1 The measurements

The measured spectra of scattered sunlight are analysed using the DOAS technique based on a least-squares spectral fitting method [Platt, 1994]. The direct results of this fitting are the DSCDs, i.e. the integrated concentrations of the absorbers along the effective light path of the scattered photons relative to the concentrations of the absorbers in a reference spectrum. For tropospheric profiling purposes, one can eliminate the stratospheric contribution to the measured DSCD by subtracting for each scan the DSCD measured at zenith from the off-axis DSCDs [Wagner et al., 2004; Friess et al., 2006]. The O_4 DSCD, needed for the aerosol profile retrieval, are retrieved at 360, 477,577, and 630 nm in the wavelength intervals 344.7-365 nm, 455-500 nm, 540-588 nm, and 602-645 nm. These wavelength regions were optimized to obtain optimal sensitivity for O_4 while minimizing correlations with interfering absorption structures. In addition to the O_4 cross-section (xs) other trace gas cross-sections such as O_3, H_2O, BrO, were included in the fitting routine, along with a Ring interference spectrum and a low-order polynomial closure term.

As a consistency check, we compared the O_4 DSCDs measured on clear-sky days with relatively low aerosol pollution at 30° elevation with O_4 DSCDs simulated using retrieved aerosol profiles and ancillary aerosol information. Under these conditions, the O_4 DSCDs are rather insensitive to changes in the aerosol profile or other atmospheric parameters. Therefore, a good agreement between the O_4 DSCD is expected [Wagner et al., 2009]. We noticed, however, that depending on location and wavelength the simulated O_4 DSCDs were systematically lower by a factor of about 0.8-0.9. Possibly, the difference is induced during the DOAS retrieval, maybe because of errors in the absolute values of the O_4 cross-section. To account for this, we applied a corresponding correction to the absolute value of the O_4 cross-section.

II.1.2.3.2 Semi-blind intercomparison of NO_2 and O_4 columns during CINDI

In June-July 2009, over thirty different in-situ and remote sensing instruments all capable of measuring atmospheric nitrogen dioxide (NO_2), were jointly operated during the Cabauw Intercomparison campaign for Nitrogen Dioxide measuring Instruments (CINDI). The campaign took place in The Netherlands at the Cabauw Experimental Site for Atmospheric Research (CESAR), which is managed by the Royal Dutch Meteorological Institute (KNMI). Its main objectives were to determine the accuracy of state-of-science ground-based NO_2 measuring techniques and to investigate their use in satellite validation. During the first two weeks of the campaign a semi-blind intercomparison was performed involving 22 MAXDOAS and Zenith Sky instruments from a number of institutes worldwide [Roscoe et al., 2010]. These instruments (among them the BIRA-IASB MAXDOAS system) pointed in the same direction and scanned almost the same air mass every 20-30 minutes. The wavelength ranges and inversion algorithm to obtain slant columns of NO_2 and O_4 were prescribed to minimise differences caused by these algorithms. The 30-minute averages of the slant column densities of NO_2 and O_4 matched within 5% for most participating instruments and all elevation angles (see Figure 16 and Figure 17).

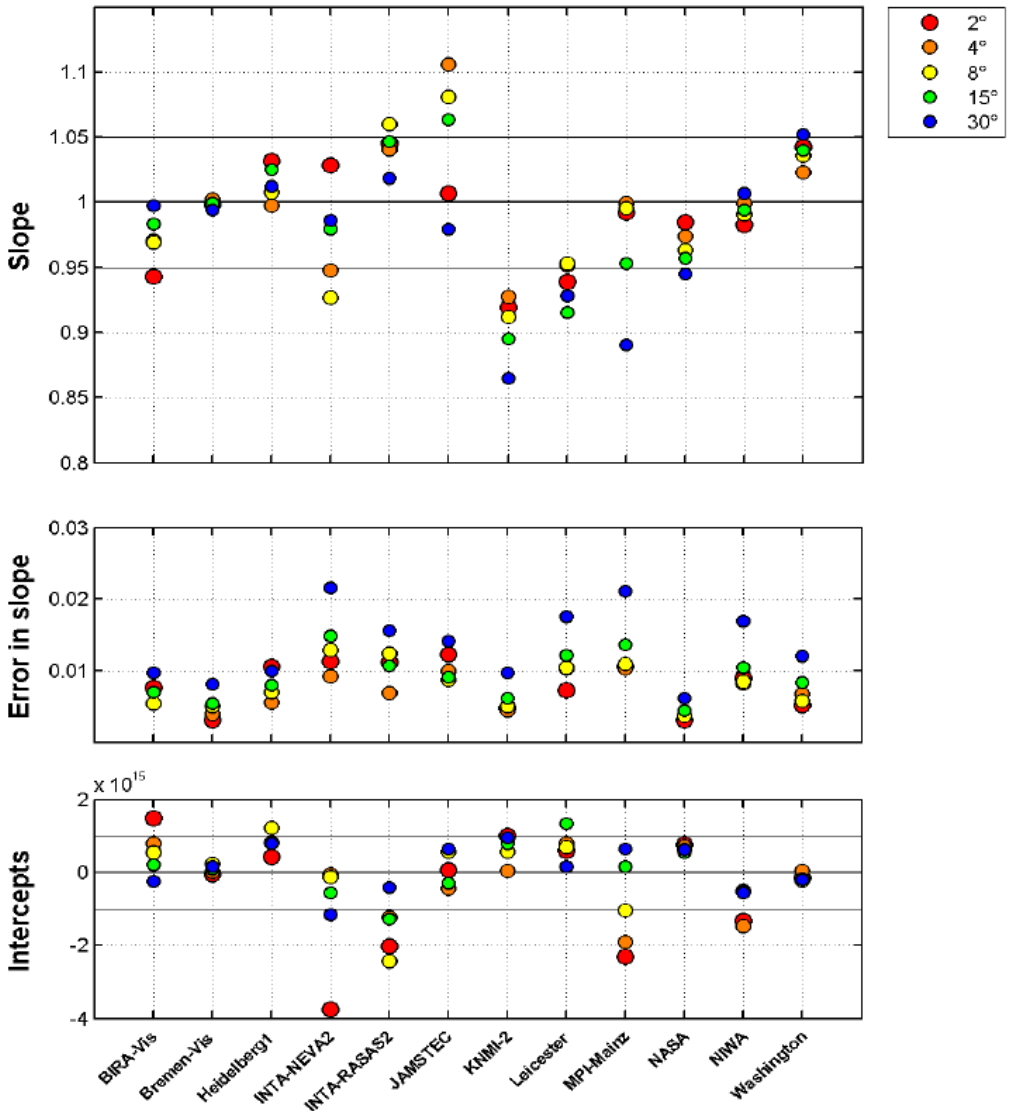

Figure 16 : Straight-line slopes and their standard errors of NO_2 slant columns against those of the reference data set, for each instrument at visible wavelengths and for the whole campaign. Colours refer to elevation angles shown top right [Roscoe et al., 2010].

Note that such results are comparable to those obtained in previous intercomparions which were only for zenith-sky instruments hence focussing on stratospheric NO_2. The fact that during CINDI an almost as good agreement was found in MAXDOAS measurements of NO_2, which have a much shorter heritage than zenith measurements, and that an almost as good agreement was found for MAXDOAS measurements of O_4, which are important to diagnose the state of cloud and aerosol in the troposphere, bodes well for the future of measurements of tropospheric NO_2 by this important technique. From this study it became clear that a proper calibration of the elevation angles is crucial for the interpretation of the measurements. Also, the variability of the NO_2 with time is observed to be quite large, and a significant part of the scatter in the comparisons is caused by time differences in the measurements.

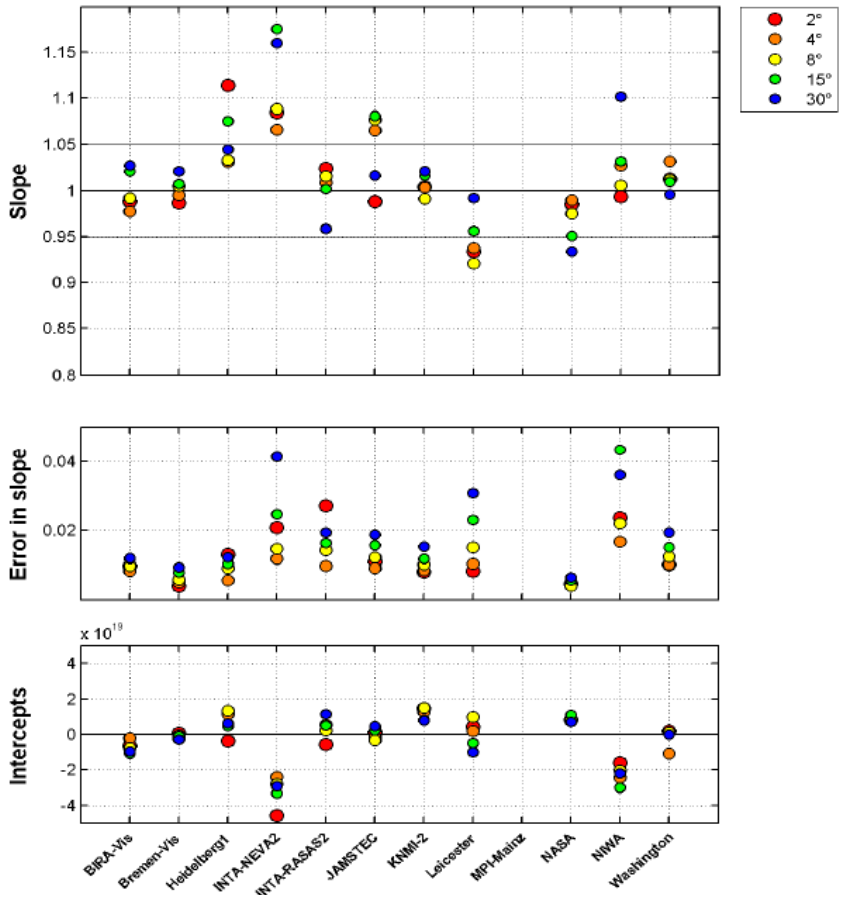

Figure 17 : Straight-line slopes and their errors of O_4 slant columns against those of the reference data set, for each instrument at visible wavelengths and for the whole campaign. Colours refer to elevation angles shown top right. MPI-Mainz used a non-standard wavelength range for analysis, which did not produce an O_4 amount.

II.1.2.3.3 Retrieval of aerosol extinction profiles

General algorithm description

An inversion algorithm was developed for the retrieval of aerosol extinction profiles at different wavelengths from MAXDOAS measurements. A detailed description of the algorithm was already given in AGACC200806 and AGACC200812; here we just repeat a short summary.

The aerosol extinction vertical profile is obtained by combining the retrieved O_4 DSCDs for different line of sight (LOS) directions. [Wagner et al., 2004; Hönninger et al., 2004; Friess et al., 2006; Li et al., 2008; Irie et al., 2008] In general, the length of the light path through the atmosphere and thus the observed DSCD of an atmospheric absorber depend not only on the concentration of the trace gas but also on the vertical distribution and optical properties of the aerosol present in the atmosphere [Wagner et al., 2004; Friess et al., 2006]. Consequently, when the vertical distribution of an absorber is well known and nearly constant – the O_4 concentration varies with the

square of the O_2 monomer [Greenblatt et al., 1990] – DSCD measurements provide information on the aerosol optical properties.

For the inversion we used the OEM [Rodgers, 2000]. Herein, the aerosol extinction vertical profile k is retrieved given an *a priori* profile k_a, the measurements y (here, a set of DSCDs for different LOS directions), their respective uncertainty covariance matrices (S_a and S_ε), the matrix K of weighting functions, and a forward model operator F usually implemented as a numerical model. Aerosol extinction profile retrieval is a non-linear problem, and the inverse solution has to be determined iteratively:

$$k_{i+1} = k_i + \left(S_a^{-1} + K_i^T S_\varepsilon^{-1} K_i\right)^{-1} \left[K_i^T S_\varepsilon^{-1} \left(y - F(k_i)\right) - S_a^{-1} \left(k_i - k_a\right)\right] \quad (1)$$

The weighting functions display the sensitivity of the measurements to changes in the vertical profile. The forward model F describes the physics of the measurement, and in our application is based on the linearized discrete ordinate radiative transfer model (LIDORT v3.3) [Spurr, 2008]. A major advantage of this code is that it includes an analytical calculation of the weighting functions needed for the inversion step. Consequently the algorithm is relatively fast, which is a major advantage since it allows for near real time automated retrievals. An important parameter for the characterization of the retrieval is the sensitivity of the retrieved state to the true state [Rodgers, 2000]. The averaging kernels – which are the rows of the averaging kernel matrix A – express this relationship. They provide a measure for the vertical resolution of the measurement and the sensitivity of the retrieval to the true state at particular altitudes. The trace of A is the Degrees of Freedom of Signal (DFS), a measure of the number of independent pieces of information extracted from the retrieval.

Retrieval parameter settings

With optimal estimation, the choice of the *a priori* profile and the error covariance matrices has an important impact on the results. There is a trade-off between maximizing the DFS and eliminating the occurrence of spurious oscillations in the retrieved profiles.

The O_4 DSCDs calculated using the forward model not only depend on the aerosol extinction profile but also on aerosol single scattering albedo and phase function. To obtain a good estimate of these optical aerosol parameters, we used the inversion products (size distribution and refractive index) reported on the AERONET website [Holben et al., 1998] from a CIMEL sunphotometer located next to the MAXDOAS instrument. The AERONET AODs were used for a first validation of the aerosol extinction profiles retrieved from the MAXDOAS measurements.

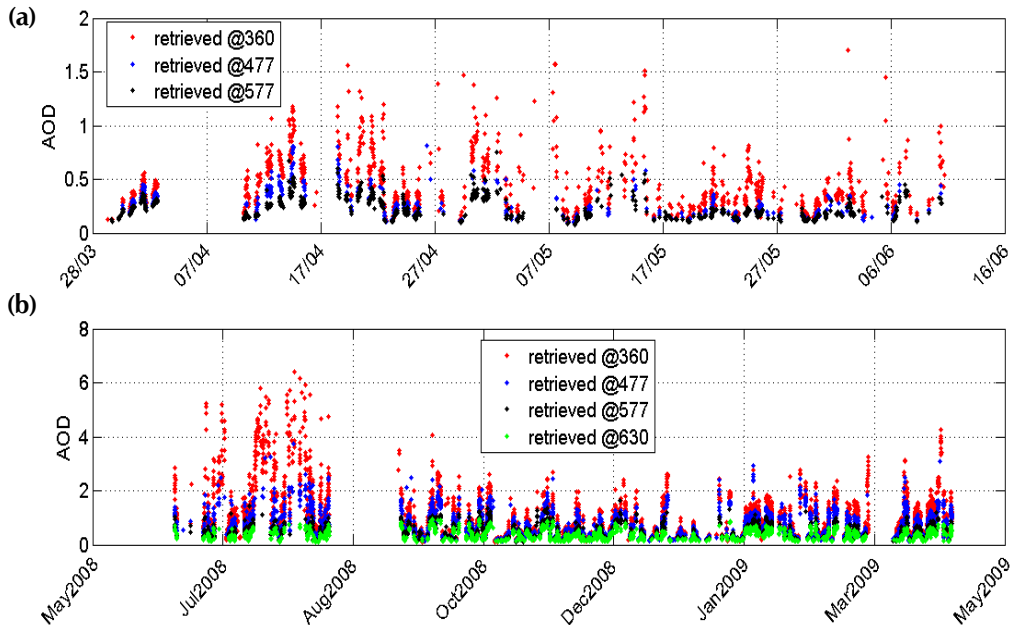

Figure 18: Time series of retrieved tropospheric AODs (a) in Brussels and (b) in Beijing.

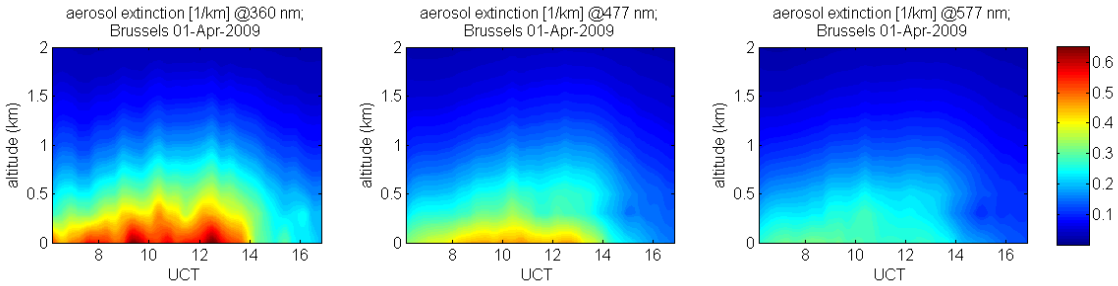

Figure 19 : Contour plots of the aerosol extinction profiles retrieved from MAXDOAS measurements made in Brussels on the 1st of April 2009.

Results

The MAXDOAS instrument in Brussels (50.5°N, 4°E) was installed on the roof of the building of the Royal Meteorological Institute, with the telescope pointing north-west for the MAXDOAS measurements. The instrument operated continuously from March until June 2009. Due to mechanical problems with the suntracker the measurements were then paused, but will recommence in the near future. The MAXDOAS instrument in Beijing (N39°58'37" E116°22'51"), on the roof of the Institute of Atmospheric Physics, was installed with the telescope pointing north. The instrument operated continuously from June 2008 until April 2009, with the exception of a short period between the 21st of August and the 16th of September 2008, when no measurements were taken due to instrumental problems.

A full MAXDOAS scan comprised 10 elevation angles (0°, 2°, 4°, 6°, 8°, 10°, 12°, 15°, 30°, zenith) and required approximately 15 minutes measurement time. In

addition to the MAXDOAS observations, also direct sun and almucantar (azimuthal scans) measurements were performed.
Aerosol extinction profiles were retrieved from MAXDOAS spectra measured in Brussels and Beijing for, respectively, three (360, 477, 577nm) and four (360, 477, 577, 630nm) wavelengths. Only those profiles are retained for which the measured and simulated DSCDs agree within 10%.
The time series of quality-checked AODs retrieved from the Brussels and Beijing MAXDOAS measurements using the profiling tool are shown in Figure 18. It can be seen that the AODs in Beijing are much higher than the values for Brussels. Especially during June and July 2008, the AODs in Beijing were very high (AODs at 360 nm up to 6).
As an example, the aerosol extinction profiles retrieved from MAXDOAS measurements made on the 1st of April -a clear-sky day- in Brussels, are represented as contourplots in Figure 19.

II.1.2.3.4 Auxiliary results: Retrieval of trace gas vertical profiles

One of the main obstacles for tropospheric trace gas vertical profile retrievals from MAXDOAS measurements is the sensitivity of the length of the light path -and thus the observed DSCD of an atmospheric absorber- to the presence of aerosol in the atmosphere [Heckel et al., 2004; Wittrock et al., 2004; Sinreich et al., 2005]. Consequently, it is impossible to retrieve trace gas vertical profiles without first retrieving the aerosol extinction vertical profiles. Therefore the retrieval algorithm we developed to obtain aerosol information was a first class point of departure for the development of a more general algorithm for the near real time retrieval of aerosol extinction and trace gas vertical profiles. The existing algorithm was extended such that in a first step the aerosol extinction profiles are retrieved from O_4 DSCDs and, in a second step, the derived aerosol information is used as input to retrieve tropospheric trace gas (e.g., NO_2) profiles from the (e.g., NO_2) DSCDs obtained from MAXDOAS measurements in the same wavelength interval.

II.1.2.4 Comparison of aerosol measurements

II.1.2.4.1 Comparison of the MAXDOAS AOD data with CIMEL and Brewer data, at Ukkel and Beijing

To obtain an indication of the quality of the retrievals, we compared hourly averages of the retrieved AODs with AODs measured by a co-located CIMEL sunphotometer. The CIMEL values were converted to the wavelengths of the AODs retrieved from the MAXDOAS measurements making use of the angström coefficients which are also

reported on the AERONET site. Figure 20 displays the scatter plots. A very good correlation is obtained (see Figure 16b, red line) between our retrieved AODs and those measured by the CIMEL instrument in Beijing. For the AODs retrieved in Brussels, the situation is slightly different as it appears that the data can be divided in two subgroups. For those situations where the AOD is lower than 0.5, a good correlation with correlation coefficients 0.84 to 0.89 is obtained for the wavelengths 360, 477 and 577 nm, comparable with the results for Beijing (see Figure 16a, the magenta line). When the AOD in Brussels is higher, however, the data is more scattered and the MAXDOAS retrieval seems to underestimate the AOD especially at 477 and 577nm. Possibly, in those cases, the measurements of the MAXDOAS as well as the sunphotometer were influenced by the presence of thin homogenous, possibly sub-visible, clouds [Wagner et al., 2009]. Further work is needed to address this problem. The linear regression and statistical parameters corresponding to these comparisons are summarized in Table III.

Table III: Overview of the linear regression fit parameters (slope and offset) and statistical parameters (correlation coefficient R, bias, standard deviation (stdev), number of points (N°)) from the comparison of retrieved AODs and the values from a sunphotometer in Beijing and Brussels.

	Beijing				Brussels			Brussels AOD < 0.5		
	360nm	*477nm*	*577nm*	*630nm*	*360nm*	*477nm*	*577nm*	*360nm*	*477nm*	*577nm*
N°	725	672	410	546	130	84	129	72	72	91
Slope	1.1	1.1	1.3	1.5	1.2	1.5	1.5	0.81	0.74	0.84
Offset	-0.04	0.09	-0.08	-0.1	-0.01	-0.1	-0.06	0.06	0.05	0.01
R	0.91	0.80	0.72	0.67	0.74	0.65	0.48	0.84	0.89	0.89
Bias	-0.04	0.01	-0.06	-0.06	-0.08	-0.05	-0.08	0.0	0.02	0.03
stdev	0.31	0.31	0.29	0.28	0.26	0.26	0.26	0.05	0.04	0.04

We also intercompared hourly averaged MAXDOAS AODs with the hourly averaged AODs at 340 nm from the Brewer measurements. Again the angstrom coefficients from the AERONET were used, this time to convert the Brewer AODs at 340 nm to 360 nm. To avoid interference by clouds, as much as possible, only those data points were retained for which there was cloud-screened CIMEL data available. Because of these restrictions only 28 data points were left, resulting in relatively poor statistics. Nevertheless a good agreement (correlation coefficient 0.85) was obtained between the instruments. The scatter plots are shown in Figure 20.

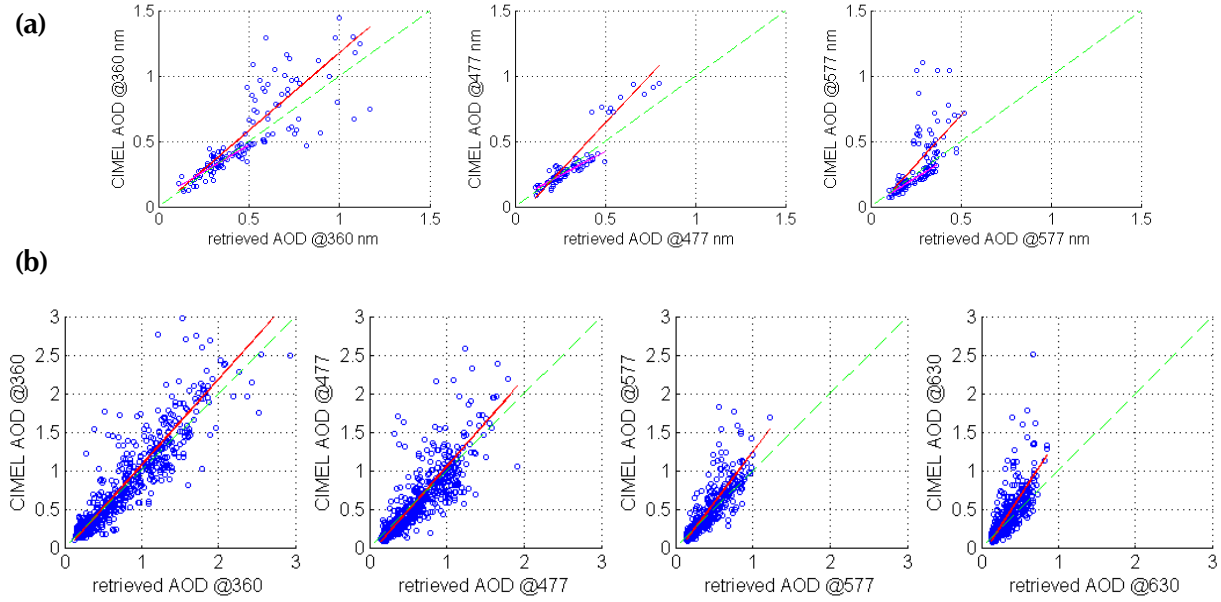

Figure 20 : Scatter plots of (a) the AODs at 360, 477, and 577nm retrieved from the MAXDOAS measurements in Brussels versus the AODs from a co-located CIMEL sunphotometer and (b) the AODs at 360, 477, 577, and 630nm retrieved from the MAXDOAS measurements in Beijing versus the values from a co-located CIMEL instrument. Also shown are the linear regressions fits (red line) for the whole dataset and in Brussels for the AODs smaller than 0.5 (magenta line). The corresponding fit parameters and statistical parameters are shown in Table III.

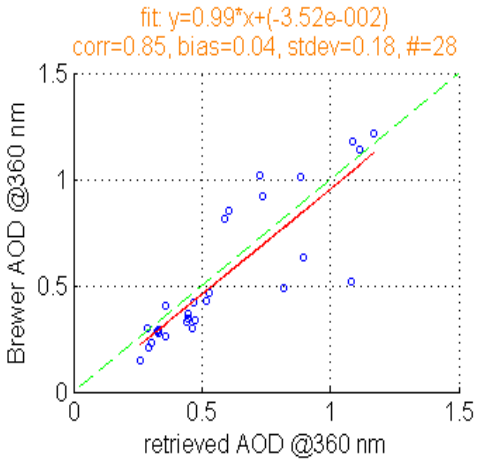

Figure 21 : Scatter plot of the hourly averaged AODs at 360nm retrieved from the MAXDOAS measurements versus AODs from the Brewer (only clear-sky data points are selected). Brewer AOD at 360nm has been derived from measurements at 340nm. Also shown are the linear regression fits and the corresponding statistical parameters (correlation coefficient R, bias, standard deviation (stdev), number of points (N°)).

II.1.2.4.2 Comparison of the MAXDOAS profile extinction data with Lidar and in-situ data during CINDI

As part of the CINDI post-campaign activities, vertical profiles and optical depths of aerosol have been retrieved by several MAXDOAS groups. Frieß et al. [2010] performed

an intercomparison between these retrievals, see Figure 22. A reasonable agreement is found between the different algorithms as to the boundary layer vertical structure. Note also that the aerosol optical depth is in good agreement with the AERONET measurements, although it tends to be too low in the afternoon. This might be related to difficulties in retrieving aerosol properties for measurements taken in a direction close to the sun.

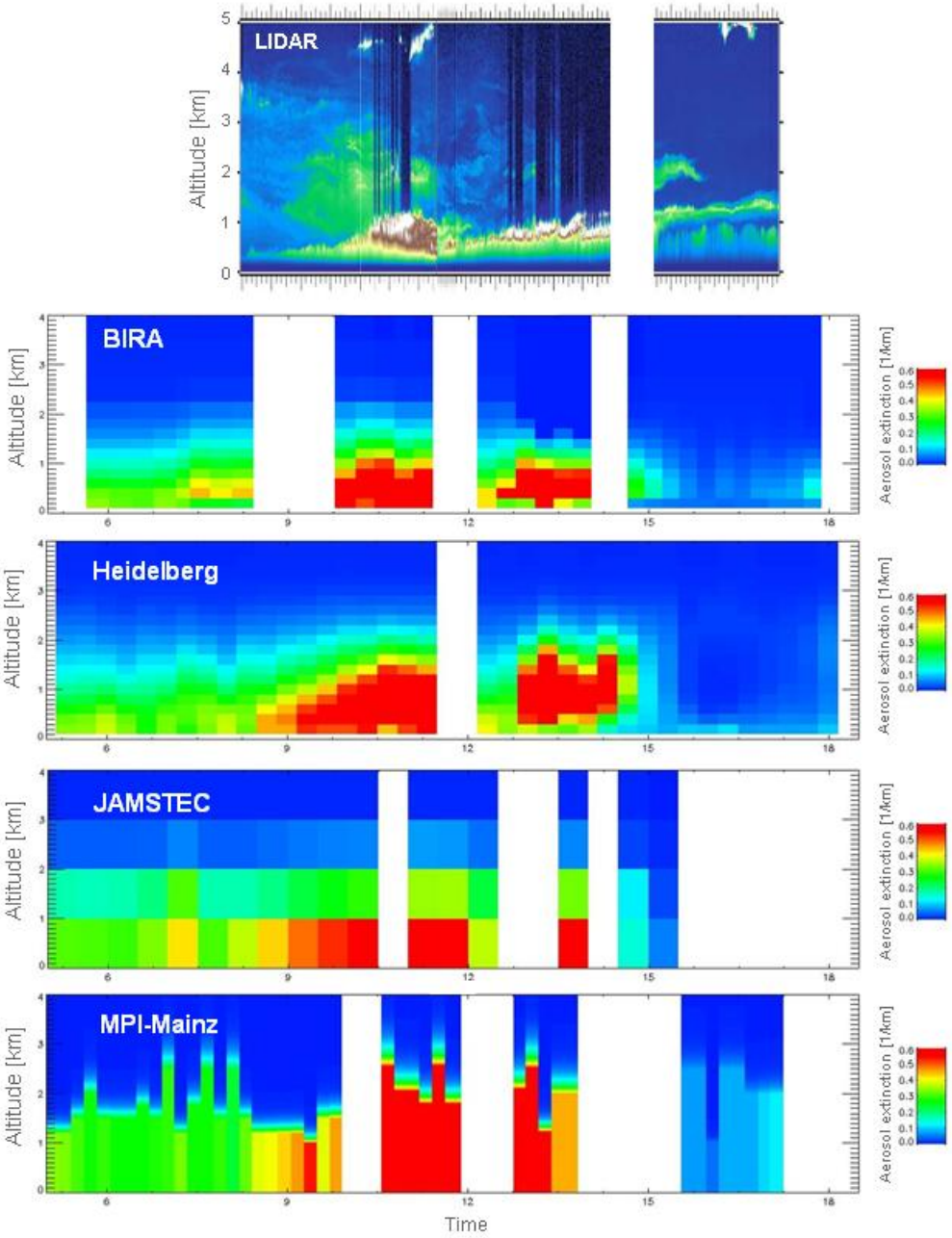

Figure 22 : MAXDOAS aerosol profile intercomparison and comparison to the CAELI lidar [Friess et al., in preparation]

Zieger et al. [2010] also compared MAXDOAS retrieved surface aerosol extinction with in-situ measurements. The values agree better than expected, where the agreement is better for low AOD (from sun photometer) and low PBL cases. The retrieval for some of the instruments improves when ambient in-situ measurements are used as input.

Possible reasons for this could be for instance the stability of the boundary layer, the influence of upper layers, the influence of homogeneous gradient of aerosol concentration, or maybe the influence of nitrate partitioning.

Good correlation was found between in-situ and MAXDOAS measurements as can be seen from Figure 23. For certain cases (low AOD and low PBL height) good agreement was found, but for most of the time MAXDOAS retrieved a 1.5 – 3.4 higher extinction coefficient. Differences could have been caused by e.g. particle losses in the inlet system (all remote-sensing instruments were measuring generally higher extinction) or by the fact that the limited vertical resolution of the MAXDOAS retrieval overestimated the extinction in the lowest layer when lofted layers were present. In addition, the MAXDOAS retrieval could have been influenced by the horizontal aerosol gradient, which could have exhibited large variations. The smaller slope of the regression line for the MPI measurements (panel d) could indicate that the coarser resolution with more simplified assumptions leads to a more robust MAXDOAS aerosol retrieval..

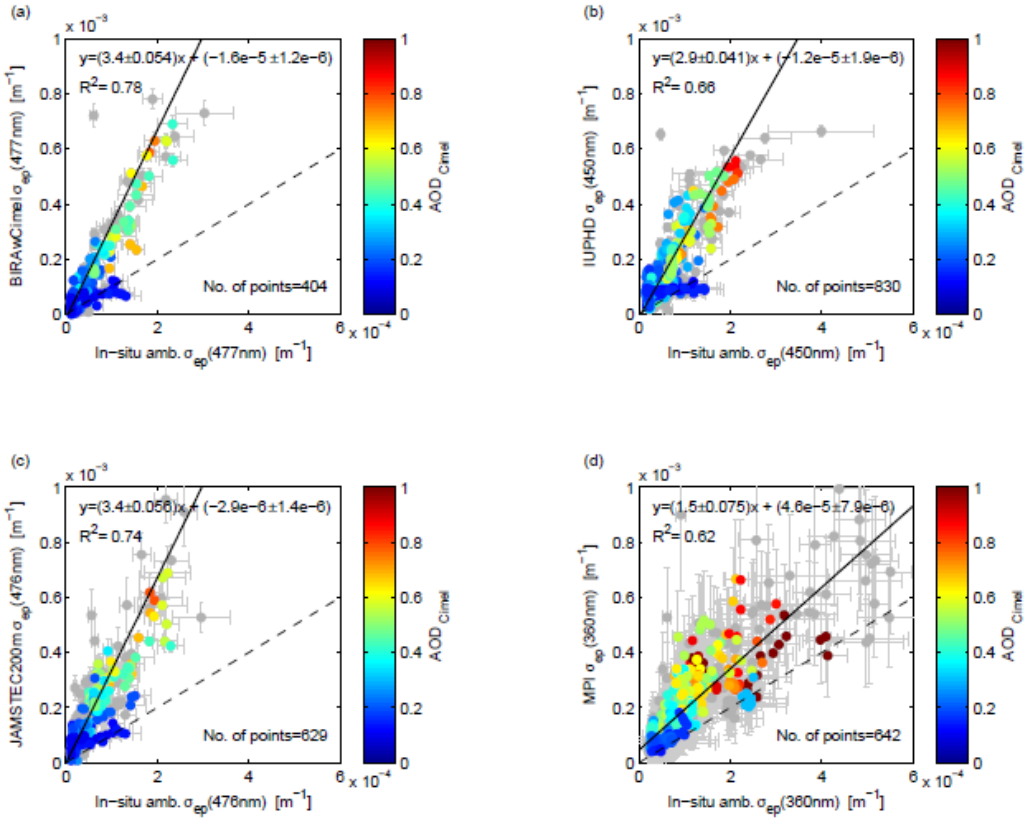

Figure 23 : Ambient extinction coefficient retrieved by four MAXDOAS systems (respectively from BIRA, IUPH, JAMSTEC and MPI) vs. in-situ measurement brought to ambient conditions. The color code denotes the AOD measured by the CIMEL sun photometer (grey points are times with no sun photometer measurements). The solid black line represents a bivariate linear regression including weights (with calculated uncertainty of slope and intercept). The dashed line is the 1:1-line [Zieger et al., 2010].

II.1.2.4.3 Comparisons between the CIMEL and Brewer spectrometer at Ukkel

We have compared the AODs retrieved with the Langley plot method [Cheymol et al., 2006] from the Brewer measurements at 320nm with the AODs from CIMEL at 340nm. We have found that the diurnal variation of the AODs calculated from the CIMEL or the Brewer is very similar. Next, all simultaneous clear-sky data ($\Delta t < 3'$) of the CIMEL-Brewer intercomparison campaign were selected, which corresponds to a dataset of 368 measurements, and the AODs were calculated at 320nm and 340nm for the Brewer and CIMEL instruments respectively. We obtained a very good agreement between both instruments (the correlation coefficient being 0.96).

The retrieval of the AOD at 320nm from both Brewers is now pre-operational. This means that whenever it is necessary the data can be produced up to the current day.

The relative intensities of sunlight from the CIMEL and the Brewer have been compared on clear sky days. The CIMEL filter is centered at 340 nm whereas the Brewer originally operates at 320 nm. To eliminate the difference in ozone absorption at both wavelengths in the comparison of the intensities of both instruments, an adapted observation routine was created for the Brewer#178 instrument in August 2006, so that it also records the direct sun intensities at 340nm. Additionally, as the Brewer measures with a very narrow bandwidth, the data at several adjacent wavelength steps are filtered to mimic the CIMEL band-pass. With this new observation mode, we get an excellent agreement between the Brewer and CIMEL relative intensities at this wavelength. We have built up a database of simultaneous intensities of the direct solar irradiance at 340nm in order to compare the AODs derived from both instruments. Adapted algorithms and new software have been developed to derive the AODs at 340nm. The algorithm uses the same principle as the method for 320nm. First a number of clear days are selected. These days are used to determine the calibration coefficients of the instrument by the refined Langley-Plot method [Cheymol et al., 2009]. With this calibration coefficient the AOD can be calculated for each individual clear sky observation. Different selection criteria had to be built into the analysis software in order to eliminate measurements with obscured sun [De Bock et al., 2010]. In the future, the cloud-screening algorithm needs to be further improved.

In an initial stage we calculated the Brewer AODs at 340nm for a period from August 2006 until May 2009. We extended this period and obtained nearly 3000 individual AOD values for a period from 1 September 2006 until 31 August 2010. These observations were compared with the CIMEL level 2.0 data.

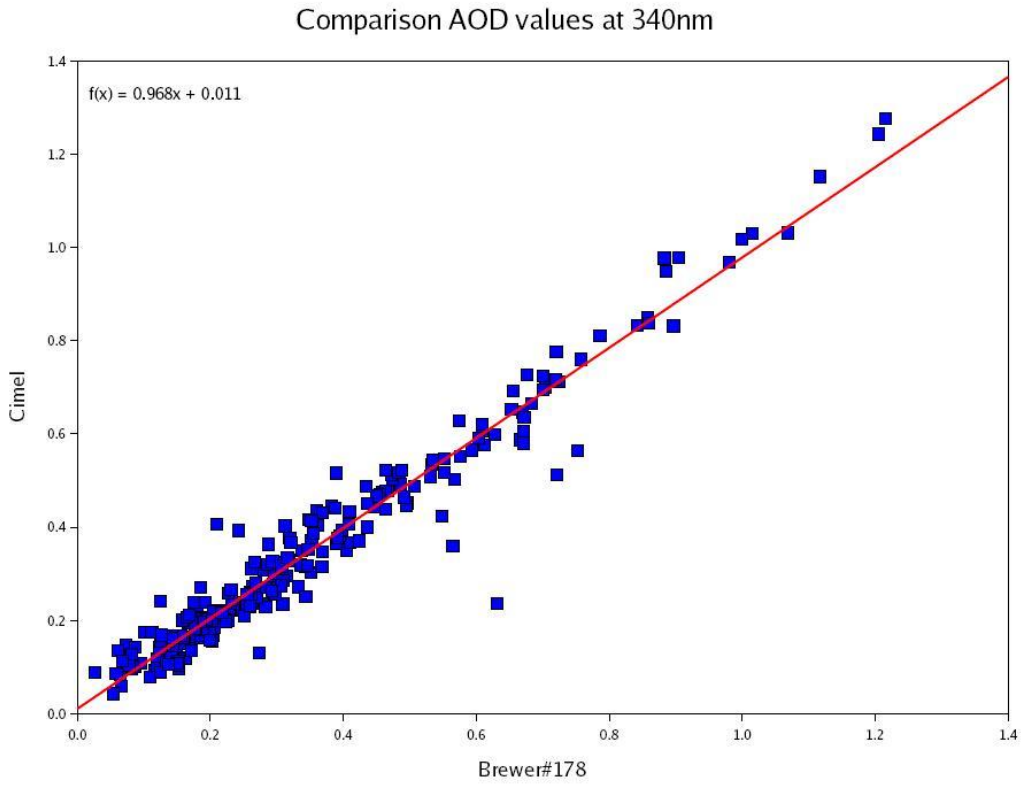

Figure 24: Scatter plot of the AODs at 340nm measured with Brewer#178 and CIMEL at Ukkel.

Figure 24 shows the scatter plot of 251 quasi-simultaneous AOD observations of Brewer 178 and the CIMEL at Ukkel. The correlation between both is 0.97, the slope 0.968+/-0.014 and the intercept 0.011+/-0.006. This illustrates that with the proposed method it is possible to obtain good quality AOD observations at 340 with a double monochromator Brewer instrument.

II.1.2.5 Brewer AOD and UV index prediction

II.1.2.5.1 AOD variability in Uccle

The highest AOD values at Uccle (at 340nm) can be observed in summer (respectively 0.63(+/-0.35), 0.59(+/-0.34), 0.53(+/-0.27) and 0.58(+/-0.37) for 2007, 2008, 2009 and 2010) and spring (respectively 0.55(+/-0.32), 0.58(+/-0.35), 0.63(+/-0.38) and 0.51(+/-0.30) for 2007, 2008, 2009 and 2010 [(De Bock et al. (2010)]. These findings are consistent with other studies reporting on higher AOD values during spring and summer and lower values in autumn and winter. This seasonal cycle can be clearly seen in Figure 25.

The small apparent offset between Brewer and CIMEL data in this figure may be due to the fact that the cloud-screening of the Brewer data is not yet optimal; the improvement of the cloud-screening algorithm is in progress.

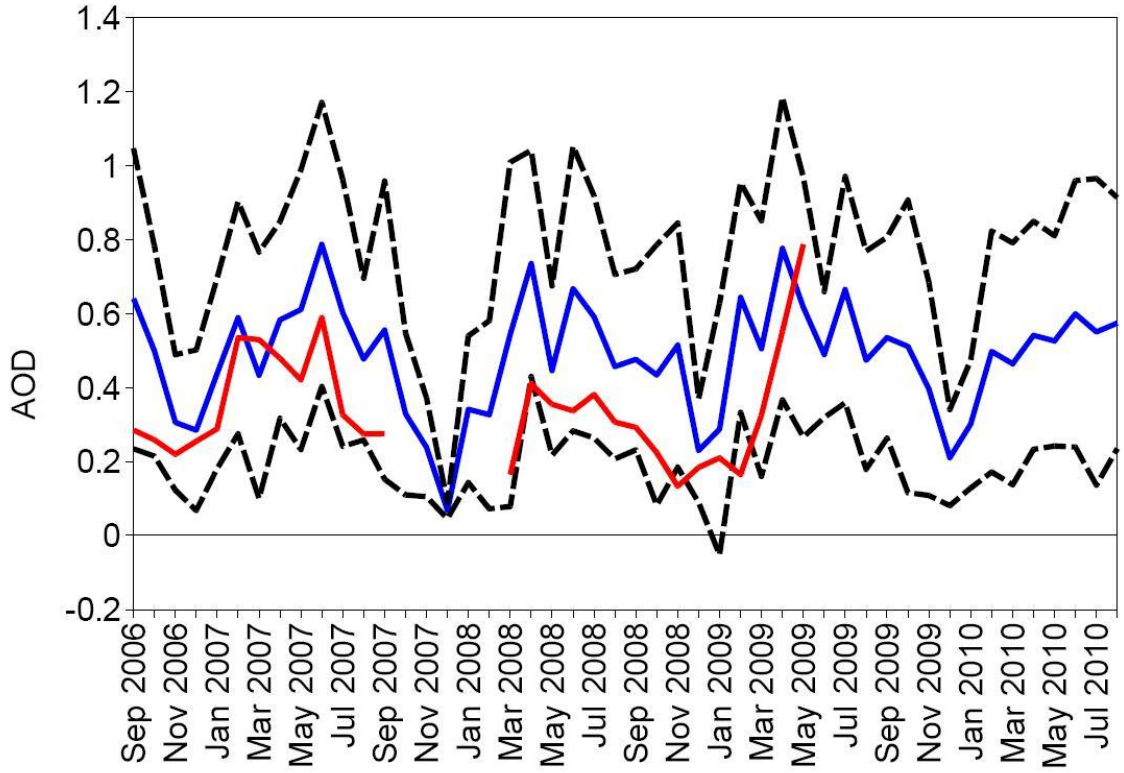

Figure 25 : Monthly variation in AOD (at 340nm) at Uccle (based on Brewer data from September 2006 until the end of August 2010). The blue line is the mean monthly value, whereas the dashed black line represents the mean value +/- its standard deviation. The CIMEL level 2.0 monthly means are shown in red.

II.1.2.5.2 **AOD impact on UV index prediction at Uccle**

In order to improve the operational UV index prediction at Ukkel, we have investigated the impact of the AOD, measured by the Brewer spectrophotometer #16, on the UV index.

Therefore, we implemented the daily/monthly/annual mean of the Brewer AOD at 320 nm in the Madronich TUV index forecast model, instead of using the AOD at 340nm given by the standard Elterman aerosol profile. For 50 clear days, these *simulated* UV indices are compared with the *observed* UV indices, measured by the Brewer instrument. We found that using the daily mean of the observed Brewer AODs improves the UV index forecast significantly and to a larger extent than using monthly or annual means. Another important conclusion is that the AOD impact on the UV index increases with the solar zenith angle (SZA) [Cheymol et al., 2007], i.e., a certain increase of AOD reduces the UV index relatively stronger at higher SZA than at lower SZA.

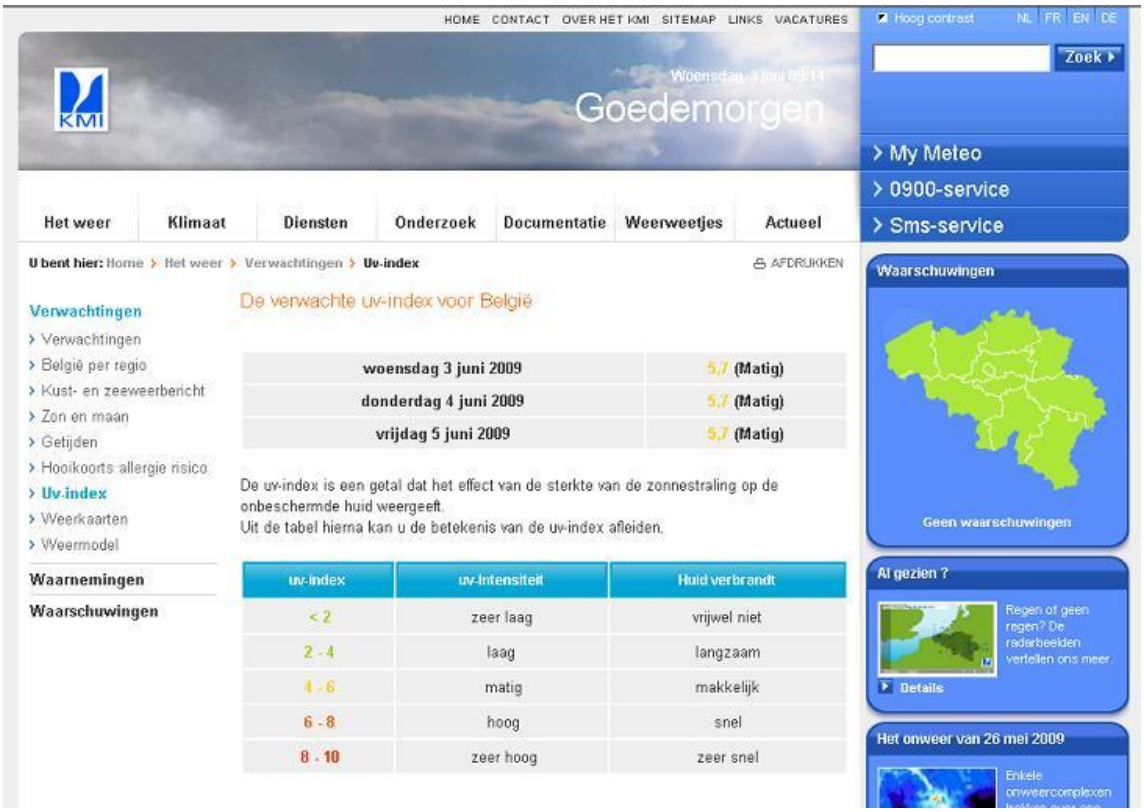

Figure 26 : Example of the dissemination of the UV index prediction on the web pages of RMIB.

Recently the UV-index prediction period was extended to two days. Now the predicted UV index for clear sky is available for the current day, the next day and the day after (Figure 26). The prediction is based on the stratospheric ozone forecast by the Deutsche Wetterdienst.

In order to improve the quality of the predictions a student of the University of Antwerp made a modelling study to investigate the impact of the aerosol composition, used in the modelling, on the quality of the predictions.

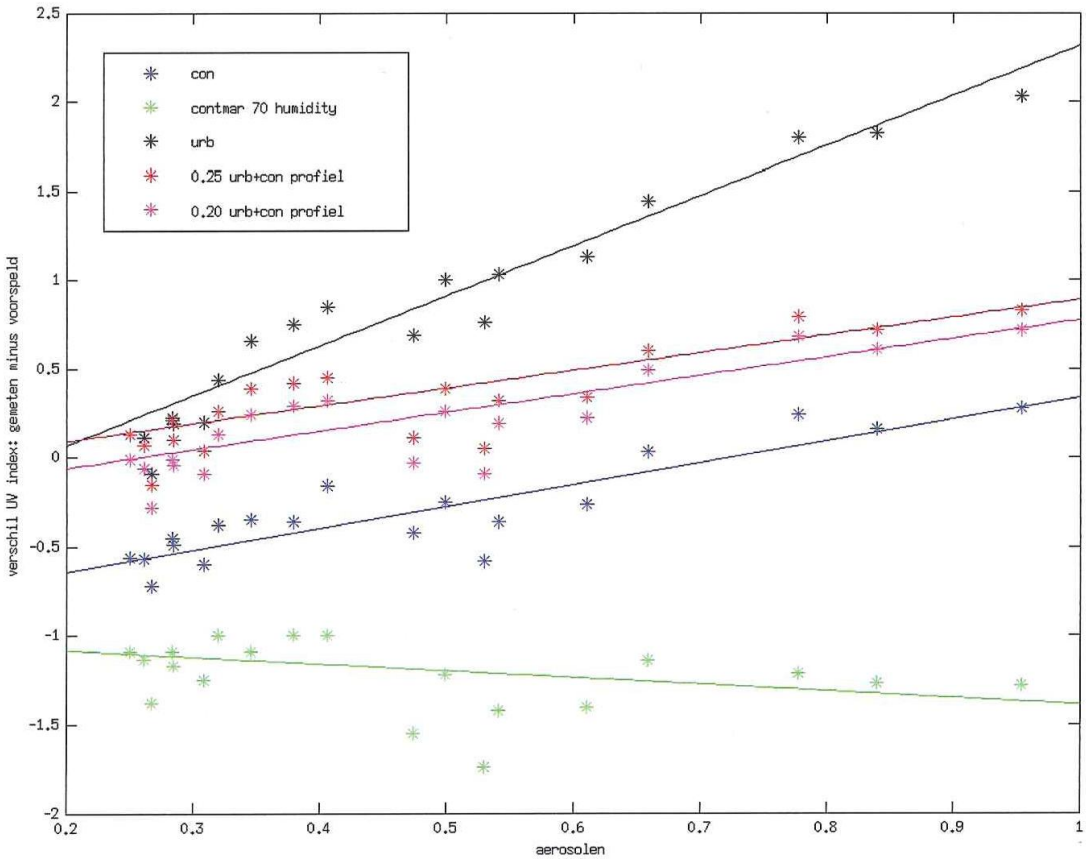

Figure 27 : The difference between the measured and the predicted UV-index as function of the amount of aerosols (AOD) for different aerosol models (con = standard continental; conmar = continental marine with 70 % relative humidity; urb = standard urban, 0.25 urbicon = 0.25 standard urban + 0.75 continental, 0.2 urbicon = 0.20 urban + .80 continental).

Figure 27 shows that the lowest aerosol dependence is obtained when a mixed aerosol model (0.20 urban + 0.80 continental) is used [Geens, 2008]. However, it seems that the composition of the aerosol particles may depend on the AOD itself. This is probably linked to the origin of the air masses, which in its turn, depends on the actual meteorological situation. The relative importance of clouds, ozone and aerosol on the UV radiation and its trends has been studied [De Backer, 2009]. To that end the correlation coefficients between the daily erythemal UV doses and the total radiation, the ozone column and the AOD were calculated for each calendar month. At the same time the modification factor for each of these parameters was calculated. The latter factor represents the percentage change of the daily erythemal UV dosis for a 1 percent change of the correlated parameter. Figure 28 shows that the correlation with total radiation is very high (larger than 0.9 most of the year). The anti-correlation with ozone is lower (of the order of –0.5) and with AOD is even still lower. However, the modification factors for the AODs are higher than those for ozone, in such a way that the effect of AOD on the daily erythemal UV dosis is larger than the effect of ozone. This illustrates the importance of the aerosol on the UV radiation reaching the surface,

and the need to include aerosol information as an input parameter in the models used for the prediction of the UV-index.

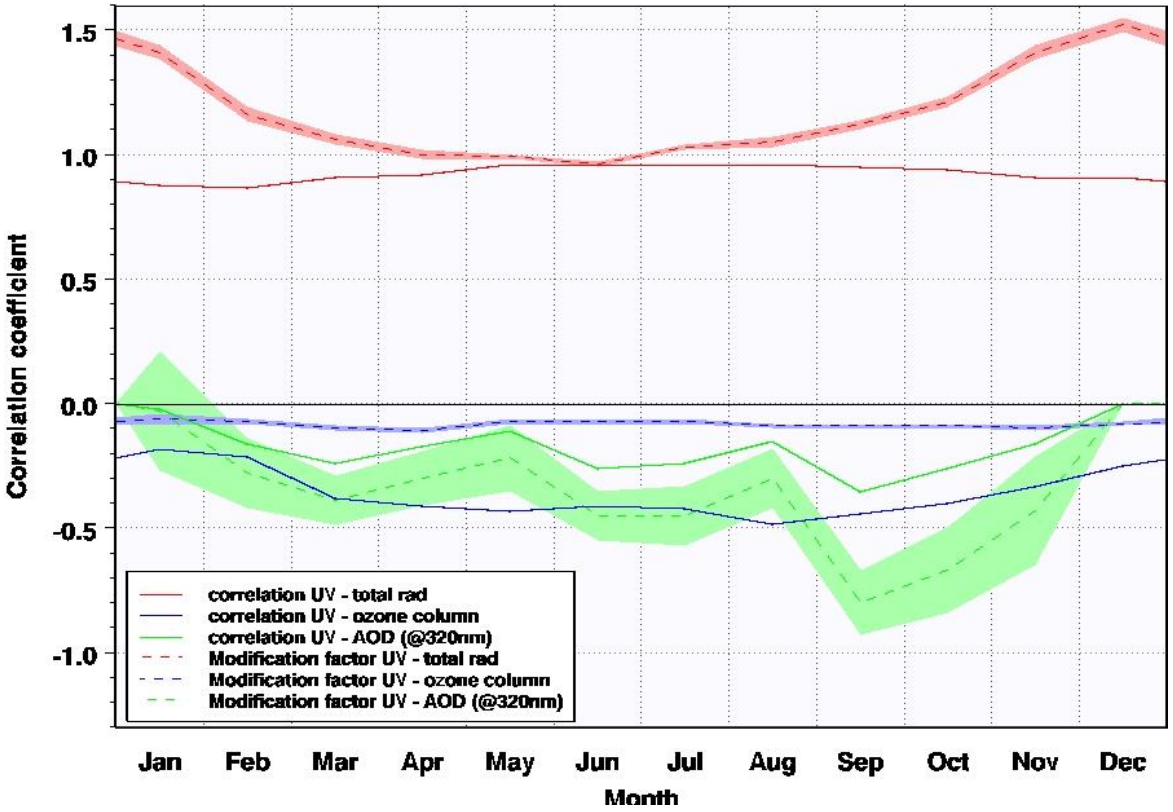

Figure 28: Seasonal correlation coefficients and modification factors (see text) for the relation between daily erythemal UV doses and total solar radiation, ozone column and AOD in the UV-B. The shaded areas are the 1σerror estimates for the modification factors.

The AODs from the Brewer instruments (at 320 and 340 nm) will soon be made available on a regular basis. A next step is to use this information in the prediction of the UV index. For the past couple of months, the UV forecast model has been running in a test mode using the mean AOD over the past 15 days as input instead of the climatological monthly mean that is currently used. The results of these tests will be analyzed in the near future.

II.1.2.6 Major conclusions

Several measurement techniques are now operational in the AGACC consortium for the ground-based monitoring of aerosol properties. These are the Brewer spectrometer and CIMEL observations at Ukkel, the latter contributing also to the AERONET network since July 2006, and the MAXDOAS observations, currently performed at Beijing and Ukkel for development and validation purposes but with the objective to provide measurements at other interesting locations, e.g., within NDACC but also during measurement campaigns. Unlike CIMEL and Brewer measurements, that provide the total AOD, it has been demonstrated that the MAXDOAS measurements also provide

additional information about the vertical distribution of the aerosol extinction in the lowest kilometers of the troposphere.

The measurements have been compared among each other and show good agreement within their respective uncertainties. The MAXDOAS measurements also contributed to the international CINDI campaign in Cabauw, The Netherlands (June-July 2009). The CINDI results include interesting comparisons between MAXDOAS aerosol extinction profiles and lidar and in-situ aerosol extinction data. They have given us more confidence and insight into the ultimate capabilities of the technique, and will allow us to contribute to the definition of new standards for tropospheric aerosol and trace gas profile measurements using the MAXDOAS technique.

The combination of Brewer, CIMEL and MAXDOAS instruments gives us a remote-sensing dataset that will enable a more comprehensive characterization of the tropospheric aerosol optical properties.

The usefulness of these aerosol observations has already been demonstrated in the better understanding of the UV irradiation received at the Earth's surface and in the improvement of the UV-index predictions for the general public. Another application is their use as input data in the retrieval of trace gases from MAXDOAS measurements, like tropospheric NO_2.

II.1.3 Detection of other climate-related trace species

II.1.3.1 Rationale

It is well known that human activities are changing the chemical composition of the troposphere and the whole atmosphere, especially after the industrial revolution, at a regional and global scale. This composition change has significant effects on our environment: it affects the penetration of the solar radiation through the atmosphere, air quality and climate. Changing greenhouse gas and aerosol concentrations directly affect the radiative budget of the atmosphere, and therefore climate. But many species known as pollutants like carbon monoxide (CO), nitrogen oxides (NO_x) and hydrocarbons, - often related to fossil fuel or biomass burning -, also affect climate through their role in chemical reactions that produce tropospheric ozone, which is a well-known greenhouse gas, or that modify the lifetime of gases like methane (CH_4), and the oxidation capacity of the atmosphere.

Therefore in AGACC, we have focused on the measurement of a number of trace gases that are subject to changing concentrations, that directly or indirectly affect climate, and that are either difficult to monitor or that have not yet been measured from the ground. We have included attempts to observe distinctly some isotopologues, because the isotopic ratios observed in an airmass provide information on its history, and

because the FTIR solar absorption measurements provide a rather unique capability herefore.
The investigated species are the isotopologues of CH_4, hydrogen cyanide (HCN) and the isotopologues of CO as examples of biomass burning tracers, some hydrocarbons like formaldehyde (HCHO), ethylene (C_2H_4) and acetylene (C_2H_2), and HCFC-142b, a replacement product for CFCs and a greenhouse gas.

II.1.3.2 Hydrogen cyanide (HCN)

II.1.3.2.1 Introduction

Recent investigations have resulted in the revision of the lifetime of hydrogen cyanide (HCN) from 2.5 years to 2-5 months, more in line with its important and well documented variability in the troposphere. The main HCN source is believed to be biomass burning (0.1 to 3.2 Tg N/yr; [Li et al., 2003]), making this species a useful tracer of fires, e.g. the widespread and intense 2004 boreal fires. Oxidation by the OH radical is among the identified sinks, while uptake by oceans has been hypothesized as the dominant removal process (0.73 to 1.0Tg N/yr). The magnitude of sources and sinks are still affected by significant uncertainties.

II.1.3.2.2 HCN above Jungfraujoch

In the 3260-3310 cm^{-1} spectral region, there are several HCN lines that can be used for the retrieval of HCN from ground-based FTIR spectra. A systematic and careful look at Jungfraujoch "dry and wet spectra" has allowed identifying 6 candidate lines close to 3268, 3277, 3287, 3299, 3302 and 3305 cm^{-1}. The major interferences are water vapour, two of its isotopologues ($H_2{}^{18}O$ and $H_2{}^{17}O$) and C_2H_2. Each of the identified lines has been characterized in terms of information content. Using a representative subset of spectra, a mean DOFS of 1.6 was computed for the 3287 line, values close to 1.1 were found for the 3268, 3277, 3299 and 3305 lines while the 3302 interval provides less information, with a mean DOFS of 0.75. This latter microwindow was therefore omitted in the final retrieval strategy which simultaneously uses five HCN lines. Two additional windows are included to help in the fitting of water vapor interferences (see Figure 29). Typically, a mean DOFS of 2.2 is achieved.

Table IV : Microwindows used simultaneously to retrieve HCN at Jungfraujoch.

Limits (cm-1)	Fitted species
3267.895 – 3268.300	HCN, H_2O, $H_2{}^{18}O$, $H_2{}^{17}O$
3277.775 – 3277.950	HCN, H_2O
3286.168 – 3288.482	H_2O
3286.950 – 3287.350	HCN, H_2O
3299.120 – 3299.620	HCN, H_2O, $H_2{}^{18}O$
3301.030 – 3301.300	$H_2{}^{17}O$
3304.825 – 3305.600	HCN, H_2O, $H_2{}^{18}O$, $H_2{}^{17}O$, C_2H_2

This retrieval approach has been applied to available Jungfraujoch observations from 1994 onwards. Resulting time series for daily mean partial tropospheric columns are displayed in Figure 29 (left frame).

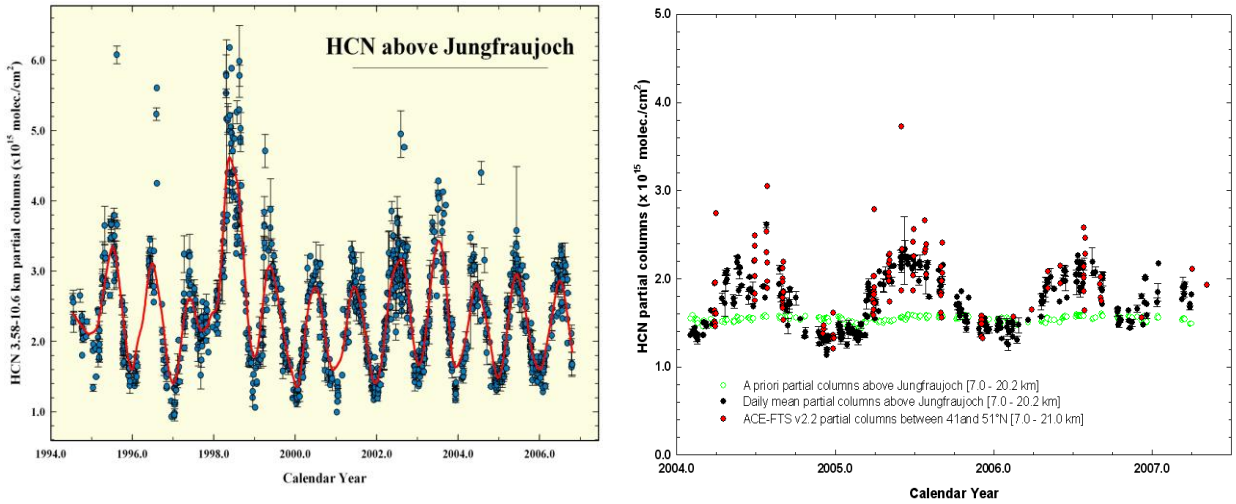

Figure 29: Daily mean tropospheric columns of HCN above the Jungfraujoch station from 1994 onwards (left frame) and comparison with ACE-FTS zonal partial columns (7-21 km) (right frame).

Among striking features, we notice the very high columns observed in 1998 (and to a lesser extent in 2003) correlated with documented high values of carbon monoxide resulting from important biomass burning; also obvious is the strong seasonal variation with maximum columns generally observed in July. For years corresponding to background conditions (e.g. 2000-2001), the peak-to-peak amplitude amounts to 80% of the mean tropospheric column.

Our retrievals provide good sensitivity up to 20 km, allowing to perform comparisons with ACE-FTS (Atmospheric Chemistry Experiment – Fourier Transform Spectrometer onboard the Canadian SCISAT satellite) measurements. 117 occultations recorded between 03/2004 and 05/2007 in the 41-51°N latitudinal belt provide information on the HCN distribution down to 7 km. 7-21 km ACE partial columns have therefore been

computed for comparison with the corresponding ISSJ time series. Results are respectively reproduced as black and red circles in the right frame of Figure 29 (while ISSJ a priori partial columns are reproduced in green). These two data sets are in excellent agreement in terms of absolute value, amplitude and phase of the seasonal modulation. An independent check has also been performed, using Jungfraujoch spectra of 2006-2007 and making no use of ACE inputs. This verification has further confirmed the excellent agreement noted above.

The Jungfraujoch time series for total and UTLS partial columns of HCN have been confronted to model calculations (GEOS-Chem global 3-D CTM, version 7.4.11, collaboration with the School of GeoSciences, University of Edinburgh, Edinburgh, UK). ACE-FTS data have also been included in the comparison. Figure 30 shows the comparison over the 2001-2006 time period between the model run (grey dots), Jungfraujoch (black dots) partial or total columns and ACE-FTS data (red dots).

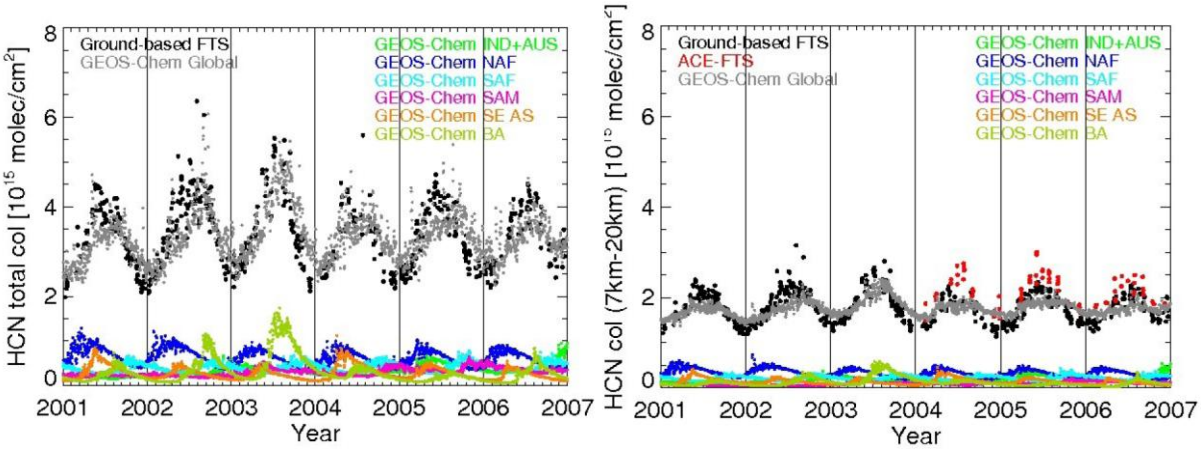

Figure 30 : Comparison between model (grey dots), Jungfraujoch FTIR (black dots) and ACE-FTS (red dots) column data [Li et al., 2009].

Also shown on the plots are the various contributions to the total or partial column values of GEOS-Chem, associated to biomass burning emissions in northern Africa (NAF), southern Africa (SAF), South America (SAM), Southeast Asia (SE AS) and boreal Asia (BA), with color codes identified in Figure 30. Emissions from Europe and northern America are an order of magnitude lower. The model simulation indicates that, globally, biomass burning emissions have reached 0.63 to 0.77 Tg N/yr in the 2001-2006 time frame. Although not displayed in Figure 30, emissions associated to domestic biofuel burning are also included in this study, they amount on average to 0.22 Tg N/yr and essentially originate from Asia. Regarding the sinks, the ocean uptake has been analyzed, its seasonal variation presents a maximum in September-December due to higher surface sea temperature in the southern hemisphere. Globally, we estimate the corresponding loss to 0.73 Tg N/year. The main atmospheric HCN sink has been evaluated using the most recent kinetic data for the HCN + OH chemical reaction, this loss corresponds to the removal of 0.12 Tg N/yr.

Figure 30 shows a very good agreement between GEOS-Chem and observations in terms of absolute values, strong seasonal modulations (amplitudes and phases) and interannual variability. Our study further indicates that the seasonal cycle above Jungfraujoch is primarily influenced by NAF and BA biomass burning emissions, with obvious impact of the strong 2002 and 2003 BA fire seasons on the total column measurements. Further details about these comparisons can be found in Li et al. [2009].

II.1.3.2.3 HCN above Ile de la Réunion

As outlined above, the retrieval of HCN is subject to relatively strong H_2O interferences. Therefore it was not certain from the beginning whether the retrieval strategies applied at the Jungfraujoch station could be successfully applied at the Reunion station.
One of the key features of the Jungfraujoch strategy was to expand and add certain micro-windows in order to include more H_2O (and H_2O isotopologue) lines, followed by a joint full profile retrieval of both HCN and H_2O. Applied to Reunion, this method failed to produce a meaningful result.
Instead, a two step method was applied in which the $H_2{}^{18}O$ profile was first determined from the 3299.0-3299.6 cm^{-1} microwindow ($H_2{}^{17}O$, H_2O and HCN as interfering species). After this, these individual profiles acted as the H_2O (and isotopologue) a-priori for each individual spectrum, the total columns of which are scaled during the HCN retrieval. The micro-windows and interfering species are listed in Table V.

Table V: Microwindows used for HCN retrieval at Ile de la Réunion

Limits (cm^{-1})	Interfering species
3268.0500 - 3268.4000	H_2O, $H_2{}^{18}O$, $H_2{}^{17}O$
3287.1000 - 3287.3500	H_2O
3299.4000 - 3299.6000	H_2O, $H_2{}^{18}O$, $_{C2H2}$

For the retrieval of HCN profiles, the HCN a priori vertical distribution as well as the diagonal elements of the a priori covariance matrix (S_a) in the 14-65 km altitude range have been derived from ACE FTS; a Gaussian inter-layer correlation with a 2.5 km width was added to S_a.

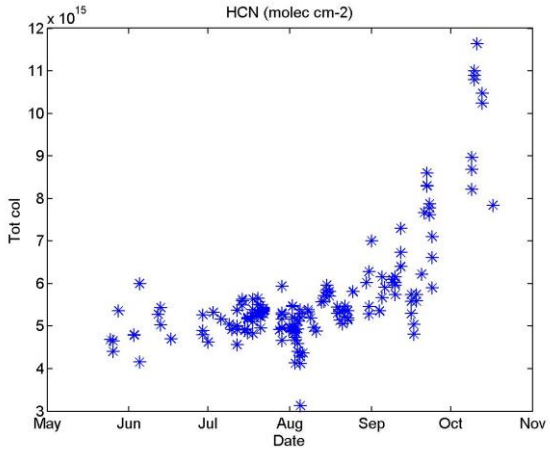

Figure 31: Time series of total columns of HCN during the 2007 campaign at Ile de La Réunion.

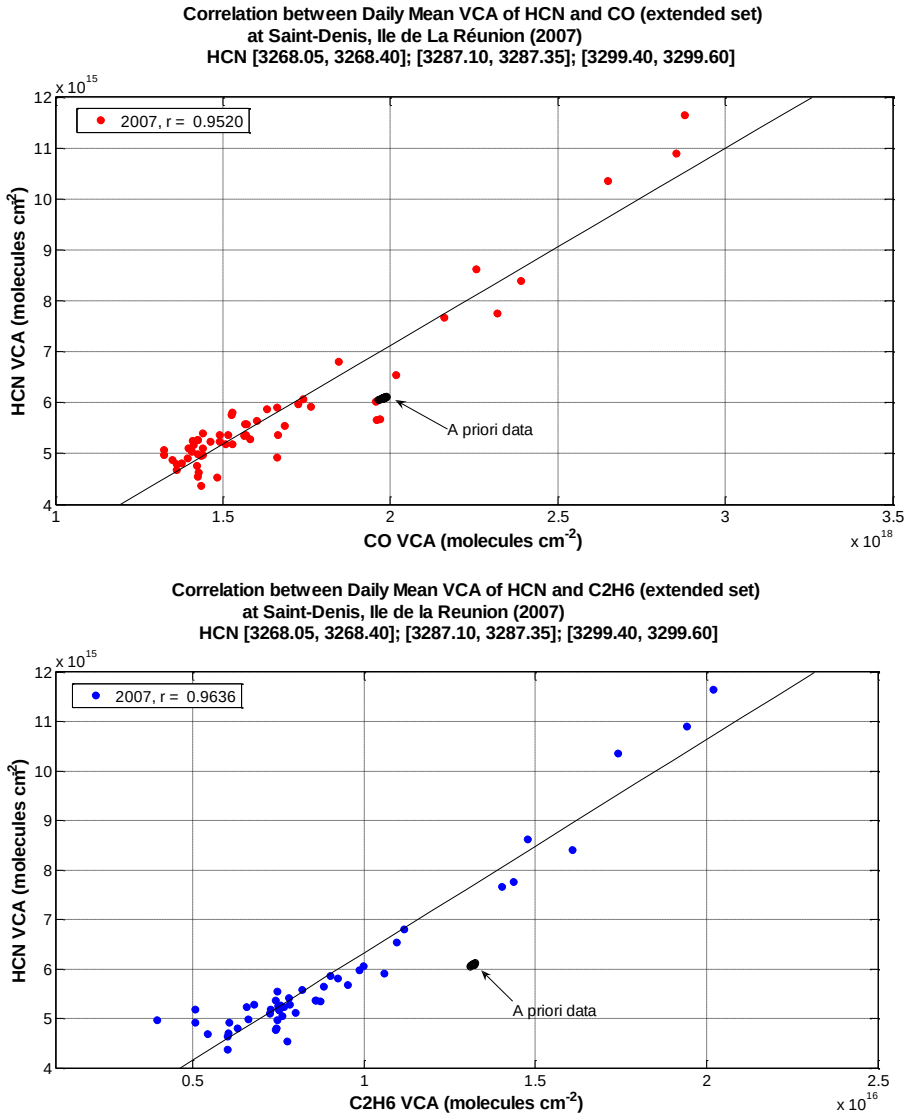

Figure 32 : Correlation of the observed total columns of HCN with CO (top) and with C_2H_6 (bottom) during the 2007 campaign at Ile de La Réunion.

Using this approach we obtain a mean DOF (2007 campaign) of 1.63 ± 0.14, and an average total column value of (5.68 ± 1.35) E+15 molec/cm^2 – see Figure 31. We also observe a strong correlation between HCN and CO (R=0.95, as shown in) and C_2H_6 (R=0.96) – see Figure 32 (as expected since HCN is strongly linked to biomass burning activities, as are the other species). The seasonal variation is dominated by the impact of the biomass burning season in the southern hemisphere (August – October).

In the frame of a publication about observations of biomass burning products at Ile de La Réunion, the retrieval strategy for HCN is being revised, and a complete error budget is being evaluated [Vigouroux et al., in preparation for publication in 2011].

II.1.3.3 Formaldehyde (HCHO)

II.1.3.3.1 Introduction

Formaldehyde (HCHO) is one of the most abundant carbonyl compounds and a central component of the oxidation of volatile organic compounds (VOC). Both NOx and VOC concentrations determine the production of ozone in the troposphere, a climate gas. The main sources of HCHO in the atmosphere are the photochemical oxidation of methane and non-methane volatile organic compounds (NMVOCs), among which are biogenic VOCs (isoprene), and anthropogenic hydrocarbons. HCHO is also released during biomass burning. The sinks of formaldehyde are photolysis, oxidation by OH and dry and wet deposition [Stavrakou et al., 2009a]. HCHO is a major source of CO. Due to its short lifetime of only a few hours, its global distribution closely resembles the distribution of its sources. Therefore, over land, observations of formaldehyde provide new constraints on the emissions of reactive NMVOCs (in particular isoprene), as demonstrated by several inverse modeling studies using satellite retrievals of HCHO [e.g., Abbott et al., 2003; Stavrakou et al., 2009b]. Far away from the emission regions, e.g. over oceans, formaldehyde observations might provide an opportunity to test our current knowledge regarding methane oxidation, and possibly also to quantify the effect of long-range transport of NMVOCs from source regions.

II.1.3.3.2 HCHO at Ukkel

Formaldehyde (HCHO) profiles and columns have been retrieved for some days in April-May 2007 ay Ukkel using ground-based MAXDOAS and FTIR observations performed during the dedicated measurements campaign – see AGACC07 Annex. A CIMEL photometer measuring the aerosol optical depth (AOD) and several meteorological instruments were also involved in this campaign. Hereafter, we report on

the MAXDOAS and FTIR HCHO retrievals and on the comparison between profiles and columns retrieved using both techniques.

MAXDOAS and FTIR capabilities for HCHO profile and column retrievals

Technical details about the retrieval strategies have been given in AGACC2007 – Annex. The information content has been characterized through the calculation of the averaging kernel matrices A for both MAXDOAS and FTIR retrievals. Typical examples of averaging kernels are presented in Figure 33.

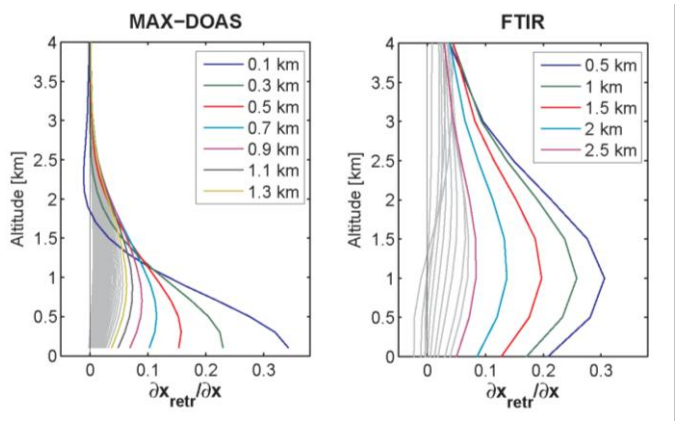

Figure 33: Averaging kernels obtained from MAXDOAS (left) and FTIR (right) HCHO retrievals in Ukkel on 15/04/2007 using measurements around 9:40h UT.

Most of the information on the vertical distribution of HCHO contained in the MAXDOAS and FTIR measurements is located below 1.5 km and 2.5 km of altitude, respectively. These plots also show that both techniques present some complementarities regarding the altitude range where they have their maximum of sensitivity to HCHO: mainly below 0.5 km for MAXDOAS and between 0.5 and 1.5 km for FTIR. Concerning the number of degrees of freedom for signal (trace of A), which represents the number of independent pieces of information contained in the measurements, it ranges from 1.2 to 1.7 for FTIR and from 1.2 to 1.5 for MAXDOAS. Figure 34 shows an example of HCHO profile retrievals from MAXDOAS measurements – presented as contour plots - on 15/04/2007 using all MAXDOAS scans below 85° SZA.

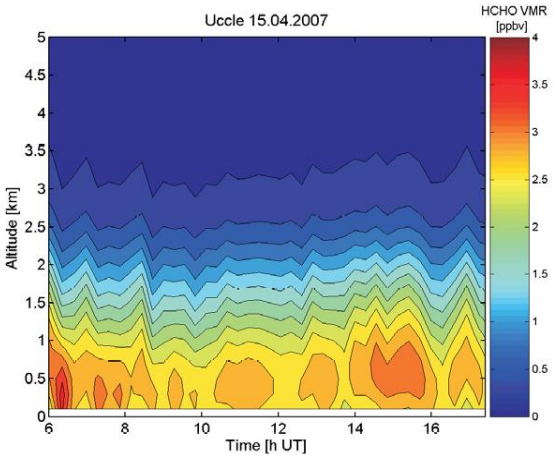

Figure 34: Contour plots of the HCHO profiles (in VMR) retrieved on 15/04/2007.

Observation results for HCHO profiles and columns in April-May 2007

Time-series of HCHO Differential Slant Column Densities (DSCDs) from MAXDOAS observations and maximum air temperature for the April-May 2007 period in Ukkel are presented in Figure 35. A clear correlation is found between high HCHO DSCDs and high temperature events. A possible explanation for this feature could be that the high temperatures combined to the high surface pressures observed during April-May 2007 in Belgium have favoured the accumulation of formaldehyde precursors (mainly hydrocarbons) and their confinement near the surface as well as their transformation into formaldehyde. Further investigations are needed to confirm this explanation.

As to the FTIR observations, we focused our analysis on five days during which the meteorological conditions allowed several successive measurements with the same instrumental setup. These days are the 15th, 16th, 21st and 22nd of April 2007 and the 1st of May for which 25, 17, 12, 18 and 10 spectra are recorded, respectively. The obtained degree of freedom on the retrieved HCHO profile lies between 1.2 and 1.7, and the estimated error on the HCHO total column is about 20%.

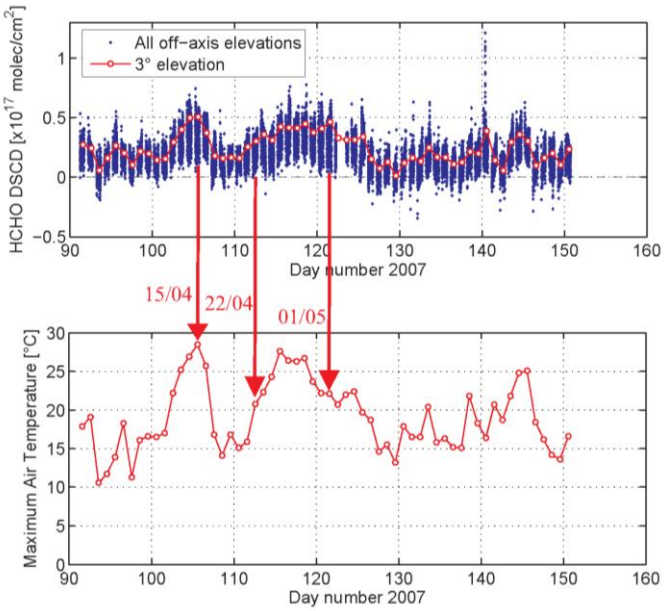

Figure 35: Time series of HCHO DSCDs from MAXDOAS observations (upper plot) and maximum air temperature (lower plot; data from KMI-IRM) in Ukkel for the April-May 2007 period. In the upper plot, blue dots correspond to DSCDs at all elevation angles except zenith (reference) and the red dots are the daily averages of HCHO DSCDs at 3° of elevation.

Figure 36 shows the comparison between HCHO total column amounts calculated from MAXDOAS and FTIR profiles for three selected clear-sky days (April 15 and 22, and May 1, 2007). On 22/04/2007 and 01/05/2007, a very good agreement is found between both techniques with relative differences generally smaller than 9 % and never larger than 13 %. We see also that MAXDOAS and FTIR total columns display almost identical short-term variations. On 15/04/2007, larger discrepancies are obtained, especially in the afternoon where FTIR gives significantly larger column values (up to +38 %) than MAXDOAS. Different sensitivity tests have shown that the FTIR retrieval settings and the impact on the MAXDOAS retrieval of the assumption made on the aerosol loading cannot explain this feature. Since in the afternoon, the MAXDOAS and FTIR instruments are pointing in opposite direction (NE for MAXDOAS and SW for FTIR), we cannot exclude that both instruments probe air masses with very different HCHO content: due to the presence of a large forest area in the South of Ukkel and the high air temperature observed on 15/04/2007 (see Figure 35), large biogenic emissions of HCHO could occur, and with favourable wind direction and speed, would only be detected by the FTIR instrument. We will investigate on this scenario in the near future using tropospheric modelling studies. Concerning the comparison with SCIAMACHY, a very good agreement is obtained on both 15/04/2007 and 01/05/2007. It is also interesting to note that the FTIR data also show a strong correlation between HCHO total column and precipitable water.

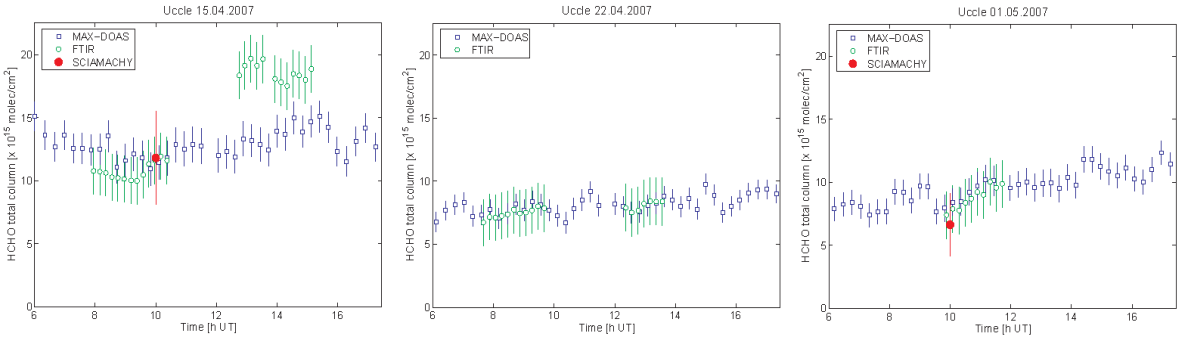

Figure 36: Comparison between MAXDOAS and FTIR HCHO total columns in Ukkel on 15/04/2007 (left plot), 22/04/2007 (middle plot), and 01/05/2007 (right plot). When data exist, the SCIAMACHY nadir column amount corresponding to the daily average of all pixels falling within a radius of 500 km around Ukkel also appears in the plots.

Figure 37 shows examples of comparison results between coincident (time difference smaller than five minutes) FTIR and MAXDOAS profiles on 15/04/2007 and 22/04/2007. As expected from the total column comparisons, a very good agreement is found between FTIR and MAXDOAS HCHO profiles on 22/04/2007. On 15/04/2007, the afternoon example shows that the FTIR profile is significantly higher than the MAXDOAS one on the whole 0-5 km altitude range. Concerning the morning comparison, the opposite feature is obtained in the 0-2 km altitude range with MAXDOAS profile higher than FTIR. Above 2 km, a good agreement is found between both profiles. The comparison between profiles retrieved on 15/04 and 22/04/2007 also shows that significantly larger HCHO concentrations are obtained on 15/04/2007 up to 3 km altitude and not only in atmospheric layers close to the ground.

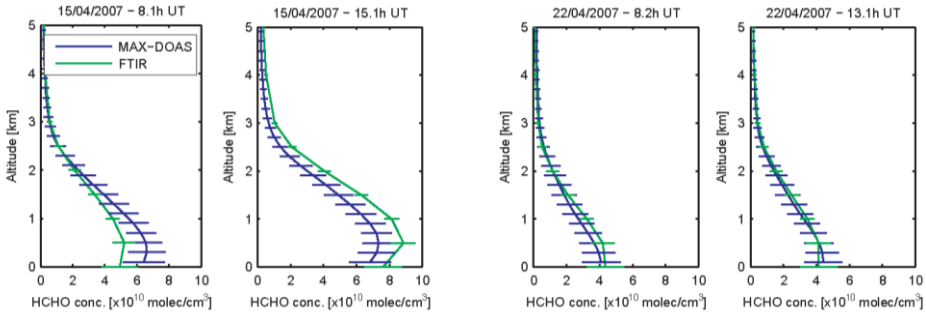

Figure 37**:** Comparison between coincident MAXDOAS and FTIR HCHO profiles in Ukkel on 15/04/2007 (left) and 22/04/2007 (right). The error bars on the profiles correspond to the total retrieval errors.

II.1.3.3.3 HCHO at Jungfraujoch

At the Jungfraujoch high-altitude site, even the most favorable IR absorptions of HCHO are very weak. Up to now, reliable formaldehyde retrievals were only possible using averaged spectra, thus preventing proper characterization of its variability and the production of data for validation. Specific efforts have been undertaken to improve the signal-to-noise ratio (S/N) of the solar observations, with the hope to be able to retrieve

HCHO total columns from individual spectra, with good precision. An experimental setup based on a tunable optical filter covering here the 2810 to 2850 cm^{-1} spectral range has been tested. The combination of a narrower interval with a larger aperture has allowed improving the S/N by more than a factor 4, with the resolution unchanged.

The specific experimental setup has been regularly used since December 2005, allowing to record more than 1600 atmospheric spectra. Retrievals have been performed using SFIT-2 (v3.91), HITRAN-2004, a microwindow extending from 2833.07 to 2833.35 cm^{-1} and encompassing a single HCHO line at 2833.19 cm^{-1}. Interferences by HDO, CH_4 and O_3 have to be accounted for. HCHO total columns have been retrieved for the December 2005 to December 2010 time period (see Figure 38) These first results indicate that: (i) minimum values of about $3x10^{14}$ molec./cm^2 are found in February-March; (ii) higher columns ranging up to $1x10^{15}$ molec./cm^2 are observed during summer; (iii) summer is characterized by higher variability; (iv) two strong pollution events were detected on 27 July 2006 and 6 August 2008, with HCHO column about 10 times higher than expected.

The precision achieved on a single measurement has been estimated from inter-spectra variability, to about 10%.

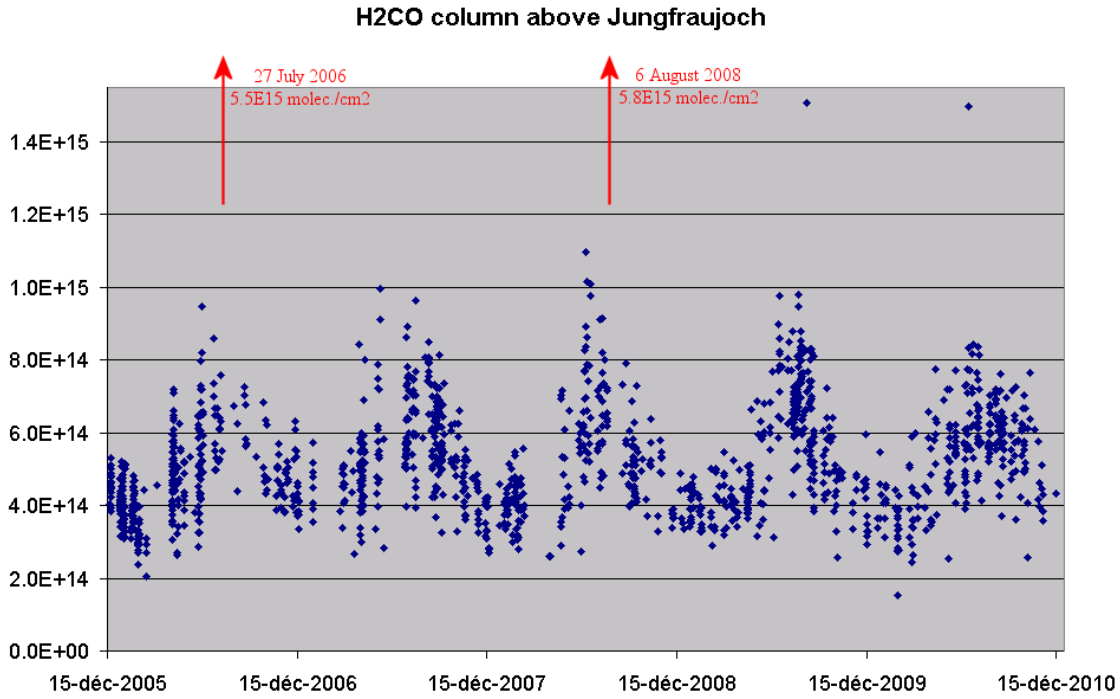

Figure 38: Timeseries of formaldehyde total columns above the Jungfraujoch station.

II.1.3.3.4 HCHO at Ile de la Réunion

Introduction

At Reunion Island in the Indian Ocean, methane oxidation is the dominant formaldehyde source. However, it is located only 700 km from the East coast of Madagascar and about 2000 km from southeastern Africa, a region with large biogenic NMVOC emissions as well as extensive vegetation fires during the May-November period. Although formaldehyde itself has a too short lifetime (a few hours) to be directly transported over such distances, pyrogenic and biogenic NMVOC precursors (e.g. ethane, methanol, acetic acid, etc.) and oxidation products (e.g. certain organic nitrates, hydroperoxides, etc.) can be transported to Réunion Island and lead to enhanced formaldehyde formation.

Three measurement campaigns have been performed at Saint-Denis in order to prepare for the quasi-continuous observations, that started in May 2009. During the second campaign (August-October 2004), HCHO has been measured both by Fourier Transform InfraRed (FTIR) and Multi-Axis Differential Absorption Spectroscopy (MAXDOAS) techniques. As the measurement of HCHO is a challenge, it is very interesting to compare the results obtained by two independent measurements, as was done also at Ukkel. The ground-based total column data of HCHO are also compared to satellite products retrieved at BIRA-IASB from GOME/ERS-2 (2002) and SCIAMACHY/ENVISAT (2004 and 2007), and to simulations from the 3D chemistry transport model IMAGES. At last, we used FLEXPART results to help us identify events impacted by long-range transport.

All details of the work can be found in Vigouroux et al. [2009] where we focused on the 2004 and 2007 data. Since that publication, the FTIR data since May 2009 up to end of 2010 have also been analysed for HCHO. Small modifications have been made to the retrieval strategy described in the paper (cf. Table VI of the present report). The a priori profiles of the interfering species are not anymore the daily means of preliminary retrievals, but the individual retrieved profiles (i.e, a different a priori profile per spectrum). Therefore, we had to select other microwindows for the retrievals of $H_2{}^{16}O$ and HDO (2924.10 - 2924.32 and 2855.65 - 2856.4 cm^{-1}, respectively) because the lines used in Vigouroux et al. [2009] were saturated for the high solar zenith angles spectra. Then, the HDO microwindow, now fitted prior to the target retrieval, was removed from the set of six microwindows used for HCHO in the paper (Table VI). Our FTIR time-series for HCHO have been sent to Eloise Marais, from Harvard University, for comparisons with OMI data above the African continent for the period 2005-2009.

Spectral data analysis and characterization of the information content

The retrieval strategies for HCHO from MAXDOAS and FTIR observations developed at Ukkel have been revised for Ile de La Réunion because of the different atmospheric conditions. The FTIR retrievals have been performed with SFIT-2; the microwindows are listed in Table VI : the upper windows are used to first retrieve the interfering species; the lower ones to fit HCHO itself. The spectroscopy has been taken from HITRAN2004, except for the lines of HCHO for which we used the recent linelist from Perrin et al. (2009). The a priori profile for both the FTIR and MAXDOAS retrievals is the same: it has been constructed (1) from aircraft data from the PEM-Tropics-B campaign, from the ground to 12 km, (2) from the IMAGES model between 12 and 20 km, and (3) based on MIPAS data in the upper atmosphere. In the FTIR profile retrieval, we used a Tikhonov L1 regularization.
The MAXDOAS measurements have been made in the period August 2004 – July 2005, at the following elevation angles: 0, 3, 6, 10, 18, and 90° (zenith). The retrieval of HCHO is done in the 336-358 nm wavelength range, taking into account the spectral signature of O_3, NO_2, BrO, the collision pair of oxygen molecules O_4, and the Ring effect. The cross-sections for HCHO are taken from Meller and Moortgat [2000]. The retrievals are made using the WinDOAS software [Van Roozendael et al., 1999], using OEM [Rodgers, 2000].

Since the light path of the different off-axis directions is strongly dependent on aerosols, a good estimate of the aerosol extinction profile is required to calculate accurate HCHO weighting functions for vertical profile retrieval. For this purpose, we have used MAXDOAS measurements of the oxygen collision complex O_4 similarly to Heckel et al. [2005]. Ideally, an aerosol extinction profile should be retrieved at each MAXDOAS scan since the aerosol loading can vary during the day. However, using the RTM UVspec/DISORT, this would require unrealistically large computing time. Therefore, we derive a mean aerosol profile for each selected clear-sky morning or afternoon using a look-up table (LUT) approach like in Irie et al. [2008]. This could in the future be improved by exploiting the newly developed algorithm for aerosol retrieval (Section II.1.2.3.3). Figure 39 and Figure 40 show the averaging kernels that were obtained for the FTIR and MAXDOAS retrievals, respectively.

Table VI: Microwindows (in cm^{-1}) used for the independent retrievals of H_2O, HDO, CH_4, N_2O, and HCHO, in Vigouroux et al. (2009). The retrieved profiles of the first four compounds are used as a priori profiles in the retrievals of HCHO.

Target gas	Microwindows (cm^{-1})	Interfering species
H_2O	2925.10 – 2925.30	CH_4
	2941.60 – 2941.90	CH_4, O_3, solar CO
HDO	2660.00 – 2661.20	CH_4, CO_2
CH_4	2613.70 – 2615.40	HDO, CO_2
	2650.60 – 2651.30	HDO, CO_2
	2835.50 – 2835.80	HDO
	2903.60 – 2904.03	HDO, H_2O
	2921.00 – 2921.60	HDO, H_2O
N_2O	2806.20 – 2806.48	
HCHO	2763.425 – 2763.600	CH_4, HDO, N_2O, O_3, CO_2 solar CO
	2765.725 – 2765.975	CH_4, HDO, N_2O, O_3, CO_2 solar CO
	2778.200 – 2778.590	CH_4, HDO, N_2O, O_3, CO_2 solar CO
	2780.800 – 2781.150	CH_4, HDO, N_2O, O_3, CO_2 solar CO
	2810.000 – 2810.350	CH_4, HDO, N_2O, O_3 solar CO
	2855.650 – 2856.400	CH_4, HDO, H_2O, O_3, CO_2, solar CO

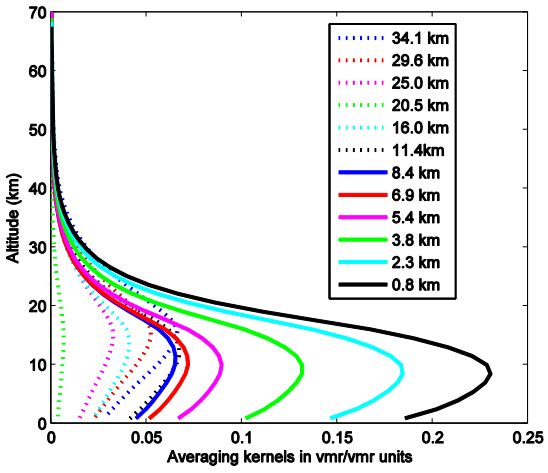

Figure 39 : FTIR volume mixing ratio averaging kernels (ppv/ppv) for the altitudes listed in the legend

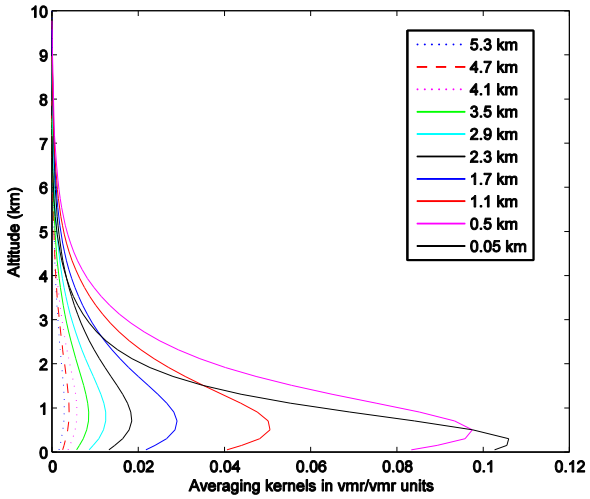

Figure 40 : Averaging kernels (ppv/ppv) obtained for MAXDOAS observations of HCHO at Réunion Island on 26/08/2004 (morning) using measurements at all elevation angles at a sola zenith angle of about 64°

For the FTIR retrievals, we obtain a mean DOFS of 1.1 and its standard deviation (1σ) for all measurements at different solar zenith angles (SZA) is 0.1. The retrieved profile is sensitive only to a change in the true profile that occurs between the ground and about 20 km, with a maximum of sensitivity around 10 km. For the MAXDOAS retrievals, we see that, according to the observation geometry, most of the information on the vertical distribution of HCHO contained in the measurements is located below 2.5 km of altitude. The trace of A (DOFS) is 0.7 ± 0.1 on average for a scan. Both observation techniques are therefore complementary to a certain extent.

A complete error budget of the retrievals has also been evaluated and has been taken into account in the comparisons mutually and with the satellite and model data, see Vigouroux et al. [2009].

In the next discussions of the geophysical results, we will also use SCIAMACHY and model IMAGES v2 data for HCHO: the SCIAMACHY data are described in detail in De Smedt et al. [2008]; the global IMAGESv2 chemistry-transport model (CTM) is an updated version of the IMAGES model, in which the NMVOC chemical mechanism has been revised in order to provide a more reliable representation of the formaldehyde produced by pyrogenic and biogenic hydrocarbon emissions [Stavrakou et al., 2009a]. Two different versions of the model have been run: the standard version (S1) and a version (S2) in which prescribed monthly mean climatological OH fields from Spivakovsky et al. [2000] are used to test the influence of OH on the calculated HCHO columns.

Diurnal, seasonal and interannual variations of HCHO above Réunion

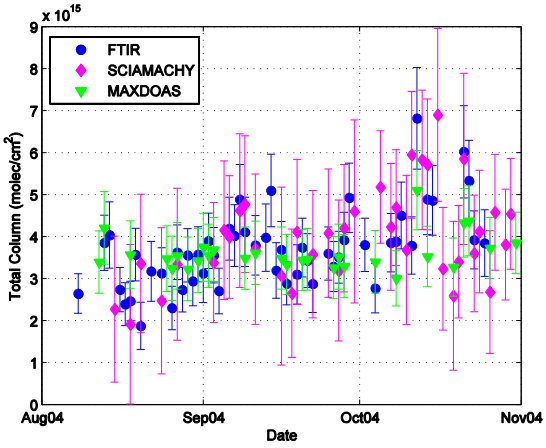

Figure 41 : Daily means of formaldehyde total columns above Saint-Denis from FTIR, MAXDOAS and SCIAMACHY measurements during the 2004 campaign.

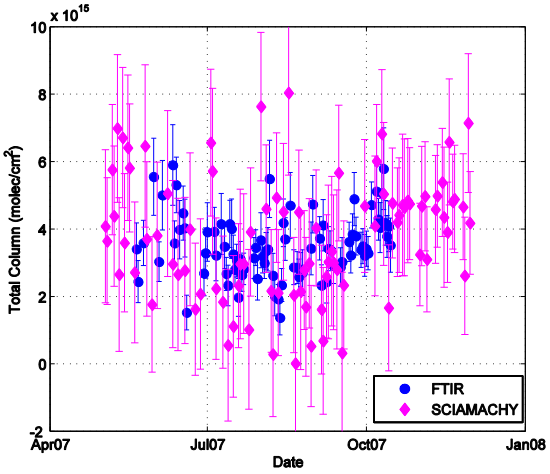

Figure 42 : Formaldehyde daily mean FTIR total columns and daily averaged SCIAMACHY columns in a region of 500 km around Saint-Denis during the 2007 campaign.

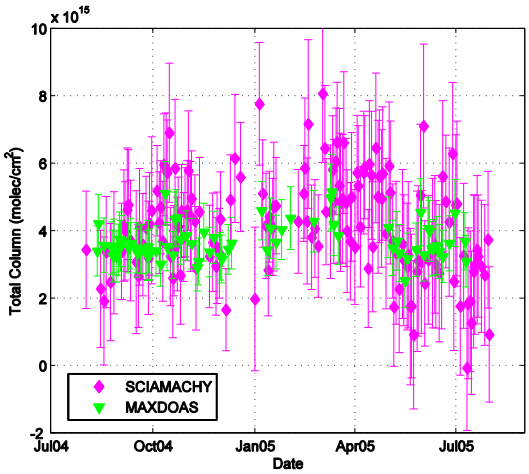

Figure 43 : Daily means of formaldehyde total columns above Saint-Denis from MAXDOAS and SCIAMACHY measurements from August 2004 to August 2005.

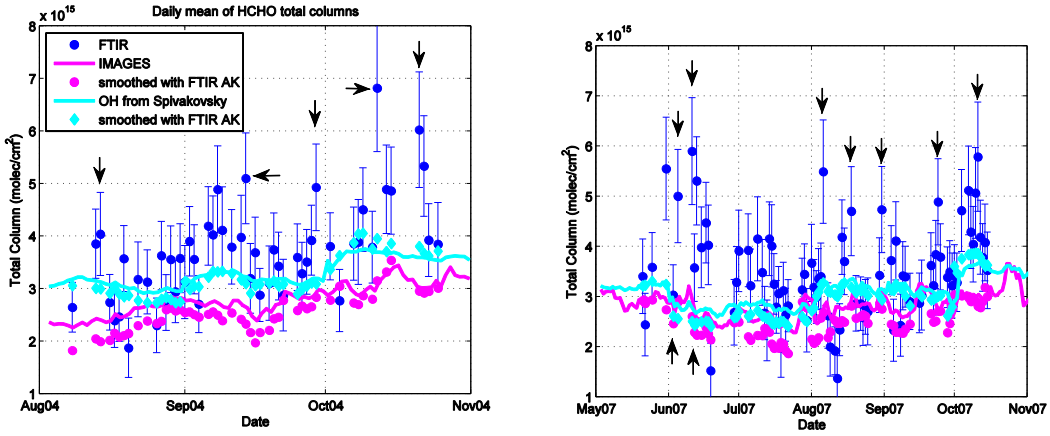

Figure 44 : FTIR and IMAGESv2 formaldehyde total columns during the two FTIR campaigns in 2004 (left) and 2007 (right). The arrows correspond to dates mentioned in the discussion (Sect. 7) : the 14th August, 14th and 29th September, 12th and 21th October 2004 (left plot) ; and the 3rd, 5th, 11th and 12th June, 6th, 18th, and 31th August, 24th September, and 11th October 2007 (right plot).

Figure 41 to Figure 45 show the time series of formaldehyde obtained in 2004-2005 and 2007 including all data sources; the error bars represent the total error on each data point. The model data have been plotted once directly, at the model resolution, once after smoothing with the FTIR or MAXDOAS averaging kernels (AK).

First, we observe a good agreement between all experimental data, taking into account the errors, and especially the smoothing error that represents the effect of the different vertical resolutions and sensitivities of the instruments. A quantitative statistical evaluation of the differences has demonstrated that the experimental data sets agree within their error bars. The situation is slightly different when one compares with the model data (after smoothing): the model slightly underestimates the columns, it shows less day-to-day variations and does not capture the events with large column abundances (indicated by the arrows in Figure 44).

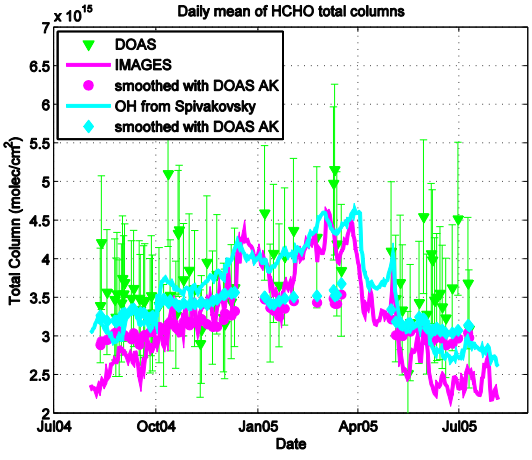

Figure 45 : MAXDOAS and IMAGESv2 formaldehyde total columns.

Second, we observe a clear seasonal cycle with a minimum in local winter, which is due primarily to the lower radiation and humidity levels prevailing during this period, which lead to lower OH concentrations and therefore to lower methane oxidation rates. The model predicts a maximum of formaldehyde in January–March (Figure 45), also found in the MAXDOAS and SCIAMACHY measurements (Figure 43). The amplitude of the seasonal cycle appears slightly smaller in the MAXDOAS measurements: this is due to its lower information content. A maximum in February is also seen in FTIR measurements in 2010 (Figure 46), but unfortunately only few data are available.

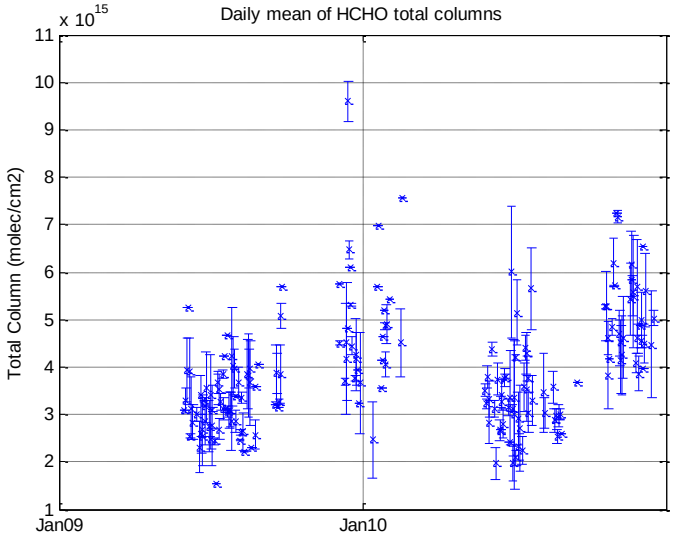

Figure 46 : FTIR daily means of formaldehyde total columns at Saint-Denis in 2009-2010. Error bars are the standard deviations of the daily means.

Third, we observe a fairly clear diurnal cycle: Figure 47 shows the diurnal cycle obtained from FTIR and MAXDOAS measurements at Réunion Island.

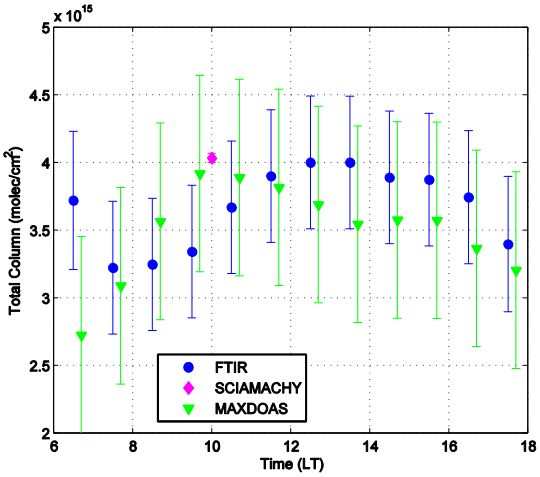

Figure 47 : Diurnal cycle obtained from FTIR and MAXDOAS measurements at Ile de la Réunion

Each data point at a given hour (from 6.5 a.m. local time (LT) to 5.5 p.m.) is the mean of all the retrieved total columns within 1 hour (during the two campaigns 2004 and 2007 for FTIR, and during the whole campaign 2004-2005 for DOAS). The diurnal cycle obtained with the FTIR measurements shows a maximum at about 13:00 LT, and a minimum at early morning (7:30 to 8:30 LT). The MAXDOAS measurements also show an increase during the morning and a decrease in the middle afternoon. The diurnal cycle comes from the fact that deposition is the only active process during the night. This leads to net destruction of formaldehyde during nighttime. During the day this loss and the additional photochemical removal processes are compensated by photochemical oxidation of methane and NMOVCs which produce formaldehyde. Therefore, a diurnal cycle is expected. This is also reproduced by the model IMAGES (S1), but with a much lower amplitude.

Fourth, the observed total columns show a high day-to-day variability (Figure 41 and Figure 42), which is not captured by the model. The large temporal variability of FTIR formaldehyde columns might be partly elucidated by their good correlation (0.7) with CO total columns measured with the same instrument [Senten et al., 2008] during the period from August to November, when the fire season is at its maximum in southeastern Africa and Madagascar. This result suggests that long-range transport of HCHO precursors from these regions can explain the large temporal variability of observed HCHO columns. To assess the role of long-range transport on the observations at Réunion Island, we used the Lagrangian particle dispersion model FLEXPART v.6.2 [Stohl et al., 2005]. One of the major uncertainties in FLEXPART simulations is the emission injection height. At Réunion Island, the dominant transport pathway at low altitudes (below 4 km during most of the fire season) originates from the South-East. At these low altitudes, African-Madagascar emissions reach Réunion Island only via a roundabout way. Given the short lifetime of HCHO and of its pyrogenic precursors that could be emitted by fires (a few hours to a few days) it is unlikely that these pathways contribute significantly to the observed HCHO concentrations. Above 4 km, the air masses generally take a direct eastward pathway and any African-Madagascar emissions that reach this altitude band are transported within a short timeframe towards Réunion Island. It was found that the best correlation between the observed HCHO and simulated tracer data with FLEXPART was obtained when restricting the runtime to ≅ 1 day and by allowing emission into the 4-6 km altitude layer. Within the 1 day backward trajectory, the FLEXPART simulations indicate that emissions / transport originate from Madagascar only. Longer runtimes yielded lower correlations, indicating that sources further inland do not significantly contribute to the observations at Réunion Island. Under these conditions, we can fairly well reproduce the high HCHO enhancements and their day-to-day variability in the burning season observed in the FTIR data. The general underestimation of the modeled columns against FTIR measurements (by ca.

25% on average) and the fact that IMAGES does not so well reproduce the day-to-day variations would therefore reflect either an underestimation of pyrogenic and biogenic NMVOC emissions in Southeast Africa and Madagascar in the model, as indicated by an inverse modeling study based on SCIAMACHY data [Stavrakou et al., 2009], or an underestimation of the role of long-range transport from these source regions to the measurement site. Uncertainties in the determination of OH concentrations in the model may possibly contribute to the underestimation.

II.1.3.4 Methane (CH_4) and its isotopologues

II.1.3.4.1 Introduction

Methane (CH_4) is the third most important greenhouse gas, after water vapour and carbon dioxide. Due to its high warming potential and its relatively long chemical lifetime (8-10 years), atmospheric methane plays a major role in the radiative forcing responsible of the greenhouse effect. Natural processes (e.g. wetlands, termites) as well as anthropogenic activities (e.g. fossil fuel exploitation, rice agriculture, biomass burning, etc.) release methane in the atmosphere. Methane is removed from the troposphere via oxidation by OH, leading to HCHO, CO, and, in high NOx environments, to O_3. In the stratosphere, methane oxidation by OH forms water vapour. Therefore methane also affects climate by influencing tropospheric ozone and stratospheric water.

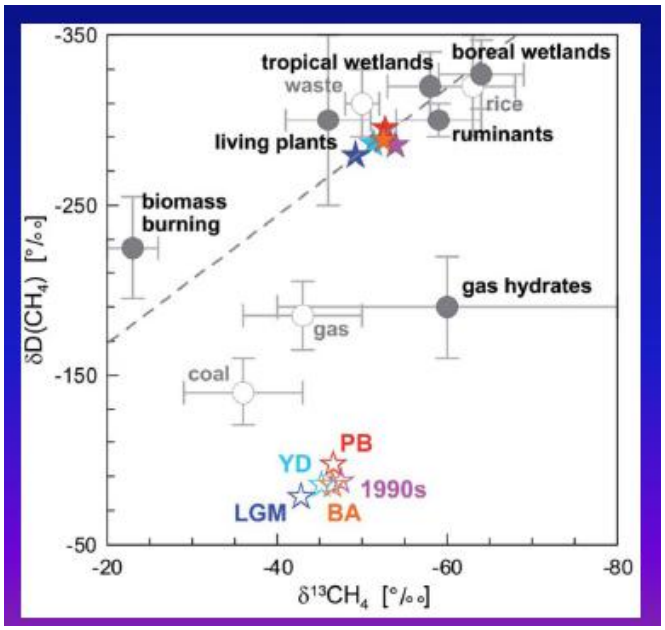

Figure 48 : Typical carbon and hydrogen isotopic signatures of different CH4 sources used in the Monte Carlo model. (From Fischer et al. [2008])
Mainly anthropogenic sources are indicated by open circles, mainly natural sources by dark grey dots. The error bars indicate the spread of reported values10. No δD values for plant emissions are available so far. Open stars indicate the modelled average atmospheric δ^{13}CH4 and δD(CH4) for the 1990s, preboreal Holocene (PB), Younger Dryas (YD), Bølling/Allerød (BA) and Last Glacial Maximum (LGM). Filled stars represent best-guess model estimates for average δ^{13}CH4 and δD(CH4) emitted, where we limited atmospheric lifetimes to values larger than 5 yr. The dashed line represents a linear fit through these isotopic emission averages. δD = [(D/H)sample/ (D/H)standard]-1 in ‰, where standard is standard mean ocean water (SMOW); $\delta^{13}C = [(^{13}C/^{12}C)sample/(^{13}C/^{12}C)standard]-1$ in ‰, where standard is Vienna PeeDee belemnite (VPDB).

The cycle of methane is complex and to understand it a complete study of its sources and sinks, including its main isotopologues, has to be made. Measurements of the

$^{13}C/^{12}C$ isotopic ratio and of the D/H ratio are useful to differentiate between various biological and fossil fuel related sources of atmospheric methane, as illustrated in Figure 48.

Biogenic sources tend to favour the production of lighter elements but not in all cases: some sources tend to favour CH_3D over CH_4. Measurements of atmospheric $^{12}CH_4$ and $^{13}CH_4$ and of CH_3D can therefore be used to investigate individual source strengths as well as their spatial and temporal distributions, and to help models to constrain estimates of the global methane budget.

II.1.3.4.2 Retrieval of $^{12}CH_4$ and $^{13}CH_4$ above Jungfraujoch

Several retrieval strategies of the $^{12}CH_4$ and $^{13}CH_4$ methane isotopologues have been investigated in AGACC. Finally, the best results maximizing the information content while avoiding oscillations in the vertical distributions were obtained for both species by using a Tikhonov L_1 regularization scheme [Duchatelet et al., 2009]. Microwindows used as well as ancillary informations about the retrieved products are summarized in Table VII. The official 2004 version of the HITRAN line parameter compilation [Rothman et al., 2005] has been used for the $^{13}CH_4$ retrievals. For the main isotopologue, HITRAN 2004 including updates derived from laboratory measurements has been assumed [Duchatelet et al., 2008].

Table VII : Microwindows selected for the retrievals of $^{12}CH_4$ and $^{13}CH_4$. The statistics (mean ± 1σ) provided for the degree of freedom for signal (DOFS) were derived from the whole time series (1998-2008). Total errors affecting the total columns are equal to 1 and 6%, respectively for $^{12}CH_4$ and $^{13}CH_4$.

Microwindow range (cm^{-1})	Interfering species	Mean DOFS	Typical partial column limits and associated error
$^{12}CH_4$			
2613.70 – 2615.40	HDO, CO_2, solar lines	2.47 ± 0.20	[3.58 – 7] km (2%) [7 – 17] km (1.5 %)
2650.60 – 2651.30	HDO, CO_2		
2835.50 – 2835.80	None		
2903.60 – 2904.03	NO_2		
2921.00 – 2921.60	HDO, NO_2		
$^{13}CH_4$			
1234.04 – 1234.44	$^{12}CH_4$, $^{13}CO_2$, COF_2	1.57 ± 0.29	[3.58 – 18] km (7%)

Time series of $^{12}CH_4$ and $^{13}CH_4$ have been produced, using all available Jungfraujoch observations recorded with the Bruker instrument from 1998 to 2008, inclusive. The

two upper panels of Figure 49 display partial column daily means computed in the 6 – 18 km altitude range. The lower panel shows the $\delta^{13}C$ time series, with $\delta^{13}C$ defined as:

$$\delta^{13}C = \left(\frac{(^{13}CH_4 / ^{12}CH_4)_{meas}}{(^{13}CH_4 / ^{12}CH_4)_{std}} - 1 \right) \times 1000$$

where the accepted value for the standard $^{13}CH_4/^{12}CH_4$ ratio is 0.0112372 (Vienna Pedee Belemnite). To our knowledge, it is the first time that a $\delta^{13}C$ data set is derived from ground-based FTIR observations. The three time series have been fitted using a first order polynomial and a Fourier series including four first harmonics (solid lines on each panel). This helps appraising the seasonal variations affecting the three ensembles.

The mean $\delta^{13}C$ value computed over the whole Jungfraujoch time series is equal to (-48.4 $\pm$ 9.1) ‰, it agrees well with experimental values deduced from ground-based or aircraft in situ sampling reported in the literature (generally close to -47 ‰ at ground level, see e.g. Miller et al. [2002]. The seasonal variations affecting the data sets have been evaluated after removal of the linear components deduced from the fits reproduced in Figure 49. For $\delta^{13}C$ and after combination over a 1-year time period, the seasonal cycle exhibits a significant peak-to-peak amplitude of 10 ‰, with a maximum found in July/August and a minimum in winter (December-January). Although the phase of this modulation is in agreement with previous results, e.g. Bergamaschi et al. [2000], its amplitude is 10 times larger. Model comparisons will be performed to determine if the fact that our FTIR measurements focus on the UTLS region of the atmosphere (6-18 km) is responsible for the discrepancy on the signal amplitude.

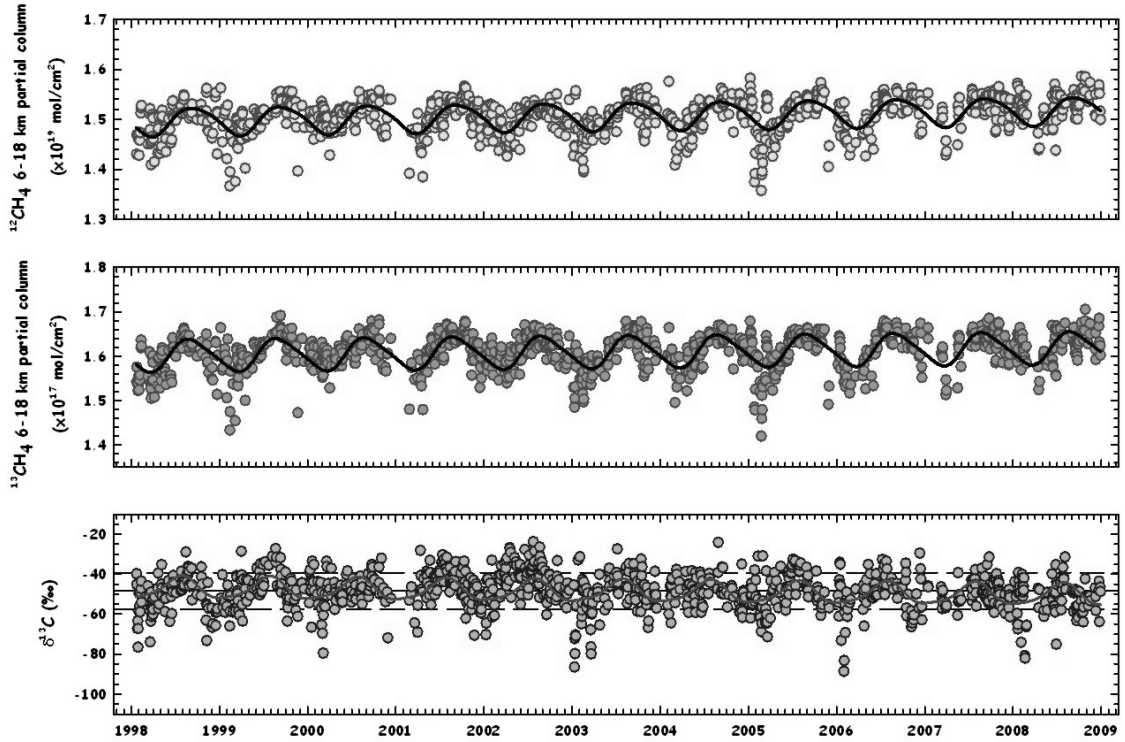

Figure 49 : Time series of daily mean partial columns (6-18 km) for $^{12}CH_4$ (top panel) and $^{13}CH_4$ (middle panel). The lower panel shows the $\delta^{13}C$ dataset, with the mean value and corresponding 1-σ standard deviation, computed over the whole time series, reproduced as solid and dotted lines, respectively.

$^{13}CH_4$ partial columns obtained with the AGACC strategy have been compared to daily mean values derived from occultation measurements performed from February 2004 to July 2008 by the ACE-FTS instrument in the [41-51]ºN latitudinal belt. The comparisons have been performed in the 6 – 18 km altitude range, where a good sensitivity is available for both experiments. Figure 50 reproduces the 41 ACE-FTS data points as dark and light blue circles, with the latter identifying the 13 days for which coincident Jungfraujoch measurements (in yellow) are available. Relative differences between Jungfraujoch FTIR and ACE-FTS time series are reproduced for coincident days on top panel of Figure 50. An excellent agreement is observed, with maximum differences always lower than 10%, with a mean non significant bias of -0.18 $\pm$ 3.19 % (1-σ).

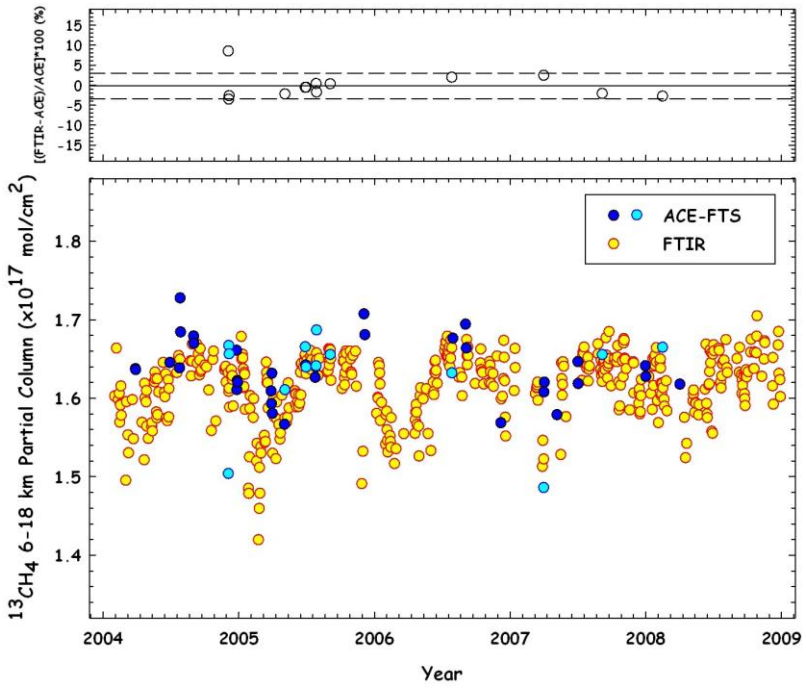

Figure 50 : Comparison between the ACE-FTS and Jungfraujoch FTIR daily mean $^{13}CH_4$ 6-18 km partial column time series. Top panel shows relative difference for coincident days

Finally, we have analyzed the evolution with time of both $^{12}CH_4$ and $^{13}CH_4$ amounts, based on their long-term (1985-2009) total column time series derived with the retrieval strategies described in Table VII. Both $^{12}CH_4$ and $^{13}CH_4$ datasets indicate a strong increase until the end of the nineties, followed by a significant slowdown between years 2000 and 2005. Since then, atmospheric methane is on the rise again. Present $^{12}CH_4$ total column abundances are about 40% higher than those derived from pioneering observations performed at the same site in 1950-1951.The temporal evolutions of $^{12}CH_4$ and $^{13}CH_4$ growth rates are plotted in Figure 40 (as blue and red dots, respectively). Error bars correspond to 2-σ uncertainties. Similar behaviors are observed for both isotopologues. In particular, the only significant decrease in atmospheric methane burden is observed when considering the 1999-2003 time period. In the future, additional FTIR observations are definitely necessary to assess if the upward trend currently observed is the beginning of a new rapid growth era for methane.

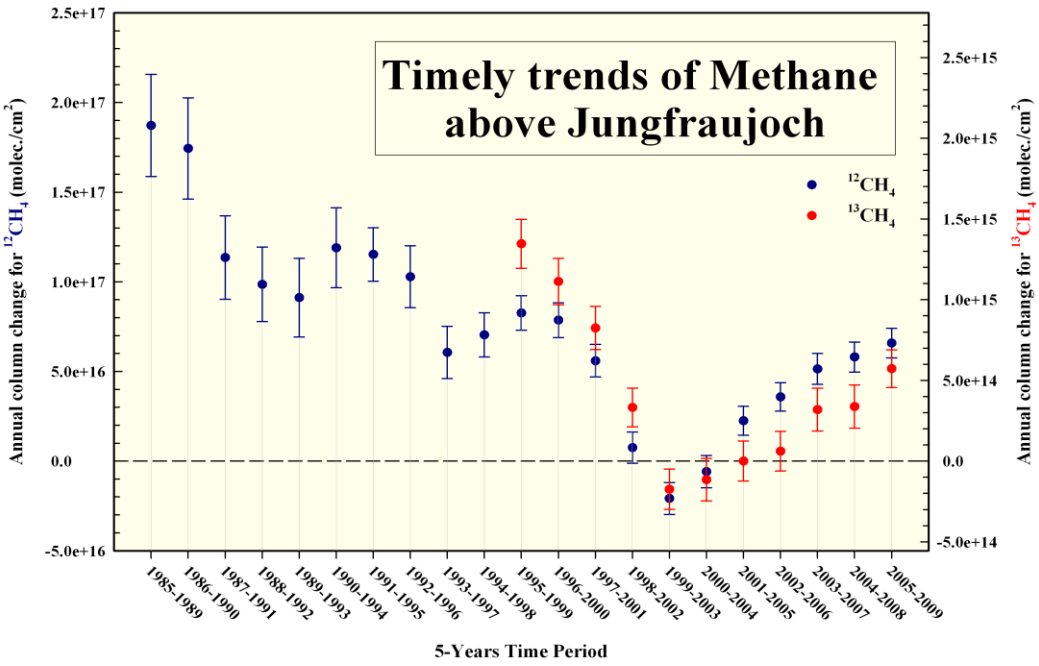

Figure 51 : Annual change in total column of $^{12}CH_4$ (blue dots) and $^{13}CH_4$ (red dots) for successive 5 years time periods.

II.1.3.4.3 CH_3D at Jungfraujoch

Retrievals of CH_3D are more difficult than those of $^{13}CH_4$. Four microwindows were identified early in AGACC (see AGACC2007 Annex), but unfortunately 3 of them are polluted by interfering absorptions due to water vapour or HDO. Hence they may not be usable at low altitude and latitude FTIR ground-based stations. It was therefore important to check if the use of the sole microwindow not affected by water vapour could provide enough information. We have compared the information content related to three different fitting procedures: (i) the use of this microwindow in a single spectrum fitting procedure; (ii) its use in a multi-spectra fitting procedure; (iii) the simultaneous use of the four microwindows in a single spectrum fitting procedure. The multi-spectra approach consists of combining several FTIR spectra recorded during the same day and at the same spectral resolution to increase the information content (Duchatelet et al., 2009).

Figure 52 plots daily means CH_3D total columns above Jungfraujoch for the year 2005 and derived from the multi-spectra (yellow triangles) and multi-microwindows (light blue dots) retrieval strategies. Relative differences between the two approaches are plotted in the upper panel. A slight significant relative difference of 1.5 $\pm$ 1.0 % can be observed, with the multi-microwindows approach giving higher abundances. A priori CH_3D total columns have also been added (green dots) to emphasize the quite good sensibility of each retrieval strategy. Low insert panel plots relative differences between each time series and a priori values.

The next section discusses the application of the retrieval strategy to the low altitude, low latitude site of Ile de La Réunion.

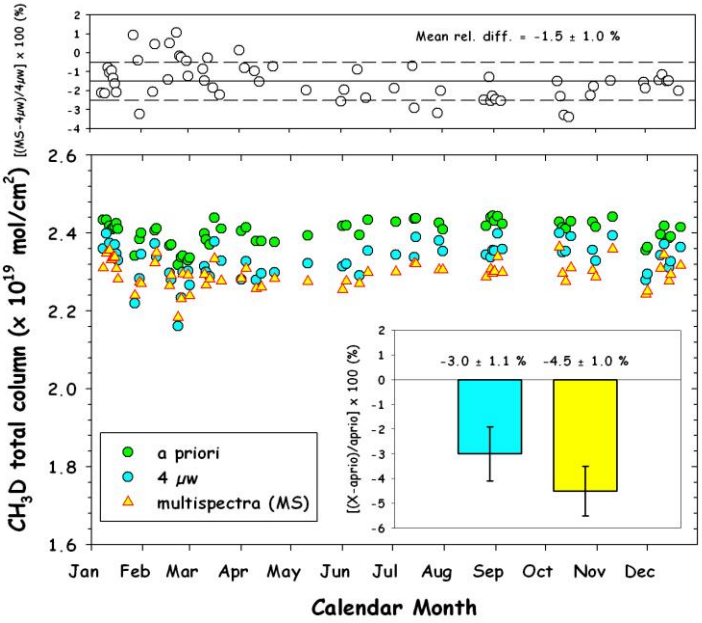

Figure 52: CH_3D total columns derived from the multi-microwindows (light blue dots) and the multispectra (yellow triangles) approaches for the year 2005. *A priori* total columns are plotted in green. Lower right insert panel: mean relative differences between each retrieved time series and *a priori* values. Top panel: relative differences between both retrieved time series.

II.1.3.4.4 CH_3D at Ile de la Réunion

The retrievals of CH_3D at Ile de la Réunion have been tested following the same strategy as performed at the Jungfraujoch (47°N, 8°E) site. Réunion being a humid site, the retrievals are far more sensitive to the interferences with water vapour absorptions than at the Jungfraujoch, a relatively dry high mountain site. The multi-spectra, multi-windows and single microwindow (3070.71-3071.00 cm^{-1}) approaches were tested for retrievals at La Réunion. It turned out that a simultaneous multi-microwindows fitting procedure still yielded the highest information content, with a DOFS equal to (0.65±0.1) versus (0.4±0.1) for the multi-spectra approach and (0.15±0.1) for the single window approach. Moreover, the multi-spectra approach requires at least 7 spectra/day which limits the number of possible retrievals too much. Note also that only spectra with a solar zenith angle between 70 and 80° have been processed. Lower SZA angle spectra have insufficient information content (DOFS $<<$ 1 for the multi-window fit).

It turned out that at Ile de La Réunion, the retrieval works better if one eliminates one of the microwindows and slightly changes the limits of another one. The final choice is given in Table VIII. A priori profile and covariance matrix (Sa) were derived from ACE-FTS (global ± 10° latitude around Reunion), using a correlation width of 4 km. We achieve a DOFS of order 1, for spectra with SZA > 62°.

Table VIII: Microwindows used for CH_3D retrieval at Ile de la Réunion. The last column lists the number of CH_3D lines in the window.

µwindow limits	Interfering species	Line #
3070.71 - 3071.00	CH_4, O_3	2
3072.58 - 3073.15	CH_4, H_2O, O_3, solar lines	2
3089.15 - 3089.70	CH_4, H_2O, O_3	2

At present, we still face the problem that we have a bias in the CH_3D columns retrieved from spectra taken with two different bandpass filters (including the selected microwindows). More work is needed to derive a final reliable product for CH_3D at Réunion.

II.1.3.5 Carbon monoxide (CO) and its isotopologues

II.1.3.5.1 Introduction

Although carbon monoxide (CO) is not considered as a direct greenhouse gas, it is able to elevate concentrations of methane and tropospheric ozone, through scavenging of atmospheric constituents, e.g. the hydroxyl radical OH. Carbon monoxide is created when carbon-containing fuels are burned incompletely. Through natural processes in the atmosphere, it is eventually oxidized to carbon dioxide. Carbon monoxide has a limited atmospheric lifetime of only a few months and as a consequence is spatially more variable than longer-lived gases.

II.1.3.5.2 Retrieval of ^{12}CO and ^{13}CO at Jungfraujoch

Commonly, carbon monoxide (CO) retrieval approaches from FTIR spectra simultaneously use three lines, one saturated line from the main isotopologue and two weaker lines from ^{13}CO. Since we aim at retrieving isotopologue ratio timeseries in AGACC, we first have to develop two new independent approaches for ^{12}CO and ^{13}CO.

For ^{12}CO, we have tested more than a dozen unsaturated lines from the (2-0) band of CO, in the 4200-4300 cm^{-1} spectral interval. 6 of these lines have finally been selected, essentially on the basis of minimum interference by CH_4, HDO and the solar spectrum.

For ^{13}CO, two dozen lines from the 2055-2155 cm^{-1} range have been looked at. Only four of them were finally kept, with interferences by O_3 and the solar spectrum only.

The same a priori profile and covariance matrix have been used for both isotopologues. Information content analyses have indicated that similar pieces of information are derived from those two independent approaches, with typical DOFS of 2.70 and 2.15,

and error affecting the tropospheric columns of 3 and 9%, for ^{12}CO and ^{13}CO, respectively.

Since the ^{12}CO and ^{13}CO are recorded with different optical filters, simultaneous measurements are not available and data taken within less than 1 hour of each other have been considered. $^{12}CO/^{13}CO$ ratios have been computed using all available observations from 1995 onwards. Monthly mean $\delta^{13}C$ (see section II.1.3.4.2) are plotted versus the month of year fraction in Figure 53.

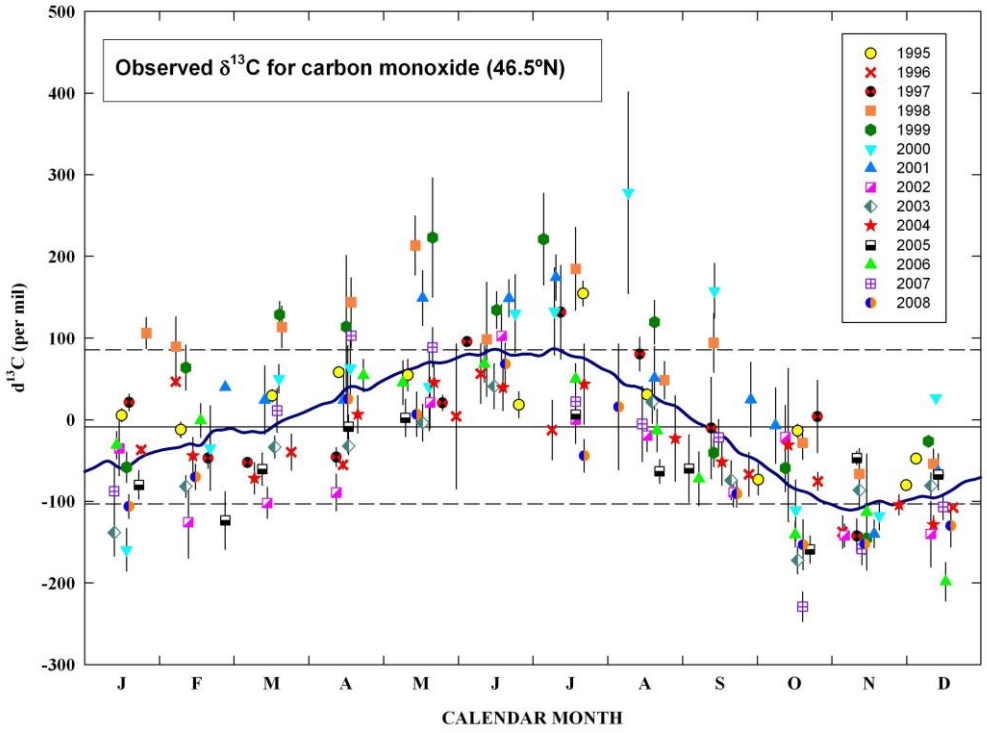

Figure 53 : Seasonal modulation of $\delta^{13}C$ above the Jungfraujoch station, derived from quasi-simultaneous measurements of the ^{13}CO and ^{12}CO mean vmr in the 3.58-8.2 km atmospheric layer. Vertical bars give the standard errors around the monthly means.

Among striking features, we notice the significant seasonal modulation, with a maximum in the middle of the year in agreement with in situ measurements in the Northern hemisphere; this probably reflects significant changes in specific sources and/or sinks of the isotopologues. We also see interannual change, with possible impact of strong biomass burning events, with e.g. 1998 showing fractional differences above the mean signal. Overall, a mean value of -9 ‰ is found, very close to the typical $\delta^{13}C$ for a background atmosphere (-8 ‰).

II.1.3.6 Ethylene

Ethylene (C_2H_4) originates from a variety of anthropogenic (e.g. cars in urban areas) and natural (e.g. plants, volcanoes, forest fires) sources [Aikin et al., 1982]. Due to its very short chemical lifetime, it is difficult to detect C_2H_4 from FTIR spectra, in particular at the

high-altitude Jungfraujoch site. However, we have selected three microwindows and showed that it's possible to clearly detect larger absorptions of ethylene in FTIR spectra recorded during special events, e.g. under enhanced biomass burning. Main characteristics of these microwindows are presented in Table IX.

Table IX : Three microwindows that allow detecting, from FTIR spectra, C_2H_4 enhancements associated to pollution events. The number of ethylene lines in each microwindow is given in third column. Last column provides lower-state energy for each line.

Range (cm^{-1})	Interfering species	Line #	Lower-state energy E'' (cm^{-1})
941.75 - 942.05	CO_2, COF_2	1	136
949.85 - 950.85	CO_2, COF_2, O_3, N_2O, H_2O, solar lines	3	98 / 81 / 357
951.50 - 952.25	CO_2, COF_2, O_3, N_2O, H_2O	3	55 / 290 / 259

Due to the limited information content, it's only possible to derive vertical total columns of C_2H_4 from spectra recorded at very high SZA (between 85 and 90°). At such high SZA, spectra are usually recorded at a "reduced" resolution of 6.1 mK. Ethylene total abundances above Jungfraujoch have been derived by using the SFIT-2 v3.91 algorithm and the HITRAN-2004 database. A realistic a priori VMR profile for ethylene has been constructed from data found in the "Spectroscopic Atlas in the middle Infra-Red", published by Meier et al. [2004].

Figure 54 presents an example of detection of ethylene enhancement above Jungfraujoch, using the first microwindow of Table IX.

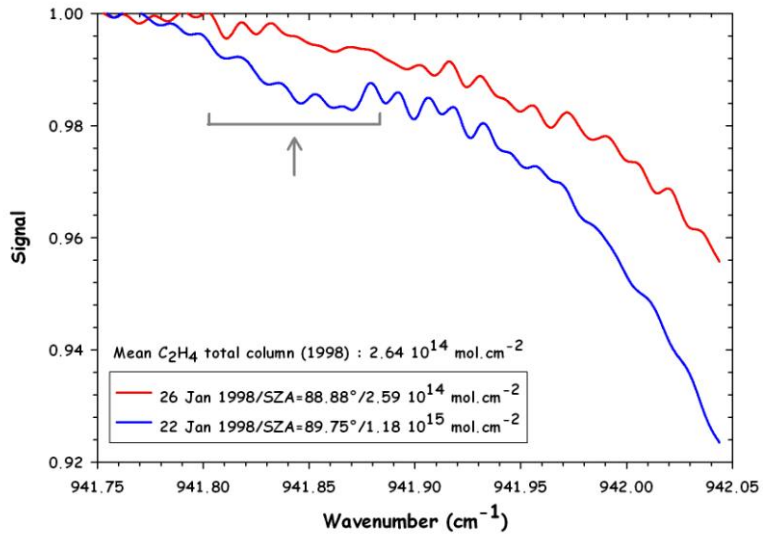

Figure 54: Comparison between spectra recorded under similar geometry and corresponding to C_2H_4 enhancement (blue curve, grey arrow) or normal conditions (red curve) (C_2H_2).

The blue curve shows a spectrum recorded at 89.8° with a strong absorption due to ethylene (see grey arrow) while the red curve reproduces an FTIR spectrum obtained under similar geometric conditions four days after, but corresponding to background atmospheric contents. A total column of 1.18 10^{15} molec./cm^2 was retrieved in the first case, i.e. about four times larger than the mean total column value of 2.64 10^{14} molec./cm^2 computed for 1998.

II.1.3.7 Acetylene

II.1.3.7.1 Introduction

Acetylene (C_2H_2) is among the nonmethane hydrocarbons (NMHCs) accessible to the infrared remote sensing technique. As a product of combustion and biomass burning, it is emitted at the Earth surface and further transported and mixed into the troposphere. Destruction by OH is the main removal process. The resulting average tropospheric lifetime is estimated at 1 month on the global scale. At mid-latitudes, it varies between 20 days in summer to 160 days in winter. This compound is appropriate to study tropospheric pollution and transport, and is often used in conjunction with other tracers of fires.

II.1.3.7.2 Observations of acetylene at the Jungfraujoch

There are exploitable C_2H_2 absorption lines in both the MCT and InSb spectral domains, more precisely in the 750-780 and 3250-3305 cm^{-1} ranges. Although all these lines are weak (~1% absorption), they can be used for the retrieval of C_2H_2 from ground-based high-resolution IR spectra. A systematic and careful look at ISSJ "dry and wet observations" has allowed identifying 5 candidate lines close to 3251, 3255, 3268, 3278 and 3305 cm^{-1}. The major interferences are water vapor (H_2O) and one of its less abundant isotopologues ($H_2{}^{18}O$). Absorptions by solar lines, O_3 and HCN have also to be accounted for. Each of the identified lines has been characterized in terms of information content using a representative subset of spectra. Mean values for the degree of freedom for signal (DOFS) range from 1.2 to 1.5. The final strategy is however reduced to four lines, owing to the fact that the fits to the 3268 cm^{-1} line are less satisfactory.

Information content and error budget have been carefully evaluated. They objectively indicate that our strategy allows to retrieve C_2H_2 tropospheric columns without contribution of the a priori; discrimination between partial columns below and above 7 km is at 92% coming from the retrieval. Typical errors amount to 4% of the tropospheric column, and to 12% of the 7-14.2 km partial columns.

The left frame of Figure 55 shows the Jungfraujoch time series of tropospheric columns retrieved with this new approach (left frame). Among striking features, we notice high tropospheric columns observed in 1998 correlated with documented high values of carbon monoxide resulting from important biomass burning. This is also consistent with record-high troposheric columns of C_2H_6 and HCN observed the same year at the Jungfraujoch (Figure 29). Our measurements also allow to characterize the strong seasonal variation of C_2H_2, with maximum columns generally observed around mid-February. On average, the peak-to-peak amplitude amounts to nearly 90% of the mean yearly column.

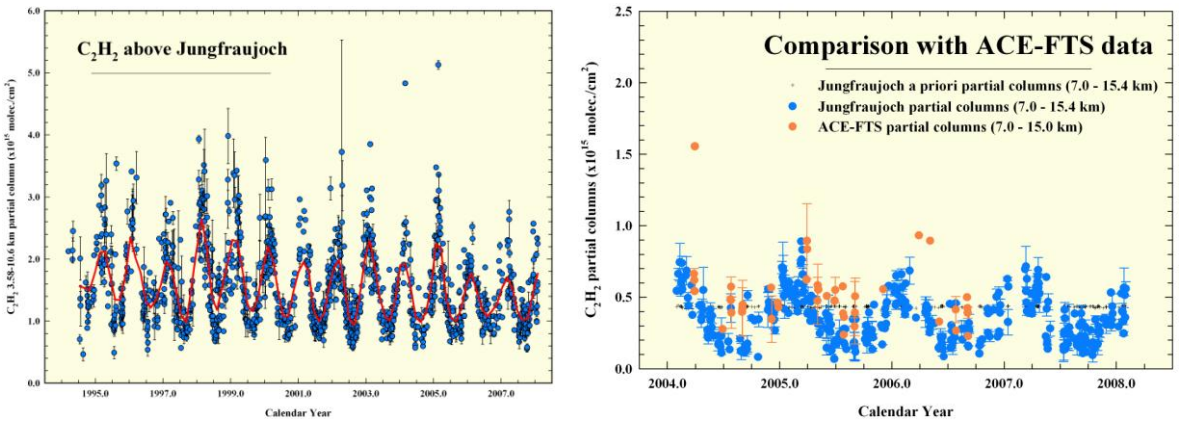

Figure 55: Timeseries of C_2H_2 above the Jungfraujoch and comparison with ACE-FTS data

As for HCN, the Jungfraujoch 7-15 km time series has been compared with ACE-FTS data. These latter correspond to an update of the standard version 2.2. ACE-FTS vertical profile distributions are retrieved using 14 lines from both the MCT and InSb domains. Over northern mid-latitudes, vmr values are generally available from 17 km down to at best 7 km. Corresponding ACE-FTS partial columns can be compared to Jungfraujoch data, since the ground-based retrievals are sensitive to that range, as shown by the information content analysis. The right frame of

Figure 55 Figure 55 compares the Jungfraujoch and the ACE-FTS data sets. The latter includes all occultation measurements obtained between 41 and 51°N latitude and extending down to 7 km.

The Jungfraujoch time series (in blue) is characterized by a clear seasonal modulation, with partial columns ranging from about 1 to $9x10^{14}$ molec./cm^2. The Jungfraujoch and ACE-FTS data sets (in orange) agree reasonably well, although the latter seems to be slightly biased high, especially during summertime. An extension in time of the ACE-FTS data set is needed to confirm these first conclusions.

II.1.3.7.3 Observations of acetylene at Ile de la Réunion

Taking into account the significant amount of water vapor at Reunion Island, we found that the best approach in this situation is to use the 3250.25 - 3251.11 cm^{-1} microwindow. Preliminary retrievals of $H_2{}^{16}O$ and $H_2{}^{18}O$ were made in the 3189.50 - 3190.45 cm^{-1} and 3299.0 - 3299.6 cm^{-1} spectral intervals, respectively. These retrieved profiles are then used as a priori in the C_2H_2 retrieval process. We show in Figure 56 the 2004 to 2010 C_2H_2 FTIR total columns time-series, together with the columns from simulations of the model IMAGES. It can be seen that during the period of intense biomass burning in Africa and Madagascar (September – October), the emissions of C_2H_2 were probably underestimated in the model.

The work on C_2H_2 will be published in 2011, together with other biomass burning products measured by our FTIR instrument at Saint-Denis, by Vigouroux et al.

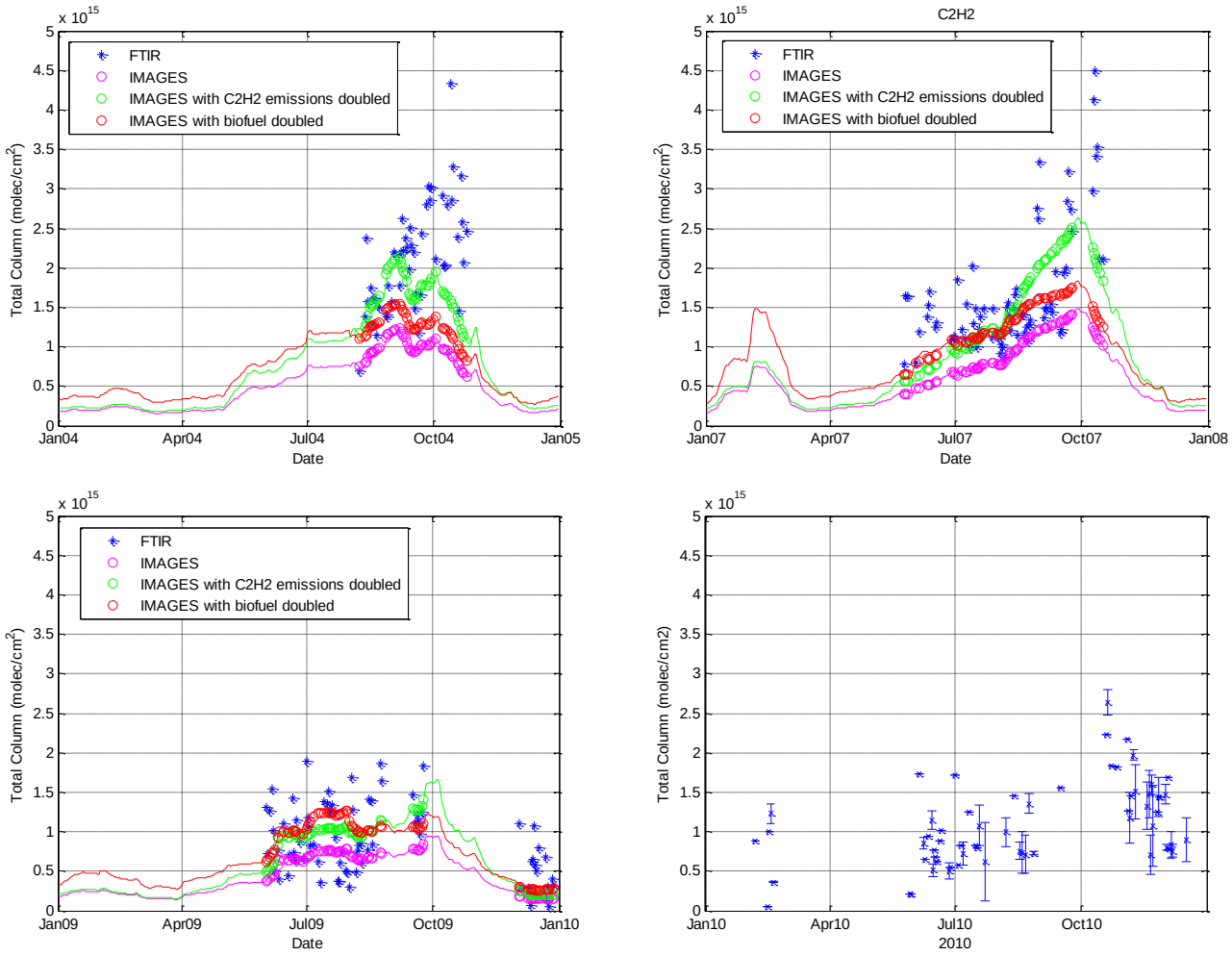

Figure 56 : FTIR daily means of C_2H_2 total columns at Saint-Denis in 2004-2010, together with C_2H_2 total columns from the model IMAGES.

II.1.3.8 HCFC-142b

II.1.3.8.1 Introduction

Among the replacement products for the CFCs, one of the most commonly used is the HCFC-142b (CH_3CClF_2), with applications in refrigeration and foam blowing. This has resulted in significant emissions to the atmosphere, and hence to large growth rates, e.g. 4.2%/yr for the period 2003-2004 (WMO, 2006). At present times, it is the third most abundant HCFC in the atmosphere, after HCFC-22 and HCFC-141b. Its mean global vmr was 15.38 pptv in 2004, based on the AGAGE network *in situ* measurements.
HCFCs, which are ozone depleting substances – since they are relatively long-lived chlorine-bearing source gases – have recently started to be regulated under the Montreal Protocol, with 100% phase-out production actually settled for 2029. It is therefore important to monitor their accumulation in the atmosphere, in order to make sure that the observed growth rates are consistent with the reported emissions. In addition, these species are also potent greenhouse gases, with several absorption features in the infrared.

II.1.3.8.2 HCFC-142b observations at the Jungfraujoch

For HCFC-142b, relatively broad absorption features have been identified close to 904, 967, 1134, 1192 and 1202 cm^{-1}. In all cases, the absorptions are still very weak, even in the most recent observations, and several interferences by H_2O, HDO, CO_2, O_3, CH_4, CH_3D, HNO_3 and CFC-12 have to be carefully accounted for. After several tests, we have selected three microwindows to evaluate the possibility to retrieve HCFC-142b total columns from Jungfraujoch observations, namely the 904, 967 and 1192 cm^{-1}. Corresponding intervals are reproduced in Figure 57.
In all cases, the synthetic atmospheric spectrum is the lower trace, in black, while individual absorptions by the target and interfering species are offset for clarity, and identified on the right-hand side of the figure. Although the calculations have been performed for low sun conditions (zenith angle of 85º), the total absorption for the target gas remains weak, with values of 0.36, 0.12 and 0.47%, to be compared to total absorptions of 7.1, 11.1 and 26.6% in the 904, 967 and 1192 cm^{-1} intervals, respectively.

In order to reach sufficient information content despite these unfavourable and challenging conditions, we have performed the retrievals using simultaneous fits of the three microwindows, further combining several consecutive observations of the same day. Table X summarizes the settings adopted for the HCFC-142b retrievals.

Table X : Adopted settings for the HCFC-142b retrievals. The solar spectrum was also fitted

Limits (cm^{-1})	Fitted interferences (scaling)
903.26 – 905.67	HNO_3, H_2O, CO_2
965.40 – 968.80	CO_2, O_3, H_2O
1191.6 – 1194.9	HDO, O_3, H_2O, N_2O, CH_4, CH_3D

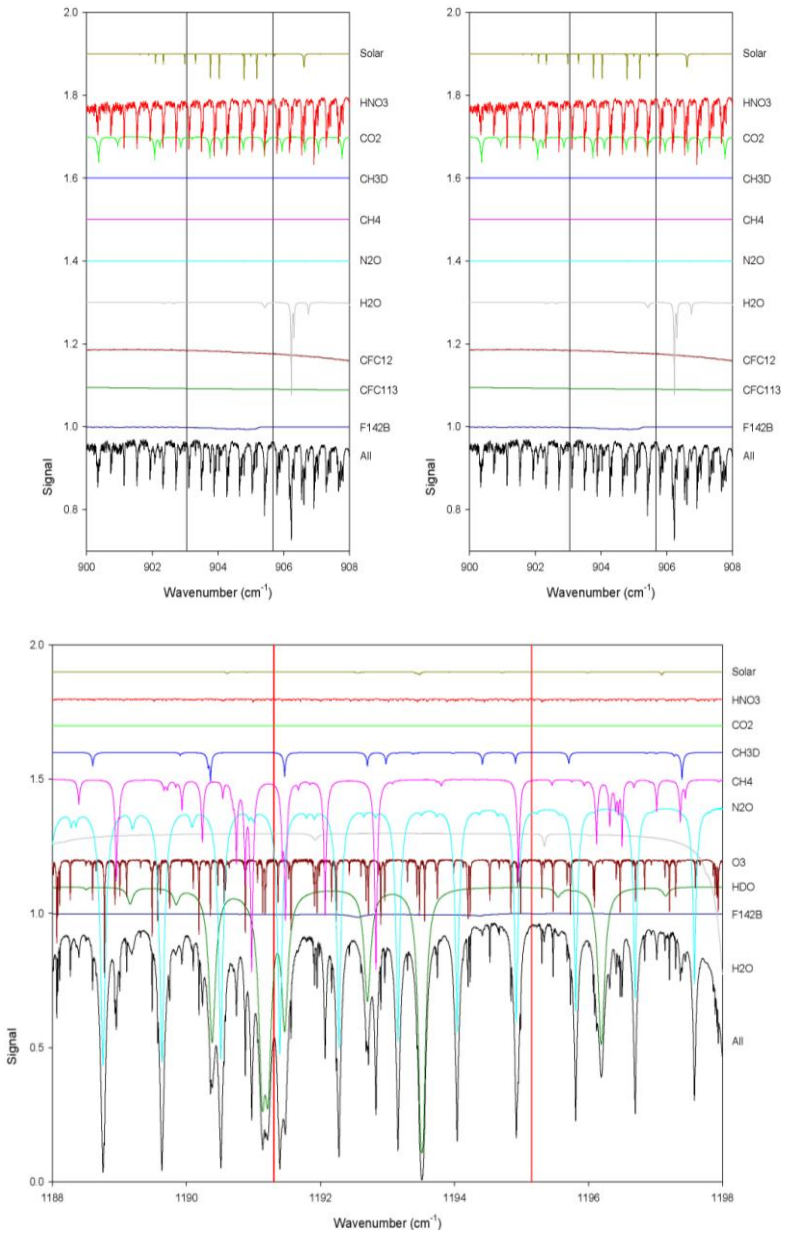

Figure 57: Synthetic spectrum calculations performed for the microwindows used for the retrieval of HCFC-142b, further extended to the left and the right to allow the identification of adjacent absorptions that could influence the local continuum. Total as well as individual absorptions are reproduced and identified on the right of each frame. The individual absorptions have been offset for clarity.

Jungfraujoch observations collected over the 2002-2007 time period have been systematically fitted to produce a consistent time series. Monthly mean total columns have been computed, they are ranging from about 1.0E14 to 2.5E14 molec./cm^2. A linear fit to the whole time series indicated a mean trend slightly lower than 8%/yr. This value is more than two times larger than expected, and we have tried to identify possible causes for this bias. The most likely one is the interference by HFC-134a, which also absorbs in the 1192 cm^{-1} microwindow (see upper frame of Figure 3 in Nassar et al., [2006]). This species is actually accumulating at a very high rate in the atmosphere (10%/yr in over 2004-2006; see e.g. Reimann et al. [2008]). Unfortunately, pseudolines for HFC-134a are actually unavailable, preventing us to perform retrievals accounting for this interference, with the current version of SFIT2.
It is therefore not possible yet to validate our approach – and hence to perform reliable HCFC-142b retrievals - until these pseudolines are available.

II.1.3.9 Major conclusions

It has been demonstrated that we can derive a number of important climate-related trace gases from FTIR solar absorption and MAXDOAS measurements, which hitherto have not yet been investigated in detail or have not yet been derived at all. In addition, we have shown that distinct isotopologue information can be retrieved for methane and carbon monoxide and that interesting features show up when considering variations in the different isotopologues' timeseries.
In many cases, retrieval strategies had to be adapted when going from one site to another with different atmospheric conditions, especially when the local humidity and abundances are very different as is the case between Jungfraujoch (dry, high altitude, mid-latitude) and Ile de La Réunion (humid, low altitude, low latitude). Still we have been able to show the feasibility of retrieving particular trace gas information even under difficult conditions. Many of our results have been compared to correlative data, to validate the approach and to gain complementary information.
It is also important to note that the retrieval strategies developed in AGACC have regularly been presented to the global NDACC UV-Vis and Infrared communities and have often been adopted by others or even proposed for adoption as a standard in the community (e.g., for HCN).
In particular:

We have been able to study the seasonal variations of HCN at the Jungfraujoch and at Ile de La Réunion, and to show the dominant impact of biomass burning products.

Formaldehyde was studied in much detail at Ukkel, Jungfraujoch and Ile de la Réunion. The challenge for detection at Jungfraujoch is the small abundance (about 10 times smaller than at Ukkel and Ile de La Réunion); a particular observation strategy was developed successfully, resulting in a time series that allows characterizing the day-to-day and seasonal variations. The new experimental set up which allows the recording of spectra with very high S/N ratio, is now routinely used for the observation of the very weak absorptions of this climate-related species at Jungfraujoch.

At Ile de La Réunion, comparisons of FTIR, MAXDOAS, satellite and model data have shown (1) the good agreement between the various data sets, but also, (2), the variability of HCHO (diurnal, seasonal, day-to-day), and (3), thanks to the complementarity of the various data sets, they have enabled us to learn more about the long-range transport of NMVOCS (precursors of HCHO) and deficiencies in the model. It was shown that fast, direct transport of NMVOCS from Madagascar has a significant impact on the HCHO abundance and its variability at Ile de La Réunion, and that this is underestimated in the model.

Notice that improvements can still be expected in HCHO retrievals from MAXDOAS spectra thanks to the development of the aerosol retrieval algorithm and by reducing the noise on the spectra and increasing the number of observation elevation angles, as is the case in the latest generation of MAXDOAS instruments (cf. Section II.1.2.3).

Significant progress was made as to the detection of $^{13}CH_4$ and CH_3D from ground-based FTIR observations, both at Jungfraujoch and Ile de La Réunion. To our knowledge, it is the first time that a $\delta^{13}C$ data set is derived from ground-based FTIR observations. More work is needed to improve the CH_3D retrieval at Ile de La Réunion, and to interpret the results, in combination with models.

Also for the first time, ^{12}CO and ^{13}CO have been retrieved individually at Jungfraujoch, a long-term timeseries of $\delta^{13}C$ has been derived, showing significant interannual and seasonal changes.

As to the hydrocarbon ethylene, it was shown that the former one can be detected at Jungfraujoch only in high SZA spectra (SZA > 85°); the mean column abundance in 1998 has been evaluated to be 2.64 molec/cm^2. Events in which ethylene is enhanced by a factor 4 have been detected.

As to the hydrocarbon acetylene, the observed time series at Jungfraujoch shows a clear seasonal variation and enhancements due to the impact of biomass burning events, correlated with enhancements in CO, C2H6 and HCN. At Ile de La Réunion, the impact of the biomass burning season in Africa and Madagascar is clearly observed in the abundance of acetylene during the period August to November. The model IMAGES nicely reproduces these enhancements if the model is run with doubled C_2H_2 emissions.

It is not clear yet whether we can reliably retrieve the concentration of HCFC-142b, a replacement product that is increasing strongly in the troposphere. New line parameters for the interfering species HCFC-134a are required to confirm/infirm the preliminary results.

The new data sets that have been derived in AGACC from FTIR and MAXDOAS observations will be archived soon in the NDACC data center, where they will be available for users (generally modelers and satellite teams). In the meantime, they are stored locally and are available to users upon request.

II.2 Supporting Laboratory data

II.2.1 Rationale

Laboratory support is necessary to improve the spectroscopic parameters that are used in retrievals of remote-sensing data. Two particular relevant problems must be addressed: (i) the need for unprecedented high accuracies of the molecular parameters required by the new generation of atmospheric remote-sensing satellites instruments [Rothman et al., 2005]; (ii) the lack of consistency between different spectral regions for one given molecule, which can lead to significant uncertainties and disagreements, e.g., as to retrieved water vapour profiles [Casanova et al., 2006]. Other examples that we are facing are inconsistencies between the UV-visible and infrared spectral data for species like formaldehyde, and even ozone.

II.2.2 H_2O and its isotopologues

To complement existing data and fulfill HITRAN database's expectations, we analysed already recorded spectra to produce line parameters covering the spectral region below 9000 cm^{-1}. We also pursued long pathlength measurements, to fill the lack of HDO line parameters in the Visible - mid-IR spectral range in the databases. Also the detection of the water vapour continuum (or dimer) absorption has been investigated by tentatively measuring the heated water vapour (up to 100°C) in spectral regions that are (i) important for solar radiative transfer, (ii) as free as possible of the water monomer interference absorption, (iii) suggested by theoreticians.

Important progress was made in the water vapor field. Linelists of HDO (11500-23000 cm^{-1}) and D_2O (8800-9520 cm^{-1}), see Naumenko et al. [2006] and Voronin et al. [2007]. Also, the experimental linelists of HDO and D_2O that cover the wide 5600-11600 cm^{-1} region have been built. They contain line positions, intensities, self- and air-broadening

coefficients, and air-induced shifts associated with their statistical uncertainties. The complete rovibrational assignment process of these lines is ongoing. In the near-IR spectral region (4200-6600 cm^{-1}), a complete linelist has been produced for the $H_2{}^{16}O$, $H_2{}^{17}O$, $H_2{}^{18}O$ and HDO isotopologues. It is accessible to the scientific community through the web (http://www.ulb.ac.be/cpm) and a paper was published [Jenouvrier et al., 2006]. The region that will fill the gap between 6600 and 8800 cm^{-1} requires great care due to strong congestion problems and to the simultaneous presence of the 3 isotopologues. This analysis has even been extended to 9250cm^{-1} because a better than previously signal-to-noise ratio could be obtained by using a different set-up.

For $H_2{}^{16}O$ in the 9250-6600 cm^{-1}, an assigned linelist was built, but disagreements with HITRAN up to 15% were observed. This problem was investigated and could be explained by experimental problems, so that new measurements were decided.

For the $HD^{16}O$ and $D_2{}^{16}O$ isotopologues, which must be analyzed together due to strong overlap between lines belonging to the two species, important progress has been achieved in two spectral regions: 11500-8800 cm^{-1} and 8800-5200 cm^{-1}. In the 11500-8800 cm^{-1} region, an assigned linelist for $HD^{16}O$ has been finalized and will be published in a next future. For $D_2{}^{16}O$, a list of experimental line parameters has been generated in continuation of our previous work [Naumenko et al., 2006] that covered a narrower spectral region (9250-8800 cm^{-1}). This linelist is mostly assigned (2690) but ambiguous lines need to be checked. In the 8800-5200 cm^{-1} spectral region, a preliminary version of experimental lists of line parameters for $HD^{16}O$ and $D_2{}^{16}O$ has been assembled and their assignments are in progress (40%).

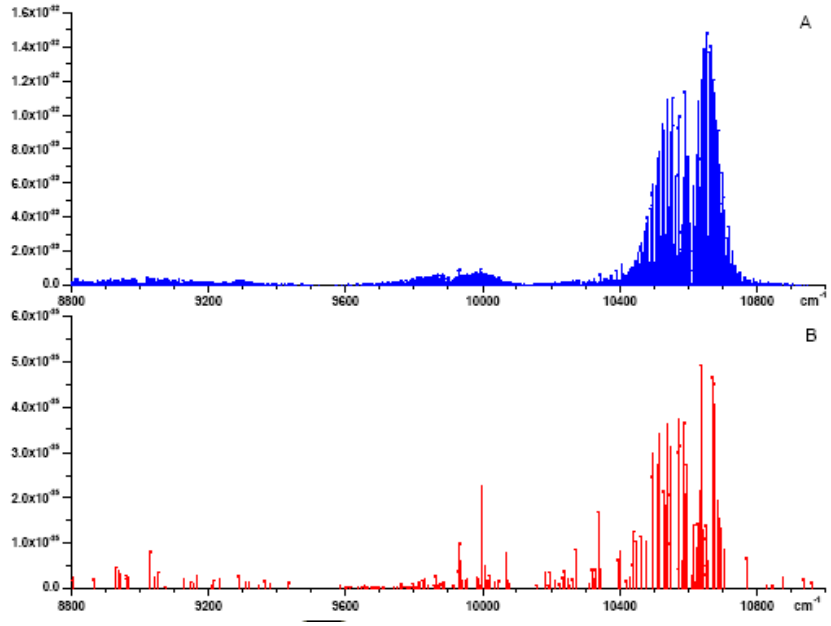

Figure 58 : Comparison between the calculated $HD^{18}O$ spectrum (upper panel) and unassigned HDO lines (lower panel) in the 8800 – 11 000 cm^{-1} region

In the course of this work, lines belonging to $HD^{18}O$ were detected in our spectra though the gas mixtures were not enriched in oxygen-18. The 11500-8800 cm^{-1} region is of particular interest because no experimental data are reported in the literature concerning this region. After having assigned the lines belonging to the $HD^{16}O$ molecule, 215 lines remained unassigned among a total of 5700 lines. The comparison of these lines with the calculated spectrum of $HD^{18}O$ shows excellent similarity which supports their identification (Figure 58). The detection of $HD^{18}O$ lines in our spectra and their assignment was not limited to this region; it was extended to the 5600-8800 and 4200-6600 cm^{-1} regions where several bands were assigned for the first time. Finally, a review of available literature data was performed, and a gathered dataset of energy levels covering 0-12000 cm^{-1} is proposed.

Finally, for the $H_2{}^{17}O$ and $H_2{}^{18}O$ isotopologues, a huge work of data collection, inventory, evaluation of line positions, transition intensities, pressure dependence, energy levels, assignments and uncertainties has been performed by the members of the IUPAC project, and will lead in a near future to a consequent publication.

This work was done in close collaboration between ULB and BIRA-IASB, and the Groupe de Spectroscopie Moléculaire et Atmosphérique (Université de Reims, France), the Université de Reims Champagne-Ardenne, the University College London, and the Tomsk Institute of Atmospheric Optics.

Laboratory data on water vapour and its isotopologues gathered in the frame of this project are included in the MARVEL database (International Union of Pure and Applied Chemistry IUPAC project; http://chaos.chem.elte.hu/marvel/).

II.2.3 Other molecules and their isotopologues

II.2.3.1 Acetylene

The objective of this work was to improve line intensities available for the ν_5 band of acetylene ($^{12}C_2H_2$) near 13.6 μm, already accurate to 5% [Mandin et al., 2000]. This is particularly challenging because of the strength of the band, forcing the use of very low sample pressures. Despite several efforts, we failed to obtain reproducible line intensities, and were not able to determine the origin of the observed variations. Although the AGACC project has ended, we will pursue this work to hopefully reach the science objectives.

II.2.3.2 Ethylene

We successfully obtained line parameters for the ν_{12} band of ethylene ($^{12}C_2H_4$), observed

near 1443 cm^{-1} [Rotger et al., 2008]. They have been incorporated into the HITRAN [Rothman et al, 2009a, 2009b] and GEISA [Jaquinet-Husson et al., 2008] databases. This work was the first step of a throughout quantitative analysis aiming to provide accurate reference line parameters for the 10 μm spectral region of this species, which is used for remote sensing of ethylene in the infrared range.

II.2.3.3 Formic acid

We showed that line intensities available in atmospheric databases, particularly HITRAN [Rothman et al., 2005] and GEISA [Jacquinet-Husson et al., 2008], for the ν_6 and ν_8 bands of formic acid (HCOOH) are a factor of about 2 lower than laboratory measurements. The sharp Q-branch of the ν_6 band, located in an atmospheric window near 9 μm, is however commonly used to probe tropospheric formic acid by infrared remote sensing techniques. An improved set of line parameters was therefore urgently needed. Using results of our recent work [Vander Auwera et al., 2007], we therefore generated a new database for the 9 micron region of the formic acid spectrum. It includes a total of 49625 lines in the ν_6 and ν_8 bands of trans-$H^{12}C^{16}O^{16}OH$ with $J'' \leq 79$, $Ka'' \leq 25$, and lower and upper state energies up to 2700 and 4000 cm^{-1} respectively. Comparisons of low and high resolution laboratory spectra with spectra calculated at the same conditions using the new line list and HITRAN showed that the former provides a significantly improved and much more accurate description of the 9 micron region of the formic acid spectrum. An article describing this work is published [Perrin and Vander Auwera, 2007]. The line list is now included in the latest version of the HITRAN [Rothman et al., 2009a, 2009b] and GEISA [Jaquinet-Husson et al., 2008] databases. It has been recently used to improve HCOOH retrievals from the ground [Zander et al., 2010]. Building upon this contribution, we also studied the ν_3 band of formic acid near 5.6 μm, and generated for the first time a list of line parameters describing this region [Perrin et al., 2009]. It has also been incorporated in HITRAN and GEISA.

II.2.3.4 Carbon monoxide istopologues

For carbon monoxide ($^{13}C^{16}O$) we recorded absorption spectra of the 1–0 band near 2096 cm^{-1} using a Bruker IFS125HR high resolution Fourier transform spectrometer available at ULB. A high-purity commercial sample (Cambridge Isotopes Laboratories, 99% purity), at pressures ranging from about 40 to 260 Pa, was contained in a 1.46 cm long stainless steel cell, temperature stabilized at 296 K. Absolute line intensities were measured by adjustment of a synthetic spectrum to the observed spectrum of each line using a least squares fitting algorithm. Each line was given a Voigt profile. The

instrumental effects arising from the truncation of the interferogram and the use of a 0.8 mm source aperture diameter were included as fixed contributions. We measured the absolute intensity of the P(20) to R(20) lines of the 1–0 band of $^{13}C^{16}O$, observed in the range 2008–2060 cm^{-1}. We estimated their accuracy to be about 2–3 %. Our results are on average 1.5 % higher than the intensity information available for these lines in the HITRAN database, characterized by a 2–5 % accuracy [Rothman et al., 2005].
This is an excellent agreement, indicating that the accuracy of 1–0 band $^{13}C^{16}O$ line intensities in HITRAN is probably close to 2 %.

II.2.4 Major conclusions

Improved line parameters have been obtained for water vapor and its isotopologues, ethylene and formic acid. We also showed that line intensities available around 2096 cm^{-1} for the $^{13}C^{16}O$ isotopologue of carbon monoxide in the HITRAN database are probably accurate to 2%, but failed to improve line intensities for the 13.6 μm region of acetylene.
The work of Frankenberg et al. [2008] has demonstrated that the H_2O spectroscopy had a significant impact on methane satellite retrievals in the 5990-6150 cm^{-1} range, and that the Brussels-Reims database brings a huge improvement as compared to HITRAN. The same is true for the region 4200-4350 cm^{-1} where an overall improvement in comparison with HITRAN is also demonstrated. The impact of water vapor on methane retrievals was found unexpectedly big. The importance of high quality water vapor spectroscopy and laboratory work, for water vapor retrieval itself but also to eliminate interferences of this highly variable gas with other species, has been highlighted in Frankenberg et al. [2008].
Laboratory data on water vapor and its isotopologues, gathered in the frame of this project, are included in the MARVEL database (International Union of Pure and Applied Chemistry IUPAC project; http://chaos.chem.elte.hu/marvel/). The updated line parameters of HCOOH and C_2H_4 have been included in the latest version of the HITRAN and GEISA databases. The half-widths of $H_2{}^{16}O$ in the region 4200-6600 cm^{-1} will be soon included in the measurement database of R. Gamache (University of Massachussetts Lowell, USA, http://faculty.uml.edu/Robert_Gamache). Local databases (http://www.ulb.ac.be/cpm and http://www.oma.be/BIRA-IASB/Scientific/Topics/Lower/Labo_Base/ Laboratory.html) are also regularly updated.

III POLICY SUPPORT

The measurements of the atmospheric composition have become central in understanding many aspects of our changing environment, from air pollution to climate change, also including the impacts on continental and oceanic ecosystems. This project, which is a concerted initiative between Belgian partners involved since a long time in the measurement of the atmospheric composition, aimed to fostering further the possible measurements of the atmospheric composition from ground-based instruments, which is an important piece of the global earth's observation network. The research was intentionally set on innovation, targeting species which were never or rarely monitored before but which could improve our understanding of key processes regulating the chemical and physical equilibrium of the atmospheric system.

The research targeted in AGACC is of fundamental nature. Nevertheless, the results will be integrated in national and international environmental assessment reports (e.g. Milieu- en natuurrapport Vlaanderen, WMO Scientific Assessments of Ozone Depletion, IPCC Assessment Reports…), that provide scientific background knowledge to policy makers for establishing or modifying environmental regulations.
The new geophysical datasets generated in AGACC are or will be integrated in international datacenters like NDACC, WOUDC, …thus contributing to the global picture of atmospheric composition changes for the benefit of the scientists, the policy makers and the public. They also serve modelers to improve their models and hence the capability to forecast future changes, which in turn helps policy makers to establish the necessary regulations. AGACC observations are also reported to GCOS, the Global Climate Observing System, and to ACCENT, 'Atmospheric Composition Change: a European Network'.
Also the new spectroscopic datasets generated in AGACC are or will be integrated in international databases like HITRAN and GEISA, to the benefit of the remote-sensing and modeling communities.

In particular:
- The work on water vapour has been presented at several occasions to the partners in the WAVACS Cost Action and to the ISSI Working Group on Atmospheric Water Vapour and will partly be included in the Report from that Group to be published in the open literature [Schneider et al., 2009]. In the end, this work will contribute to advancing our knowledge on the distribution and transport of water vapour in the atmosphere and its interaction with the changing climate. As explained above (Sect. II.2.4), the improvement in the spectroscopy of water vapour has had a large impact on the methane products from the SCIAMACHY satellite, thereby improving our knowledge on

the atmospheric methane concentrations and their evolution. As water vapour is a major interfering gas in almost all regions of the visible to infrared spectrum, one can expect that our knowledge about other atmospheric gases will be impacted for similar reasons as in the case of methane by the improved water vapour spectroscopy

- Once proven, the possibility to detect HCFC-142b will be of direct interest to the policy makers, because it will enable to verify the emission inventories and to evaluate the success of the Montreal Protocol. It should not be forgotten that the Montreal Protocol is tightly linked to Climate Change, as many of the CFC and replacement products are effective greenhouse gases.
- A first step in better evaluating the still poorly established radiative forcing of the aerosols is to observe them and to characterize them. In the end, any improvement in the operational monitoring of atmospheric aerosols, as achieved in AGACC, will contribute to decreasing the uncertainties regarding the sources of various aerosol types and their impact on the solar radiation reaching the Earth's surface and climate. The impact on the penetration of solar light has already been studied in AGACC and has resulted in an improved UV-index forecasting, of direct benefit to the general public and the policy makers.

IV DISSEMINATION AND VALORISATION

Presentations of the AGACC project to national and international policymakers, programme managers and the general public

- Participation to Kick-Off meeting of SPSDIII programme organized by Belgian Science Policy (Brussels, 26-27/3/2007)
- Development and maintenance of AGACC Web site at http://www.oma.be/AGACC/Home.html
- Redaction of AGACC fiches by coordinator, transmitted to Belgian Science Policy (February 2007)
- Workshop at Bern on 25-26/11/2008: 'Spawning the atmosphere measurements at Jungfraujoch' with oral presentations from M. Van Roozendael, F. Hendrick and M. De Mazière for BIRA-IASB and from Ph Demoulin, P. Duchatelet, E. Mahieu and Ch. Servais for ULg. Press release. For details see http://www.oma.be/AGACC/Home.html.
- Analyses of the ozone and water vapour data, performed in the frame of AGACC are included in the following report:
  Brouyaux F., Tricot, C., Debontridder, L., Delcloo, A., Vandiepenbeeck, M., De Witte, S., Cheymol, A., Joukoff, A., De Backer, H., Hus, J., Van Malderen, R., Vannitsem, S., Roulin, E., and Mohymont, B., Oog voor het Klimaat, Uitgegeven door het KMI, ISBN, 02008/0224/050, Brussel, 2009, http://www.meteo.be/meteo/view/nl/2791820-Oog+voor+het+klimaat+NL+versie.html
- Presentation of the Jungfraujoch Observatory and of the Belgian NDACC activities to minister Laruelle, Nov. 17, 2009, at Jungfraujoch, Switzerland
- MAXDOAS: a new technique for the monitoring of the tropospheric composition at the Junfraujoch, poster presentation at the attention of Minister Laruelle and co-workers, M. Van Roozendael, K. Clémer, M. De Mazière, C. Fayt, F. Hendrick, C. Hermans, G. Pinardi, Jungfraujoch, Nov. 17, 2009
- Presentation of AGACC activities and instruments during the Open Doors of the Plateau d'Uccle (Oct. 3-4, 2009).
- M. De Mazière gave part 2 of the course 'Mesurer et comprendre notre atmosphère: 50 ans d'aéronomie!' entitled 'Questions actuelles en chimie atmosphérique', voor het Collège de Belgique, Académie Royale de Belgique, 12 October 2010.

Contributions of AGACC to international research programmes

- The measurement campaigns at Ile de La Réunion also deliver products to 3 European projects: SCOUT-O3 (http://www.ozone-sec.ch.cam.ac.uk/scout-o3), HYMN (http://www.knmi.nl/samenw/hymn) and GEOmon (http://www.geomon.eu). Team

members of BIRA-IASB have participated to various working meetings in the frame of these projects.

- AGACC members contribute to the ACCENT EU Network of Excellence
- Participation in the Management Committee (KMI-IRM and ULB) and Working Groups (KMI-IRM, ULB and BIRA-IASB) of the COST action ES0604 Atmospheric Water Vapour in the Climate System (WaVaCS). This Action aims at integrating the research on water vapour and climate that is carried out in different areas (atmospheric monitoring, theory, modelling, and data assimilation);
  - Participation to WaVaCS kick-off meeting on Friday 05/10/2007 (participation of ULB and KMI).
  - Participation to WaVaCS workshop and Management Committee Meeting, Richard-Assmann Observatory, Lindenberg (Germany), 21-23 May 2008.
- Short term scientific mission to Lindenberg Observatory, Deutscher Wetterdienst, in order to adopt Leiterer's correction method for vertical humidity profiles (R. Van Malderen, KMI-IRM).
- Participation to the IUPAC project (International Union of Pure and Applied Chemistry) n°2004-035-1-100: "A database of water transitions from experiment and theory" (http://www.iupac.org/projects/2004/2004-035-1-100.html & http://theop11.chem.elte.hu/TG.htm) and to the related meetings (see below).
- Participation to meetings regarding integration of laboratory data in international data bases:
  - Boston, 28-29/06/2006: IUPAC meeting.
  - Boston, 25/06/2006: meeting of the "HITRAN Advisory Committee".
  - Bruxelles, IASB-BIRA, 12/04/2007 & 08/09/2008: IUPAC teleconferences.
  - HITRAN committee meeting, Sunday 02/09/2007, Dijon, France
  - IUPAC Task group meeting, Friday 07/09/2007, Dijon, France
  - Boston, 19/06/2010: meeting of the "HITRAN Advisory Committee"

- Participation to the Cabauw Intercomparison Campaign of Nitrogen Dioxide measuring Instruments, A CEOS, GEOMON and NDACC initiative, Cabauw, The Netherlands, June-July 2009
- Participation to the NDACC Steering Committee Meetings:
  - OHP, France, 25-29/09/2006
  - Waikoloa, Hawaii, 1-5/12/2007
  - Ilulissat, Greenland, 25-30 September 2008
  - Geneva, Switzerland, Sept. 29 – Oct. 1, 2009
  - Queenstown, New Zealand, 5-8 Oct. 2010.
- Contributions to regular NDACC Infrared and Uv-Visible Working Group Meetings

Education of students, young scientists and technical personnel

- Supervision of Naïm Rahal, student master at SCQP-ULB (2006): Stratégie d'inversion d'une distribution verticale des principaux isotopologues de la vapeur d'eau à partir de mesures FTIR sol: Mémoire présenté pour l'obtention du Grade légal de Licencié en Sciences Chimiques.
- De Mazière, M., Interpretation of FTIR observations, Invited lecture at the STAR International Research School: Atmospheric research in Suriname (Paramaribo, Suriname), March 13-17, 2006.
- S. Fally received the Young Scientists' Award in Spectroscopy, presented by the Journal of Quantitative Spectroscopy and Radiative Transfer, Elsevier, Sept. 2007
- Supervision of Valentin Duflot, student at the Université de La Réunion, who spent one month at BIRA-IASB (February 2008).
- C. Senten prepares a PhD thesis on the FTIR data analysis at Ile de La Réunion
- J.M. Metzger and V. Duflot spent two weeks at BIRA-IASB (June 15-26, 2009) to learn the operations and data analysis procedures of the FTIR experiment at Ile de La Réunion. J.M. Metzger's visit was financed by an ERASMUS grant.
- Lecturing: M. De Mazière, Ozon in al zijn facetten, Invited lecturer at the University of Antwerp, in the frame of the course Global Change in the education Milieuwetenschap, 2004, 2005, 2006, 2007, 2008, 2009.
- P.F. Coheur teaches atmospheric chemistry (CHIM-F-405) and together with J. Vander Auwera Atmospheric spectroscopy and remote sensing (CHIM-F-454) at the Université Libre de Bruxelles.
- E. Mahieu has included several of the original results produced within the framework of AGACC in the course he's giving at the University of Liège (Greenhouse gases-Measures and instruments to mitigate climate change, Master in Geographical Sciences, climatology orientation, in-depth approach, 2nd year, CLIM0007-1).
- Bert Geens, 2e Master Physics UA 2008-2009, training for mobility at KMI-IRM. "Improvement of the prediction of the UV index".
- M. Carleer and J. Vander Auwera teached Fourier transform spectroscopy (CHIM-F-453) at the Université Libre de Bruxelles.
- J. Vander Auwera presented an invited course entitled "Spectroscopie" at the *Ecole thématique* CNRS "De la spectroscopie à l'atmosphère: Mesures et modèles" (SpecAtmo), June 2009.
- De Mazière, M., The ozone saga, invited talk at the Physics Colloquium, Univ. Toronto, Nov. 28, 2010.

Added value

- Laboratory spectroscopic data are disseminated via ULB Web pages and via international databases like GEISA and HITRAN. This promotes their use by several types of users, like satellite retrieval teams, modelers of radiative transfer and budget calculations…The best example are the recent improvements in SCIAMACHY retrievals of CH_4 by C. Frankenberg using the improved spectroscopy for water vapour, and the improved retrievals of HCOOH from the satellite experiments ACE-FTS and IASI, and from the ground.
- The data of the ozone observations (total column and profiles) are stored in the NDACC and WOUDC databases.
- The FTIR data sets are archived locally and are at the disposal of interested users; they will also be archived at the NDACC Data Handling Facility (DHF) as soon as the new submission format is implemented (still in 2009)
- MAXDOAS data are archived locally and are at the disposal of interested users; they will also be archived at the NILU data base facility developed within the FP6 GEOMon project (before the end of the project).
- NDACC IRWG has extended number of molecules to be archived, among which are CO, CH_4, HCN, C_2H_6, $\Rightarrow$ AGACC helps us to satisfy NDACC commitments and more…
- Moreover, the NDACC Infrared Working Group (IRWG) is working on a homogenized retrieval strategy for the 10 target molecules, including HCN, CO and CH_4: AGACC team members play an important role in this exercise thanks to the expertise acquired in this project. M. De Mazière has been re-elected as IRWG Co-Chairman for a period of three years.
- Likewise, the NDACC UVVis WG is working on extending its measurement capability to include MAXDOAS aerosol and tropospheric trace gas data products (NO_2, HCHO and glyoxal). Algorithmic developments performed within AGACC are key activities to reach this goal.
- AGACC results are reported at ACE SCience Team Meetings, and at NDACC Brewer, UVVis and IRWG meetings.
- AGACC scientific results have been reported regularly at scientific symposia, workshops, etc. $\rightarrow$ see list here below

Oral contributions at scientific conferences

Carleer M., Clerbaux C., Coheur P.-F., Fally S., Hurtmans D., De Mazière M., Hermans C., Vandaele A. C., Daumont L., Jenouvrier A., Water, ACE science team meeting, University of Waterloo, Ontario, Canada, Oct. 31-Nov. 3, 2006.

Cheymol, A. and H. De Backer, Impact of the aerosol particle concentrations on UV index prediction, European Geosciences Union General Assembly 2007, Vienna, Austria, 15 – 20 April 2007.

Ciais, P., P. Keckhut, M. Minnock, S. Kirschke, and the GEOmon Coordination Team, Global Earth Observation and Monitoring – GEOmon, oral presentation (EGU2010-13790) at the EGU General Assembly 2010, Vienna, May 2-7, 2010.

Clémer, K., C. Fayt, F. Hendrick, C. Hermans, G. Pinardi, M. Van Roozendael, Retrieval of aerosol extinction vertical profiles from MAXDOAS measurements: algorithm development and application, KNMI, Bilt, The Netherlands, 1 April 2009.

Clémer, K., MAXDOAS retrievals of tropospheric aerosol and NO_2 profiles, KNMI, The Netherlands, April 1, 2009

Clémer, K., C. Fayt, F. Hendrick, C. Hermans, G. Pinardi, M. Van Roozendael, MAXDOAS NO_2 profiles, CINDI 2009 workshop, De Bilt, The Netherlands, 6 – 8 July 2009.

Daumont L., Jenouvrier A., Carleer M., Fally S., Vandaele A. C., Hermans C., HDO and D_2O long path spectroscopy: on-going work of the Brussels-Reims team, 9th HITRAN database conference, Cambridge, Ma, USA, 26-28 June 2006.

Daumont L., A. Jenouvrier, S. Fally, C. Hermans, A. C. Vandaele, M. Carleer, Deuterium enriched water vapor Fourier transform spectroscopy: the 8800-10800 cm^{-1} spectral region, 62nd International Symposium on Molecular Spectroscopy, Columbus, Ohio, USA, 18-22 June 2007.

De Backer H., several presentations on the activities at RMI to improve the quality of ozone sonde measurements, WMO/GAW-SPARC-NDACC Ozone sonde Expert Workshop, Jülich, Germany, 2-6 February 2009

De Backer H., Overview of WG1 activities on input data for UV maps, COST 726 Final workshop, Warsaw, Poland, 12-15 May 2009.

De Backer H. and R. Van Malderen, Study of ozone and aerosol and their influence on climate and UV radiation, STCE meeting, Brussels, 8 June 2009.

De Mazière, M., Interpretation of FTIR observations, Invited lecture at the STAR International Research School: Atmospheric research in Suriname (Paramaribo, Suriname), March 13-17, 2006.

De Mazière, M., J.C. Lambert, and M. Van Roozendael, Integrated use of ground-based and satellite measurements of atmospheric composition, International Scientific Conference in Celebration of the 75th Anniversary of the High Altitude Research Station Jungfraujoch, Interlaken, Switzerland (Congress Center Casino Kursaal), 11-14 September, 2006.

De Mazière, M., Cindy Senten, C. Vigouroux, B. Dils, M. Kruglanski, A.C. Vandaele, E. Neefs, F. Scolas, P.F. Coheur, M. Carleer, S. Fally, J. Leveau, FTIR observations at Réunion Island in support of ACE validation, 14th ACE Science Team Meeting, Waterloo University, Oct. 30-Nov. 3, 2006.

De Mazière, M., and the contributing BIRA-IASB, SCQP-ULB, LACy - Univ. Reunion teams, Belgian research at the Ile de La Réunion, International ACE Symposium, York, UK, June 9-11, 2008

De Mazière, M. and the IR team, Site report for Ile de La Reunion, oral presentation at the NDACC-IRWG annual meeting, Murramarang, Australia, June 2-4, 2010.

Demoulin, P., Water vapour retrievals from Jungfraujoch spectra: valorisation of early observations for multi-decadal trend determinations, oral presentation at the Jungfraujoch Atmospheric Workshop, Swiss Academy of Sciences, 25 – 26 November 2008, Bern, Switzerland, 2008.

Dils, B., M. De Mazière, C. Vigouroux, F. Forster, R.Sussmann, T. Borsdorff, P. Bousquet, T. Blumenstock, M. Buchwitz, S. Dalsoren, P. Demoulin, P. Duchatelet,

C.Frankenberg, J. Hannigan, F. Hase, I. Isaksen, N. Jones, J.Klyft, I. Kramer, E. Mahieu, J. Mellqvist, L. Neef, J. Notholt, K. Petersen, I. Pison, O. Schneising, A.Strandberg, K. Strong, S. Szopa, J. Taylor, P. van Velthoven, M. van Weele, S. Wood, A comparison between Methane data products from 3D Chemistry Transport Models, SCIAMACHY and FTIR data from a quasi-global network, oral presentation (EGU2010-4593) at the EGU General Assembly 2010, Vienna, May 2-7, 2010.

Hendrick, F., M. Van Roozendael, M. De Mazière, C. Fayt, J. Granville, C. Hermans, P. V. Johnston, K. Kreher, J.-C. Lambert, and N. Theys, Long-term monitoring of stratospheric composition by UV-visible spectrometry and contribution to satellite validation, Workshop on "Spawning the Atmosphere Measurements of Jungfraujoch", Bern, Switzerland, 25-26/11/2008.

Jenouvrier A., Daumont L., Regalia-Jarlot L., Tyuterev Vl. G., Carleer M., Fally S., Vandaele A. C., Hermans C., Spectrométrie de la vapeur d'eau: mesures TF avec longs trajets d'absorption, Journées de Spectroscopie Moléculaire JSM, Lyon (France), 3-5 July 2006.

Kruglanski, M., M. De Mazière, A.-C. Vandaele, C. Hermans, B. Dils, G. Hermans, A. Joos de ter Beerst and A. Merlaud, Retrieval of formaldehyde from FTIR spectra: preliminary results, NDACC IRWG, Puerta de la Cruz, Tenerife, May 1-3, 2007.

Mahieu, E., Overview of existing high-level data products derived from high-resolution Fourier-Transform Infra-Red spectra recorded at the Jungfraujoch station, typical results and their valorisation, oral presentation at the Jungfraujoch Atmospheric Workshop, Swiss Academy of Sciences, 25 – 26 November 2008, Bern, Switzerland, 2008.

Mahieu E., P. Duchatelet and the GIRPAS-team, P.F. Bernath, C.D. Boone, K.A. Walker and the ACE-team, Q. Li, C.P. Rinsland, M. De Mazière and R. Sussmann, Time series of CO and CH_4 isotopologues at northern mid-latitudes based on ACE-FTS and Jungfraujoch products, ACE Science Team Meeting, University of Waterloo, May 11-13, 2009.

Mahieu, E., S.W. Wood, R. Lindenmaier, R. Batchelor, K. Strong and B. Dils, HCN retrievals: towards an homogenized approach? NDACC-IRWG meeting, IMK-IFU, Garmisch-Partenkirchen, 8-10 June, 2009.

Mahieu, E., the GIRPAS-team, C.P. Rinsland, M. Schneider, F. Hase, T. Blumenstock, J.-M. Hartmann, and the ACE-team, Recent investigations based on Jungfraujoch FTIR solar spectra, ACE science team meeting, University of Waterloo, 26-27 May 2010, Waterloo, Canada, 2010

Pinardi, G., M. Van Roozendael, F. Hendrick, C. Fayt, C. Hermans, M. De Mazière, Ground-based MAXDOAS NO_2 observations during the DANDELIONS campaigns: geometrical approximation and OMI and SCIAMACHY validation, Fourth DOAS Workshop, Hefei, China, March 30 – April 3, 2008.

Pinardi, G., K. Clémer, C. Hermans, C. Fayt, M. VanRoozendael, MAXDOAS observations in Beijing, AMFIC meeting, Barcelona, Spain, 24 June 2009.

Senten, C., M. De Mazière, C. Vigouroux, Data comparison: ground-based FTIR versus other sounders, results from a measurement campaign at Réunion Island, oral presentation at the STAR International Research School: Atmospheric research in Suriname, Paramaribo, Suriname, March 13-17, 2006.

Senten, C., M. De Mazière, C. Hermans, B. Dils, M. Kruglanski, E. Neefs, F. Scolas, A.C. Vandaele, C. Vigouroux, K. Janssens, B. Barret, M. Carleer, P.F. Coheur, S. Fally, J.L. Baray, R. Delmas, J.M. Metzger, and E. Mahieu, Ground-based FTIR measurement

campaigns at Ile de La Réunion: Campaign specifications, retrieval method and results, Réunion Island International Symposium, St-Gilles, November 5-9th, 2007.

Van Malderen, R., KMI-IRM conference talk, Exploitation of radiosonde relative humidity measurements at Ukkel, 12/12/2007.

Van Malderen, R., EGU 2008, Trend analysis of the radiosonde relative humidity measurements at Ukkel, Belgium, 18/04/2008.

Van Malderen R. and H. De Backer, Analysis of the upper tropospheric humidity trend from radiosondes at Ukkel, MeteoClim Symposium, Louvain-La-Neuve, 28 January 2009.

Van Malderen R. and H. De Backer, "Analysis of the upper-tropospheric humidity trend from radiosondes at Ukkel, Belgium", WaVaCs Workshop, Schliersee, Germany, 17 – 19 June 2009.

Van Malderen R. and H. De Backer, Analysis of the upper tropospheric humidity trend from radiosondes at Ukkel, MOCA-09, the IAMAS-IAPSO-IACS Joint Assembly on "Our warming planet", Montréal, Canada, 19-29 July 2009.

Van Roozendael, M., Tropospheric NO_2 from space: retrieval issues and perspectives for the future, ACCENT AT-2 workshop on Tropospheric NO_2 measured by satellites, KNMI, Utrecht, The Netherlands, 10-12 Sept. 2007.

Van Roozendael, M., K. Clémer, C. Fayt, F. Hendrick, C. Hermans, G. Pinardi and M. De Mazière, MAXDOAS: a new tool for the monitoring of the tropospheric composition, Workshop on "Spawning the Atmosphere Measurements of Jungfraujoch", Bern, Switzerland, 25-26/11/2008.

Van Roozendael, M., The Cabauw Intercomparison campaign of Nitrogen Dioxide measuring Instruments – an Introduction, CINDI Opening Event, Cabauw, Netherlands, 18 June 2009.

Vander Auwera J., Vibration-rotation line intensities for constituents of planetary atmospheres, invited plenary lecture at the XXIth Colloquium on High Resolution Molecular Spectroscopy, Castellammare di Stabia (Italie), September 2009.

Vander Auwera J., Precise measurements of line parameters in high resolution far-infrared spectra, invited plenary lecture at the CNRS workshop "New experimental and theoretical developments in molecular spectroscopy: atmospheric and astrophysical applications", Synchrotron SOLEIL, Gif-sur-Yvette (France), November 2010.

Vanhoenacker-Janvier D., Oestges, C., Montenegro-Villacieros, B., Van Malderen, R. and De Backer, H., Scintillation prediction using improved pre-processed radiosounding data, 3rd European Conference on Antennas and Propagation (EUCAP), Berlin, Germany, 23-27 March 2009.

Vigouroux, C., M. De Mazière, P. Demoulin, C. Servais, T. Blumenstock, M. Schneider, F. Hase, R. Kohlhepp, S. Barthlott, J. Klyft, J. Mellqvist, M. Palm, J. Notholt, T.Gardiner, Ozone tropospheric and stratospheric trends (1995-2008) over Western Europe from ground-based FTIR network observations, oral presentation (EGU2010-8500) at the EGU General Assembly 2010, Vienna, May 2-7, 2010.

Vigouroux, C., M. De Mazière, P. Demoulin, C. Servais, T. Blumenstock, M. Schneider, F. Hase, R. Kohlhepp, S. Barthlott, J. Klyft, J. Mellqvist, M. Palm, J. Notholt, T.Gardiner, Ozone tropospheric and stratospheric trends (1995-2008) over Western Europe from ground-based FTIR network observations, oral presentation at the NDACC-IRWG annual meeting, Murramarang, Australia, June 2-4, 2010 (presented by M. De Mazière).

Poster presentations at scientific conferences

Brinksma, E.J., E Celarier, P Veefkind, MO Wenig, D Ionov, F Goutail, EJ Bucsela, J Herman, A Cede, JF Gleason, F Boersma, M Sneep, M van Roozendael, G Pinardi, A Richter, T Wagner, PF Levelt, NO_2 Verification and Validation, EOS Aura Science Team meeting, NCAR Center Green facility, Boulder, Colorado, USA, 11-15 September 2006.

Cheymol, Anne and H. De Backer, Impact of aerosol particle concentration on UV index prediction, Proceedings of the UV conference "One century of UV radiation research", Edited by J. Gröbner, PMOD, Davos, Switzerland, p 81-82, 2007.

Clémer, K., C. Fayt, F. Hendrick, C. Hermans, G. Pinardi, M. Van Roozendael, The retrieval of aerosol extinction vertical profiles from MAXDOAS measurements: algorithm development and application, European Geosciences Union General Assembly 2008, Vienna, Austria, 19 – 24 April 2009.

Clémer, K., C. Hermans, M. De Mazière, H. Brenot, H. De Backer, R. Van Malderen, S. Fally, Intercomparison of integrated water vapor measurements from radiosonde, sunphotometer, FTIR, and GPS instruments, SPARC 4th General Assembly, Bologna, Italy, 31 August - 5 September, 2008

Clémer, K., G. Pinardi, Francois Hendrick and Michel Van Roozendael, MAXDOAS: a new ground-based remote-sensing tool for the monitoring of atmospheric composition, InfoDay for Universities, BIRA-IASB, Brussels, 28 Nov. 2008

Daumont L., A. Jenouvrier, L. Regalia-Jarlot, S. Fally, M. Carleer, C. Hermans, A. C. Vandaele, S. Mikhailenko, Fourier transform infrared spectroscopy of H_2O, HDO and D_2O: line parameters in the 5500-10800 cm^{-1} spectral region, 20th Colloquium on High Resolution Molecular Spectroscopy, Dijon, France, September 3-7 2007.

Daumont L., A. Jenouvrier, M. Carleer, S. Fally, C. Hermans, A. C. Vandaele, E. Starikova, S. Mikhailenko, High Resolution Fourier Transform Spectroscopy of Water Deuterated Species in the 5600 – 8800 cm^{-1} Region , The 21st Colloquium on High-Resolution Molecular Spectroscopy International Conference, August 31 - September 4, 2009, Castellammare di Stabia, Italy.

De Backer Hugo, Time series of daily erythemal UVB doses at Uccle, Belgium, Quadrennial ozone symposium, Tromso, Noorwegen, 29 Juni-5 Juli 2008

De Backer H. and R. Van Malderen, Time series of daily erythemal UVB doses at Ukkel, Belgium, MOCA-09, the IAMAS-IAPSO-IACS Joint Assembly on "Our warming planet", Montréal, Canada, 19-29 July 2009.

De Bock, V. and H. De Backer, Comparison of AOD values at 340nm from Brewer#178 and Cimel measurements at Uccle, Belgium, 12th WMO-GAW Brewer Users Group Meeting, Aosta, Italy, September 20-26, 2009.

De Bock, V., H. De Backer, A. Mangold, and A. Delcloo, Aerosol Optical Depth measurements at 340nm with a Brewer spectrophotometer and comparison with Cimel sunphotometer observations at Uccle, Belgium, 3rd MeteoClim PhD Symposium on Meteorology and Climatology, Uccle, Belgium, November 5, 2010.

De Mazière, M., C. Vigouroux, F. Hendrick, G. Vanhaelewyn, I. De Smedt, M. Van Roozendael, B. Dils, C. Hermans, M. Kruglanski, A. Merlaud, F. Scolas, C. Senten, M. Carleer, S. Fally, V. Duflot, J.M. Metzger, J.-L. Baray, R. Delmas, P. Duchatelet, Observations of halogens, CO, CH4, and HCHO at Ile de La Réunion from ground-based FTIR and MAXDOAS campaign measurements, 4th general Assembly of SCOUT-O_3, 21-24 April 2008, Alfred Wegener Institute, Potsdam, Germany, 2008.

Demoulin, P., S. Trabelsi, E. Mahieu, P. Duchatelet, C. Servais, and G. Roland, H2O retrievals from Jungfraujoch infrared spectra: some spectroscopic problems, poster presented at the *"8th Atmospheric Spectroscopy Applications"* meeting (ASA2008), 27 30 August 2008, Reims, France, 2008.

Dils, B., Ph. Demoulin, D. Folini, E. Mahieu, M. Steinbacher, B. Buchmann and M. De Mazière, Ground-based CO observations at the Jungfraujoch: Comparison between FTIR and NDIR in situ measurements, 2nd ACCENT Symposium, Urbino, Italy, July 23-27, 2007.

Dils, B., E. Mahieu, P. Demoulin, M, Steinbacher, B. Buchmann and M. De Mazière, Ground-based CO observations at the Jungfraujoch: comparison between FTIR and NDIR measurements, EGU 2008 General Assembly, 13 – 18 April 2008, Vienna, Austria.

Dils, B., M. De Mazière, C. Vigouroux, F. Forster, R.Sussmann, T.Borsdorff, P. Bousquet, T. Blumenstock, M. Buchwitz, S. Dalsoren, P.Demoulin, P. Duchatelet, C.Frankenberg, J. Hannigan, F. Hase, I.Isaksen, N. Jones, J.Klyft, I. Kramer, E. Mahieu, J. Mellqvist, L. Neef, J.Notholt, K. Petersen, I. Pison, O. Schneising, A.Strandberg, K. Strong,S. Szopa, J. Taylor, P. van Velthoven, M. van Weele, S. Wood, A comparison of Methane data products from Chemistry Transport Models, SCIAMACHY and a quasi-global network of FTIR stations, poster presentation at the NDACC-IRWG annual meeting, Murramarang, Australia, June 2-4, 2010.

Duchatelet, P., E. Mahieu, P. Demoulin, M. De Mazière, C. Senten, P. Bernath, C. Boone, K. Walker, Approaches for retrieving abundances of methane isotopologues in the frame of the AGACC project from ground-based FTIR observations performed at the Jungfraujoch, poster presented at the EGU General Assembly, Vienna (Austria), 15-20 April 2007, 2007.

Duchatelet, P., E. Mahieu, P. Demoulin, C. Frankenberg, F. Hase, J. Notholt, K. Petersen, P. Spietz, M, De Mazi贶 and C. Vigouroux, Impact of different spectroscopic datasets on CH_4 retrievals from Jungfraujoch FTIR spectra, *"8th Atmospheric Spectroscopy Applications"* meeting (ASA2008), 27-30 August 2008, Reims, France, 2008.

Duchatelet, P., E. Mahieu, R. Sussmann, F. Forster, T. Borsdorff, P.F. Bernath, C.D. Boone, K.A. Walker, M. De Mazière, and C. Vigouroux, Determination of isotopic fractionation $\delta^{13}C$ of methane from ground-based FTIR observations performed at the Jungfraujoch, poster presented at the EGU General Assembly, Vienna, April 2-24, 2009, 2009.

Duchatelet, P., E. Mahieu, R. Zander, and R. Sussmann, Trends of CO_2, CH_4 and N_2O over 1985-2010 from high-resolution FTIR solar observations at the Jungfraujoch station, poster presented at the EGU General Assembly, Vienna, May 2-7, 2010, 2010.

Fally, S., P.-F. Coheur, M. Carleer, D. Hurtmans, M. De Mazière, C. Hermans, K. Janssens, M. Kruglanski, E. Neefs, F. Scolas, A.C. Vandaele, C. Vigouroux, B. Barret, J. Leveau, J.M. Metzger, Water vapour retrievals from ground-based FTIR observations at Ile de La Réunion: Focus on isotopologues, Poster presented at the European Geosciences Union General Assembly, Vienna (Austria), 15-20 April 2007.

Fally S., Daumont L., Hermans C., Jenouvrier A., Vandaele A. C., Carleer, M., HDO and D_2O line parameters by Fourier Transform Infrared Spectroscopy: The 8800-11600 cm^{-1} spectral region, European Geosciences Union General Assembly, Vienna, Austria, 15-20 April 2007.

Fally S., H. Herbin, P.-F. Coheur, M. Carleer, D. Hurtmans, C. Senten, M. De Mazière, C. Hermans, B. Dils, M. Kruglanski, A. Merlaud, F. Scolas, C. Vigouroux, J.-L. Baray, J.-M. Metzger, R. Delmas, Ground-based and IASI satellite FTIR measurements of water vapour isotopologues above Ile de la Réunion, RiiS Reunion Island International Symposium, St-Gilles les Bains, Ile de la Réunion, 5-9 Nov. 2007.

Hains, J., H. Volten, E. Brinksma, F. Wittrock, A. Richter, T.Wagner, M. Van Roozendael, R. Dirksen, A. Piters, M. Kroon, and P. Levelt, Validation of OMI and SCIAMACHY tropospheric NO_2 columns using DANDELIONS ground-based data, European Geosciences Union General Assembly 2008, Vienna, Austria, 13 – 18 April 2008.

Hains, J., F. Boersma, M. Kroon, H. Volten, A. Richter, M. Van Roozendael, T. Wagner, R. Cohen, A. Perring, R. Dirksen and P. Levelt, Testing and Improving OMI Tropospheric NO_2 Using Observations from the DANDELIONS and INTEX-B Validation Campaigns, EGU 2009 General Assembly, Vienna, Austria, 19-24 April, 2009a.

Hains, J., K.F. Boersma, M. Kroon, H. Volten, R. Cohen, A. Perring, A. Richter, T. Wagner, M. Van Roozendael, R. Dirksen, P. Veefkind and P. Levelt, Testing and improving OMI tropospheric NO_2 using observations from the DANDELIONS and INTEX-B validation campaigns, AGU 2008 Fall Meeting, San Francisco, USA, 15-19 December 2009b.

Jenouvrier A., Daumont L., Fally S., Carleer M., Vandaele A. C., Mikhailenko S. N., Starikova E. N., Long path FTS spectra of deuterated water vapour: new data for HDO molecule in the 8800-9100 cm^{-1} spectral region. Poster presented at the XVth Symposium on High Resolution Molecular Spectroscopy, Nizhny Novgorod, 18-21 July 2006.

Jenouvrier A., Fally S., Vandaele A. C., Naumenko O. V., Leshchishina O., Shirin S. V., The Fourier transform absorption spectrum of the D216O molecule in the 10000-13200 cm-1 spectral region, Poster presented at the XVth Symposium on High Resolution Molecular Spectroscopy, Nizhny Novgorod, 18-21 July 2006.

Lacour, J.-L., H. Herbin, D. Hurtmans, L. Clarisse, P.-F. Coheur, S. Fally, C. Hermans, M. De Mazière, Measurements of water isotopologues from IASI and ground-based FTIR at a subtropical site in the southern hemisphere, poster presentation at the Second IASI international conference (25-29 January 2010, Sévrier, France), 2010.

Litynska, Zenobia, H. De Backer, P. Koepke, A.W. Schmalwieser, J. Gröbner and +40 members, COST726: Long term changes and climatology of UV radiation over Europe, EGU General Assembly, Vienna, Geophysical Research Abstracts, Vol. 9, 08151, 2007. SRef-ID: 1607-7962/gra/EGU2007-A-08151.

Maenhaut, W., W. Wang, X. Chi, N. Raes, J. Cafmeyer, A. Cheymol, A. Delcloo, V. De Bock, and H. De Backer, Measurements on Atmospheric Aerosols and of the Aerosol Optical Depth during 2006 at Uccle, Belgium, 11th Science Conference of the International Global Atmosphere Chemistry (IGAC) Project, Halifax, Canada, July 11-16, 2010.

Mahieu, E., Curtis P. Rinsland, Tom Gardiner, Rodolphe Zander, Philippe Demoulin, Martyn P. Chipperfield, Roland Ruhnke, Linda S. Chiou, Martine De Mazière and the GIRPAS Team, Recent trends of inorganic chlorine and halogenated source gases above the Jungfraujoch and Kitt Peak stations derived from high-resolution FTIR solar observations, poster presentation (EGU2010-2420) at the EGU General Assembly 2010, Vienna, May 2-7, 2010.

Mahieu, E., P. Duchatelet, P. Demoulin, C. Servais, M. De Mazière, C. Senten, C.P. Rinsland, P. Bernath, C.D. Boone, K.A. Walker, Retrievals of HCN from high-resolution FTIR solar spectra recorded at the Jungfraujoch station, poster presented at the EGU General Assembly, Vienna (Austria), 15-20 April 2007.

Mahieu, E., P. Duchatelet, P. Bernath, C.D. Boone, M. De Mazière, P. Demoulin, C.P. Rinsland, C. Servais and K.A. Walker, Retrievals of C_2H_2 from high-resolution FTIR solar spectra recorded at the Jungfraujoch station and comparison with ACE-FTS observations, poster presented at the EGU General Assembly, Vienna, April 13-18, 2008, 2008.

Mahieu, E., P. Duchatelet, C.P. Rinsland, Q. Li, C.D. Boone, K.A. Walker, P.F. Bernath, M. De Mazière, B. Dils and the GIRPAS Team, Time series of ^{12}CO and ^{13}CO at northern mid-latitudes: determination of partial column and $\delta^{13}C$ seasonal and interannual variations, poster presented at the EGU General Assembly, Vienna, April 2-24, 2009, 2009.

Perrin A., J. Vander Auwera, First list of line positions and intensities for the n3 band of trans-formic acid near 5.6 micrometer, The 20th International Conference on High Resolution Molecular Spectroscopy, Prague (Czech Republic), September 2008.

Petersen, A.K., T. Blumenstock, B. Dils, F. Hase , C. Hermans, M. De Mazière, J. Notholt, M. Schneider, T. Warneke, Ground-based FTIR observations at the tropical and subtropical NDACC stations Paramaribo, Tenerife Is. and Ile de la Réunion, SCOUT-O3 final meeting, Schliersee, Duitsland, June 15-17, 2009.

Pinardi, G. M. Van Roozendael, C. Fayt, C. Hermans, M. De Mazière, Multi-Axis DOAS Measurements During Format And Dandelions Campaigns, Third International DOAS Workshop 2006, University of Bremen, Bremen, Germany, 20-22 March 2006.

Pinardi, G., M. Van Roozendael, C. Fayt, C. Hermans, A. Merlaud, M. De Mazière, E. Brinksma, E. Celarier, OMI NO_2 validation by ground-based Multi Axis DOAS and Direct Sun observations during the DANDELIONS campaigns, EGU General Assembly 2007, Vienna, Austria, 15-20 April, 2007.

Pinardi, G., M. Van Roozendael, C. Fayt , C. Hermans, A. Merlaud, M. De Maziere, E. Brinksma, E.Celarier, OMI and SCIAMACHY NO_2 validation by ground-based Multi Axis DOAS and Direct Sun observations during the DANDELIONS campaigns, 2nd ACCENT Symposium, Urbino, Italy, 23-27 July 2007.

Pinardi, G., M. Van Roozendael, F. Hendrick, C. Fayt, C. Hermans, A. Merlaud, M. De Mazière, OMI and SCIAMACHY NO_2 validation by ground-based Multi Axis and Direct Sun DOAS observations during the DANDELIONS campaigns, ACCENT AT-2 workshop on Tropospheric NO_2 measured by satellites, KNMI, Utrecht, The Netherlands, 10-12 Sept. 2007.

Pinardi, G., F. Hendrick, K. Clémer, J.C. Lambert, J. Bai, M. Van Roozendael , On the use of the MAXDOAS technique for the validation of tropospheric NO_2 columns measurements from satellites, EUMETSAT Conference, Darmstadt, Germany, 9 - 12/09, 2008.

Rotger M., V. Boudon and J. Vander Auwera, Line positions and intensities in the n_{12} band of ethylene near 1450 cm^{-1}: an experimental and theoretical study, 10th Biennial Hitran Database Conference, Harvard (USA), June 2008.

Rotger M., L. Régalia, V. Boudon, J. Vander Auwera, 2009, Intensity analysis of the 10 μm band system of ethylene, The 21st Colloquium on High-Resolution Molecular

Spectroscopy International Conference, August 31-September 4, 2009, Castellammare di Stabia (Italy).

Schneider, M., F. Hase, T. Blumenstock, R. Lindenmaier, K. Strong, J. Notholt, M. Palm, T. Warneke, P. Demoulin, E. Mahieu, G. Mengistu Tsidu, N. Deutscher, D. Griffith, D. Smale, and S. Wood, A network for monitoring tropospheric H_2O and δD^* profiles, poster presented at the NDACC-IRWG annual meeting, June 2-7, Murramarang, Australia, 2010

Schönhardt, A., F. Wittrock, A. Richter, H.Oetjen, J. P. Burrows, G. Pinardi, M. Van Roozendael, T. Wagner, O. Ibrahim, H. Bergwerff, S. Berkhout, R. v.d. Hoff, H. Volten, D. Swart and E. Brinksma, MAXDOAS measurements from the DANDELIONS campaigns, 2007 Annual Conference of the German Physical Society, Regensburg, Germany, March 26 – 30, 2007.

Senten, C., M. De Mazière, C. Hermans, B. Dils, A. Merlaud, M. Kruglanski, E. Neefs, F. Scolas, A.C. Vandaele, C. Vigouroux, K. Janssens, B. Barret, M. Carleer, P.-F. Coheur, S. Fally, J.L. Baray, J. Leveau, J.M. Metzger, E. Mahieu., Ground-based FTIR measurements at Ile de La Réunion: Observations, error analysis and comparisons with satellite data, Poster presented at the European Geosciences Union General Assembly, Vienna (Austria), 15-20 April 2007, Vienna, Austria, 2007.

Senten, C., M. De Mazière, C. Hermans, B. Dils, M. Kruglanski, A. Merlaud, E. Neefs, F. Scolas, A.C. Vandaele, C. Vigouroux, K. Janssens, B. Barret, M. Carleer, P.F. Coheur, S. Fally, J.L. Baray, Leveau, J.M. Metzger, E. Mahieu, Ground-based FTIR measurements at Ile de La Réunion: Observations, error analysis and comparisons with satellite data, Third SCOUT-O_3 Annual Meeting, Heraklion, Crete, Greece, 7-11 May 2007.

Senten, C., Martine De Mazière, Gauthier Vanhaelewyn, Corinne Vigouroux, and Robert Delmas Information operator approach applied to the retrieval of vertical distributions of atmospheric constituents from ground-based FTIR measurements, poster presentation (EGU2010-3479) at the EGU General Assembly 2010, Vienna, May 2-7, 2010; poster presentation at the NDACC-IRWG annual meeting, Murramarang, Australia, June 2-4, 2010.

Van Malderen, R., Poster presentation with title 'Exploitation of radiosonde relative humidity measurements at Ukkel' at the MeteoClim symposium in Leuven (10/10/2007) (KMI-IRM)

Van Malderen Roeland and H. De Backer, Trend analysis of the radiosonde relative humidity measurements at Uccle, Belgium, EGU assembly, Vienna, Austria, 13-18 April 2008.

Van Malderen, R. and H. De Backer, Analysis of the upper-tropospheric humidity trend from radiosondes at Uccle, Belgium, WaVaCs Workshop, Schliersee, Germany, June 17-19, 2009.

Van Malderen, R. and H. De Backer, A drup in UT humidity in Autumn 2001, as derived from radiosonde measurements at Uccle, Belgium, Carges International School on Water Vapour in the Climate System, Cargèse, France, September 14-26, 2009.

Vander Auwera J., K. Didriche, A. Perrin and F. Keller, Quantitative spectroscopy of formic acid leading to an improved database in the 9 micron spectral region, The 20th Colloquium on High Resolution Molecular Spectroscopy, Dijon, France, September 3-7 2007.

Vanhaelewyn, G., Pierre Duchatelet, Corinne Vigouroux, Bart Dils, Nicolas Kumps, Christian Hermans, Philippe Demoulin, Emmanuel Mahieu, Ralf Sussmann, and Martine De Mazière, Comparisons of the error budgets associated with ground-based FTIR measurements of atmospheric CH4 profiles at Île de la Réunion and Jungfraujoch, poster presentation (EGU2010-15537) at the EGU General Assembly 2010, Vienna, May 2-7, 2010; poster presentation at the NDACC-IRWG annual meeting, Murramarang, Australia, June 2-4, 2010.

Vigouroux, C., N. Theys, M. De Mazière, M. Van Roozendael, C. Senten, C. Hermans, M. Kruglanski, A.C. Vandaele, E. Neefs, F. Scolas, F. Hendrick, C. Fayt, S. Fally, M. Carleer, P.F. Coheur, and J. Leveau, Solar absorption FTIR and UV-visible MAXDOAS observations at the Ile de La Réunion, poster presentation at the SCOUT-O3 annual meeting (Zurich, Switzerland), March 20-24, 2006.

Vigouroux, C., M. De Mazière, M. Van Roozendael, I. De Smedt, B. Dils, F. Hendrick, C. Hermans, M. Kruglanski, A. Merlaud, E. Neefs, F. Scolas, C. Senten, S. Fally, M. Carleer, P.-F. Coheur, J.M. Metzger, J.-L. Baray, R. Delmas, P. Duchatelet, Observations of CH_4, CH_3D and HCHO at Ile de La Réunion from ground-based FTIR and MAXDOAS campaign measurements, poster presentation at the Réunion Island International Symposium, St-Gilles, November 5-9th, 2007; submitted for publication in the Symposium Proceedings.

Vigouroux, C., M. De Mazière, I. De Smet, B. Dils, F. Hendrick, C. Hermans, M. Kruglanski, A. Merlaud, J.-F. Müller, E. Neefs, F. Scolas, C. Senten, T. Stavrakou, M. Van Roozendael, S. Fally, J.-M. Metzger, Formaldehyde at Ile de La Réunion from ground-based FTIR and MAXDOAS measurements; comparisons with SCIAMACHY and with the CTM IMAGES, IGAC 10th International Conference Symposium, Annecy, France, September 7-12, 2008.

Vigouroux, C., F. Hendrick, T. Stavrakou, B. Dils, I. De Smedt, C. Hermans, A. Merlaud, F. Scolas, C. Senten, G. Vanhaelewyn, S. Fally, M. Carleer, J.-M. Metzger, J.-F. Müller, M. Van Roozendael, and M. De Mazière, Ground-based FTIR and MAXDOAS observations of formaldehyde at Réunion Island and comparisons with SCIAMACHY and the CTM IMAGES, ESA Atmospheric Science Conference, Barcelona, Sept. 7-11, 2009.

Vigouroux, C., Martine De Mazière, Bart Dils, Jean-François Müller, Cindy Senten, Trissevgeni Stavrakou, Gauthier Vanhaelewyn, Sophie Fally, Valentin Duflot, Jean-Luc Baray and the Instrumental Support Team, Time-series of biomass burning products from ground-based FTIR measurements at Reunion Island (21°S, 55°E) and comparisons with the CTM IMAGES, poster presentation (EGU2010-4751) at the EGU General Assembly 2010, Vienna, May 2-7, 2010; poster presentation at the NDACC-IRWG annual meeting, Murramarang, Australia, June 2-4, 2010.

V PUBLICATIONS

Peer-reviewed

2006

Baray, Jean-Luc, J. Leveau, S. Baldy, J. Jouzel, P. Keckhut, G. Bergametti, G. Ancellet, H. Bencherif, B. Cadet, M. Carleer, C. David, M. De Mazière, D. Faduilhe, S. Godin Beekmann, P. Goloub, F. Goutail, JM. Metzger, B. Morel, JP. Pommereau, J. Porteneuve, T. Portafaix, F. Posny, L. Robert and M. Van Roozendael, 2006, An instrumented station for the survey of ozone and climate change in the southern tropics, doi: 10.1039/b607762e, J. Environ. Monit., 8, 1-9.

Cheymol, A., H. De Backer, W. Josefsson, and R. Stübi, 2006, Comparison and validation of the aerosol optical depth obtained with the Langley plot method in the UV-B from Brewer Ozone Spectrophotometer measurements, J. Geophys. Res., 111, D16202, doi:10.129/2006JD007131.

Naumenko O. V., O. Leshchishina, S. Shirin, A. Jenouvrier, S. Fally, A. C. Vandaele, E. Bertseva, A. Campargue, 2006, Combined analysis of high sensitivity Fourier transform and ICLAS-VeCSEL absorption spectra of D_2O between 8800 and 9520 cm^{-1}, J. Mol. Spectrosc., 238(1) 79-90.

Simon, P. C., M. De Mazière, M. Van Roozendael and J-C. Lambert, 2006, An integrated approach to study the chemistry-climate interactions in the atmosphere, in Proceedings of the NATO Advanced Research Workshop on Remote Sensing of the Atmosphere for Environmental Security, Rabat, Morocco, 16-19 November 2005, NATO Security through Science Series C: Environmental Security, Springer, 329-343.

2007

Jenouvrier A., L. Daumont, L. Régalia-Jarlot, V. Tyuterev, M. Carleer, A. C. Vandaele, S. Mikhailenko, S. Fally, 2007, Fourier Transform measurements of water vapour line parameters in the 4200-6600 cm^{-1} region, J. Quant. Spectrosc. Radiat. Transfer,105, 326-355.

Neefs, E., M. De Mazière, F. Scolas, C. Hermans and T. Hawat, 2007, BARCOS an automation and remote control system for atmospheric observations with a Bruker interferometer, Rev. Sc. Instrum., 78, 035109-1 to -8.

Perrin A. and J. Vander Auwera, 2007, An improved database for the 9 µm region of the formic acid spectrum, J. Quant. Spectrosc. Radiat. Transfer 108, 363-370.

Rinsland, C.P., A. Goldman, J.W. Hannigan, S.W. Wood, L.S. Chiou and E. Mahieu, 2007, Long-term trends of tropospheric carbon monoxide and hydrogen cyanide from analysis of high resolution infrared solar spectra, J. Quant. Spectrosc. Radiat. Transfer, 104, 40-51.

Vander Auwera J., K. Didriche, A. Perrin, F. Keller, 2007, Absolute line intensities for formic acid and dissociation constant of the dimer, J. Chem. Phys. 126, 124311/1-124311/9.

Voronin B., O.V. Naumenko, M. Carleer, P.F. Coheur, S. Fally, A. Jenouvrier, R.N. Tolchenov, A.C. Vandaele, J. Tennyson, 2007, Assignment of the HDO Fourier

Transform absorption spectrum between 11500 and 23000 cm^{-1}. J. Mol. Spectrosc., 244, pp90-104, doi: 10.1016/j.jms.2007.03.008.

Wagner, T., J. P. Burrows, T. Deutschmann, B. Dix, C. von Friedeburg, U. Friess, F. Hendrick, K.-P. Heue, H. irie, H. Iwabuchi, Y. Kanaya, J. Keller, C. A. Mc Linden, H. Oetjen, E. Palazzi, A. Petritoli, U. Platt, O. Postylyakov, J. Pukite, A. Richter, M. Van Roozendael, A. Rozanov, R. Sinreich, S. Sanghavi, and F. Wittrock, 2007, Comparison of box-air-mass-factors and radiances for multiple-axis differential optical absorption spectroscopy (MAXDOAS) geometries calculated from different UV/visible radiative transfer models, Atmos. Chem. Phys., 7, 1809-1833.

2008

Brinksma, E. J., G. Pinardi, R. Braak, H. Volten, A. Richter, A. Schoenhardt, M. E. J. an Roozendael, C. Fayt, C. Hermans, R. J. Dirksen, T. Vlemmix, A. J. C. Berkhout, D. P. J. Swart, H. Oetjen, F. Wittrock, T. Wagner, O. W. Ibrahim, G. de Leeuw, M. Moerman, R. L. Curier, E. A. Celarier, W. H. Knap, J. P. Veefkind, H. J. Eskes, M. Allaart, R. Rothe, A. J. M. Piters, and P. F. Levelt, 2008, The 2005 and 2006 DANDELIONS NO_2 and aerosol intercomparison campaigns, J. Geophys. Res., 113, D16S46, doi:10.1029/2007JD008808.

Carleer M. R., C. D. Boone, K. A. Walker, P. F. Bernath, K. Strong, R. J. Sica, C. E. Randall, H. Vömel, J. Kar, M. Höpfner, M. Milz, T. von Clarmann, R. Kivi, J. Valverde-Canossa, C. E. Sioris, M. R. M. Izawa, E. Dupuy, C. T. McElroy, J. R. Drummond, C. R. Nowlan, J. Zou, F. Nichitiu, S. Lossow, J. Urban, D. Murtagh, D. G. Dufour, 2008, Validation of water vapour profiles from the Atmospheric Chemistry Experiment (ACE), Atmos. Chem. Phys. Discuss., 8, 4499–4559.

Celarier, E. A., E. J. Brinksma, J. F. Gleason, J. P. Veefkind, A. Cede, J. R. Herman, D. Ionov, F. Goutail, J.-P. Pommereau, J.-C. Lambert, M. van Roozendael, G. Pinardi, F. Wittrock, A. Schönhardt, A. Richter, O. W. Ibrahim, T. Wagner, B. Bojkov, G. Mount, E. Spinei, C. M. Chen, T. J. Pongetti, S. P. Sander, E. J. Bucsela, M. O. Wenig, D. P. J. Swart, H. Volten, M. Kroon, and P. F. Levelt, 2008, Validation of Ozone Monitoring Instrument nitrogen dioxide columns, J. Geophys. Res., 113, D15S15, doi:10.1029/2007JD008908.

Jacquinet-Husson, N., Scott, N. A., Chedina, A., Crepeau, L., Armante, R., Capelle, V., Orphal, J., Coustenis, A., Boonne, C., Poulet-Crovisier, N., Barbee, A., Birk, M., Brown, L. R., Camy-Peyret, C., Claveau, C., Chance, K., Christidis, N., Clerbaux, C., Coheur, P. F., Dana, V., Daumont, L., De Backer-Barilly, M. R., Di Lonardo, G., Flaud, J. M., Goldman, A., Hamdouni, A., Hess, M., Hurley, M. D., Jacquemart, D., Kleiner, I., Kopke, P., Mandin, J. Y., Massie, S., Mikhailenko, S., Nemtchinov, V., Nikitin, A., Newnham, D., Perrin, A., Perevalov, V. I., Pinnock, S., Regalia-Jarlot, L., Rinsland, C. P., Rublev, A., Schreier, F., Schult, L., Smith, K. M., Tashkun, S. A., Teffo, J. L., Toth, R. A., Tyuterev, V. G., Vander Auwera, J., Varanasi, P., and Wagner, G., 2008, The GEISA spectroscopic database: Current and future archive for Earth and planetary atmosphere studies, J. Quant. Spectrosc. Radiat. Transfer, 109, 1043-1059.

Reimann, S., M.K. Vollmer, D. Folini, M. Steinbacher, M. Hill, R. Zander and E. Mahieu, 2008, Observations of Long-Lived Anthropogenic Halocarbons at the High-Alpine site of Jungfraujoch (Switzerland) for Assessment of Trends and European Sources, Sci. Tot. Environ., 391, 224-231.

Rotger, M., V. Boudon, J. Vander Auwera, 2008, Line positions and intensities in the ν_{12} band of ethylene near 1450 cm^{-1}: An experimental and theoretical study, J. Quant. Spectrosc. Radiat. Transfer 109, 952–962.

Senten, C., M. De Mazière, B. Dils, C. Hermans, M. Kruglanski, E. Neefs, F. Scolas, A. C. Vandaele, G. Vanhaelewyn, C. Vigouroux, M. Carleer, P. F. Coheur, S. Fally, B. Barret, J. L. Baray, R. Delmas, J. Leveau, J. M. Metzger, E. Mahieu, C. Boone, K. A. Walker, P. F. Bernath, and K. Strong, 2008, Technical Note: Ground-based FTIR measurements at Ile de La Réunion: Observations, error analysis and comparisons with satellite data, Atmos. Chem. Phys., 8, 3483-3508.

Vigouroux, C., M. De Mazière, P. Demoulin, C. Servais, F. Hase, T. Blumenstock, I. Kramer, M. Schneider, J. Mellqvist, A. Strandberg, V. Velazco, J. Notholt, R. Sussmann, W. Stremme, A. Rockmann, T. Gardiner, M. Coleman, and P. Woods, 2008, Evaluation of tropospheric and stratospheric ozone trends over Western Europe from ground-based FTIR network observations, Atmos. Chem. Phys., 8, 6865–6886.

Zander, R., E. Mahieu, P. Demoulin, P. Duchatelet, G. Roland, C. Servais, M. De Mazière, S. Reimann and C.P. Rinsland, 2008, Our changing atmosphere: Evidence based on long-term infrared solar observations at the Jungfraujoch since 1950, Sci. Tot. Environ., 391, 184-195.

2009

Cheymol, Anne, L. Gonzalez Sotelino, K.S. Lam, J. Kim, V. Fioletov, A.M. Siani and H. De Backer, 2009, Intercomparison of Aerosol Optical Depth from Brewer Ozone Spectrophotometer and CIMEL Sunphotometer measurements, Atmos. Chem. Phys., 9, 733-741.

De Backer, Hugo, 2009, Time series of daily erythemal doses at Ukkel, Belgium, Int. J. Remote Sensing, volume 30, issue 1516, 4145-4151, doi: 10.1080/01431160902825032.

Laj, P., J. Klausen, M. Bilde, C. Plaβ-Duelmer , G. Pappalardo, C. Clerbaux, U. Baltensperger, J. Hjorth , D. Simpson, S. Reimann , P.-F. Coheur , A. Richter, M. De Mazière, Y. Rudich, G. McFiggans, K. Torseth, A. Wiedensohler, S. Morin , M. Schulz, J. Allan, J.- L. Attié, I. Barnes, W. Birmilli, P. Cammas, J. Dommen, H.-P. Dorn, D. Fowler, J.- S. Fuzzi, M. Glasius, C. Granier, M. Hermann, I. Isaksen, S. Kinne , I. Koren, F. Madonna, M. Maione, A. Massling, O. Moehler, L. Mona, P. Monks, D. Müllerr , T. Müller, J. Orphal, V.-H. Peuch, F. Stratmann, D. Tanré, G. Tyndall, A. A. Riziq, M. Van Roozendael, P. Villani, B. Wehner, H. Wex, A. A. Zardini, 2009, Measuring Atmospheric Composition Change, Atmospheric Environment, 43, 5351-5414.

Li, Q., P.I. Palmer, H.C. Pumphrey, P. Bernath, and E. Mahieu, 2009, What drives the observed variability of HCN in the troposphere and lower stratosphere?, Atmos. Chem. Phys., 9, 8531-8543.

Mikhailenko S. N., S.A. Tashkun, T.A. Putilova, E.N. Starikova, L. Daumont, A. Jenouvrier, S. Fally, M. Carleer, C. Hermans, A.C. Vandaele, 2009, Critical evaluation of measured rotation-vibration transitions and an experimental dataset of energy levels of HD18O, J. Quant. Spectrosc. Radiat. Transfer 110, 597–608.

Perrin, A., J. Vander Auwera, and Z. Zelinger, Z., 2009, High-resolution Fourier transform study of the ν_3 fundamental band of trans-formic acid, J. Quant. Spectrosc. Radiat. Transfer, 110, 743-755.

Rothman, L. S., L.R. Brown, and J. Vander Auwera, 2009a, SPECIAL ISSUE HITRAN Preface, J. Quant. Spectrosc. Radiat. Transfer, 110, 531-532.

Rothman, L. S., I.E. Gordon, A. Barbe, D.C. Benner, P.E. Bernath, M. Birk, V. Boudon, L.R. Brown, A. Campargue, J.P. Champion, K. Chance, L.H. Coudert, V. Dana, V.M. Devi, S. Fally, J.M. Flaud, R.R. Gamache, A. Goldman, D. Jacquemart, I. Kleiner, N. Lacome, W.J. Lafferty, J.Y. Mandin, S.T. Massie, S.N. Mikhailenko, C. Miller, N. Moazzen-Ahmadi, O.V. Naumenko, A.V. Nikitin, J. Orphal, V.I. Perevalov, A. Perrin, A. Predoi-Cross, C.P. Rinsland, M. Rotger, M. Simeckova, M.A. Smith, K. Sung, S.A. Tashkun, J. Tennyson, R.A. Toth, A.C. Vandaele, and J. Vander Auwera, 2009b, The HITRAN 2008 molecular spectroscopic database, J. Quant. Spectrosc. Radiat. Transfer, 110, 533-572.

Sussmann, R., T. Borsdorff, M. Rettinger, C. Camy-Peyret, P. Demoulin, P. Duchatelet, E. Mahieu, and C. Servais, 2009, Technical Note: Harmonized retrieval of column-integrated atmospheric water vapor from the FTIR network – first examples for long-term records and station trends, Atmos. Chem. Phys., 9, 8987-8999.

Tennyson J., P. F. Bernath, L. R. Brown, A. Campargue, M. R. Carleer, A. G. Császár, R. R. Gamache, J. T. Hodges, A. Jenouvrier, O. V. Naumenko, O. L. Polyansky, L. S. Rothman, R. A. Toth, A. C. Vandaele, N. F. Zobov, L. Daumont, A. Z. Fazliev, T. Furtenbacher, I. F. Gordon, S. N. Mikhailenko, S. V. Shirin, B. A. Voronin, 2009, IUPAC Critical Evaluation of the Rotational-Vibrational Spectra of Water Vapor, Part I. Energy Levels and Transition Wavenumbers for $H_2{}^{17}O$ and $H_2{}^{18}O$ J. Quant. Spectrosc. Radiat. Transfer 110, 573–596.

Vigouroux, C., F. Hendrick, T. Stavrakou, B. Dils, I. De Smedt, C. Hermans, A. Merlaud, F. Scolas, C. Senten, G. Vanhaelewyn, S. Fally, M. Carleer, J.-M. Metzger, J.-F. Müller, M. Van Roozendael, and M. De Mazière, 2009, Ground-based FTIR and MAXDOAS observations of formaldehyde at Réunion Island and comparisons with satellite and model data, Atmos. Chem. Phys., 9, 9523-9544.

2010

Clémer, K., M. Van Roozendael, C. Fayt, F. Hendrick, C. Hermans, G. Pinardi, R. Spurr, P. Wang, and M. De Mazière, 2010, Multiple wavelength retrieval of tropospheric aerosol optical properties from MAXDOAS measurements in Beijing, Atmos. Meas. Tech., 3, 863–878.

De Bock, V., H. De Backer, A. Mangold, and A. Delcloo, 2010, Aerosol Optical Depth measurements at 340nm with a Brewer spectrophotometer and comparison with Cimel observations at Uccle, Belgium, Atmos. Meas. Tech., 3, 1577-1588, doi:10.5194/amt-3-1577-2010.

Duflot, V., Dils, B., Baray, J.L., De Mazière, M., Attié, J.L., Vanhaelewyn, G., Senten, C.,Vigouroux, C., Clain, G., Delmas, R., 2010, Analysis of the origin of the distribution of CO in the subtropical southern Indian Ocean, J. Geophys. Res., 115, D22106, doi:10.1029/2010JD013994.

Hains, J.C. et al. (19 authors), 2010, Testing and improving OMI DOMINO tropospheric NO2 using observations from the DANDELIONS and INTEX-B validation campaigns, J. Geophys. Res. 115, D05301, doi:10.1029/2009JD012399

Paulot, F., D. Wunch, J. D. Crounse, D. B. Millet, P. F. DeCarlo, G. Gonzàlez Abad, G. C. Toon, J. Notholt, T. Warneke, C. Vigouroux, N. Deutscher, J. W. Hannigan, J. A. de Gouw, M. De Mazière, D. W. T. Griffith, J. L. Jimenez, P. Bernath, and P. O. Wennberg, 2010, Importance of secondary sources in the atmospheric budgets of formic and acetic acids, Atmos. Chem. Phys. Discuss., 10, 24435-24497.

Roscoe, H. K. et al. (50 authors), 2010, Intercomparison of slant column measurements of NO_2 and O_4 by MAXDOAS and zenith-sky UV and visible spectrometers, Atmos. Meas. Tech. Discuss., 3, 3383-3423, 2010, doi:10.5194/AMTD-3-3383-2010

Van Malderen, R., and H. De Backer, 2010, A drop in upper tropospheric humidity in autumn 2001, as derived from radiosonde measurements at Uccle, Belgium, J. Geophys. Res, 115, D20114, doi:10.1029/2009JD013587.

Zander R., P. Duchatelet, E. Mahieu, P. Demoulin, G. Roland, C. Servais, J. Vander Auwera, A. Perrin, C. P. Rinsland, and P. Crutzen, 2010, Formic acid (HCOOH) above the Jungfraujoch during 1985-2007 : observed variability, seasonality, but no long-term background evolution, Atmos. Chem. Phys. 10, 10047-10065.

Zieger, P., E. Weingartner, J. Henzing, M. Moerman, G. de Leeuw, J. Mikkila, K. Clémer, M. Van Roozendael, S. Yilmaz, U. Frieß, H. Irie, T. Wagner, R. Shaiganfar, S. Beirle, A. Apituley, K. Wilson, and U. Baltensperger, Comparison of ambient aerosol extinction coefficients obtained from in-situ, MAXDOAS and LIDAR measurements, Atmos. Chem. Phys. Discuss., 10, 29683-29734, 2010.

In press, submitted or in preparation

Irie, H, H. Takashima, Y. Kanaya, K. F. Boersma, L. Gast, F. Wittrock, D. Brunner, Y. Zhou, and M. Van Roozendael, Eight-component retrievals from ground-based MAXDOAS observations, submitted to Atmos. Meas. Tech. Discuss. (2010)

Piters, A.M.J., et al (73 authors), The Cabauw Intercomparison campaign for Nitrogen Dioxide Measuring Instruments (CINDI): Design, Execution, and First Results, to submitted to Atmos. Meas. Tech. Discuss. (2011)

Schneider, M., P. Demoulin, R. Sussmann, J. Notholt, Fourier Transform Infrared Spectrometry, in *Ground-based remote sensing and in-situ methods for monitoring atmospheric water vapour*, book to be published by the International Space Science Institute, Bern, 2011.

Vigouroux, C., et al., Ground-based FTIR observations of biomass burning products above Ile de La Réunion, in preparation for submission in the 2nd half of 2011 (C. Vigouroux is on maternity leave until June 2011).

Not peer-reviewed

2006

Cheymol, A., H. De Backer, A. Mangold, R. Lemoine, A. Delcloo, J. Cafmeyer, and W. Maenhaut, 10-15 September 2006, Aerosol Optical Depth and Aerosol Characterisation in 2006 at Ukkel (Belgium), Proceedings of International Aerosol Conference, Saint Paul, USA.

Maenhaut, W., W. Wang, N. Raes, X. Chi, A. Cheymol, and H. De Backer, September 2006, Atmospheric Aerosol Characterisation and Aerosol Optical Depth during 2006 at Ukkel, Belgium, Proceedings of IGAC, Cape Town, South Afrika.

2007

Mahieu, E., C. Servais, P. Duchatelet, R. Zander, P. Demoulin, M. De Mazière, C. Senten, K.A. Walker, C.D. Boone, C.P. Rinsland and P. Bernath, 2007, Optimisation of retrieval strategies using Jungfraujoch high-resolution FTIR observations for long-term trend studies and satellite validation, in Observing Tropospheric Trace Constituents from Space, ACCENT-TROPOSAT-2 in 2006-7, Eds., 280-285.

Mahieu, E., P. Duchatelet, P. Demoulin, C. Servais, M. De Mazière, C. Senten, C.P. Rinsland, P. Bernath, C.D. Boone, K.A. Walker, 2007, Retrievals of HCN from high-resolution FTIR solar spectra recorded at the Jungfraujoch station, Geophysical Research Abstracts, Vol. 9, 07059.

Senten, C., M. De Mazière, C. Hermans, B. Dils, A. Merlaud, M. Kruglanski, E. Neefs, F. Scolas, A.C. Vandaele, C. Vigouroux, K. Janssens, B. Barret, M. Carleer, P.-F. Coheur, S. Fally, J.L. Baray, J. Leveau, J.M. Metzger, E. Mahieu., 2007, Ground-based FTIR measurements at Ile de La Réunion: Observations, error analysis and comparisons with satellite data, European Geosciences Union General Assembly, 15-20 April 2007, Vienna, Austria, Geophysical Research Abstracts, Vol. 9, 08640.

2008

Demoulin, P., S. Trabelsi, E. Mahieu, P. Duchatelet, C. Servais, and G. Roland, 2008, H_2O retrievals from Jungfraujoch infrared spectra: some spectroscopic problems, in the Proceedings of the "8th Atmospheric Spectroscopy Applications" meeting (ASA2008), 27 – 30 August, Reims, France.

Duchatelet, P., E. Mahieu, P. Demoulin, C. Frankenberg, F. Hase, J. Notholt, K. Petersen, P. Spietz, M. De Mazière and C. Vigouroux, 2008, Impact of different spectroscopic datasets on CH_4 retrievals from Jungfraujoch FTIR spectra, Proceedings of the 8th Atmospheric Spectroscopy Applications (ASA) meeting, August 27-30, Reims, France.

Fally S., A.C. Vandaele, S. Trabelsi, E. Mahieu, P. Demoulin, C. Frankenberg, H. Vogelmann, T. Trickl, 2008, Water vapor line parameters: Some feedback from atmospheric users. Proceedings of the 8th Atmospheric Spectroscopic Applications (ASA) meeting, 27-30 Aug. 2008, Reims (France.

Geens, Bert, Report Mobiliteit, 2008, Improvement of the prediction of the UV index, Universiteit Antwerpen.

Mahieu, E., P. Duchatelet, P.F. Bernath, C.D. Boone, M. De Mazière, P. Demoulin, C.P. Rinsland, C. Servais and K.A. Walker, 2008, Retrievals of C_2H_2 from high-resolution FTIR solar spectra recorded at the Jungfraujoch station (46.5ºN) and comparison with ACE-FTS observations, Geophysical Research Abstracts, Vol. 10, EGU2008-A-08188.

Mahieu, E., C. Servais, P. Duchatelet, P. Demoulin, M. De Mazière, K.A. Walker, C.D. Boone, P.F. Bernath, C.P. Rinsland and R. Zander, 2008, Optimised approaches to invert Jungfraujoch high-resolution FTIR observations for long-term monitoring and satellite validation of tropospheric species, ACCENT-TROPOSAT final report.

Mikhailenko S. N., T. Putilova, E. Starikova, S. Tashkun, A. Jenouvrier, L. Daumont, S. Fally, M. Carleer, C. Hermans, A. C. Vandaele, 2008, A new experimental dataset of HD18O transitions and energy levels from the IR to the visible spectral region,

Proceedings of the 8th Atmospheric Spectroscopic Applications (ASA) meeting, August 27-30, Reims, France.

Van Malderen R. and H. De Backer, 2008, Trend analysis of the radiosonde relative humidity measurements at Ukkel, Belgium, Geophysical Research Abstracts, Vol. 10, EGU2008-A-02676, 2008, SRef-ID: 1607-7962/gra/EGU2008-A-02676.

2009

Duchatelet, P., E. Mahieu, R. Sussmann, F. Forster, T. Borsdorff, P.F. Bernath, C.D. Boone, K.A. Walker, M. De Mazière, and C. Vigouroux, 2009, Determination of isotopic fractionation $\delta^{13}C$ of methane from ground-based FTIR observations performed at the Jungfraujoch, Geophysical Research Abstracts, Vol. 11, EGU2009-9914-1.

Duchatelet, P., E. Mahieu, R. Sussmann, F. Forster, T. Borsdorff, P.F. Bernath, C.D. Boone, K.A. Walker, M. De Mazière, and C. Vigouroux, 2009, Determination of isotopic fractionation $\delta^{13}C$ of methane from ground-based FTIR observations performed at the Jungfraujoch, Geophysical Research Abstracts, Vol. 11, EGU2009-9914-1.

Mahieu, E., P. Duchatelet, C.P. Rinsland, Q. Li, C.D. Boone, K.A. Walker, P.F. Bernath, M. De Mazière, B. Dils, and the GIRPAS Team, 2009a, Time series of ^{12}CO and ^{13}CO at northern mid-latitudes: Determination of Partial Column and $\delta^{13}C$ seasonal and interannual variations, Geophysical Research Abstracts, Vol. 11, EGU2009-10017-1.

Mahieu, E., C. Servais, P. Duchatelet, P. Demoulin, M. De Mazière, K.A. Walker, C.D. Boone, P.F. Bernath, C.P. Rinsland and R. Zander, 2009b, Optimised approaches to invert Jungfraujoch high-resolution FTIR observations for long-term monitoring and satellite validation of tropospheric species, in The Remote Sensing of Tropospheric Constituents from Space, ACCENT-TROPOSAT-2: Activities 2007-8 & Final Report, J. Burrows and P. Borrell, Eds., 270-274.

Mikhailenko S., S. Tashkun, L. Daumont, A. Jenouvrier, S. Fally, A. C. Vandaele, M. Carleer, 2009, Line Positions and Energy Levels of the 18-O Substitutions from the HDO/D_2O Spectra between 5600 and 8800 cm^{-1}, The XVI Symposium on High Resolution Molecular Spectroscopy July, 5-10 2009, lake Baikal.

Sussmann, R., T. Borsdorf, M. Rettinger, C. Camy-Peyret, P. Demoulin, P. Duchatelet, and E. Mahieu, 2009, New multi-station and multi-decadal trend data on precipitable water. Recipe to match FTIR retrievals from NDACC long-time records to radio sondes within 1mm accuracy/precision, Geophysical Research Abstracts, Vol. 11, EGU2009-10617-1.

2010

Duchatelet, P., E. Mahieu, R. Zander, and R. Sussmann, 2010, Trends of CO_2, CH_4 and N_2O over 1985-2010 from high-resolution FTIR solar observations at the Jungfraujoch station, Geophysical Research Abstracts, Vol. 12, EGU2010-15418-2.

VI ACKNOWLEDGEMENTS

We thank Belgian Science Policy for support via AGACC and the PRODEX project SECPEA. We are grateful to our colleagues at the Laboratoire de l'Atmosphère et des Cyclones de l'Université de la Réunion, the University of Reims, the Institute of Atmospheric Optics at Tomsk, the Groupe de Spectroscopie Moléculaire et Atmosphérique de l'Université de Reims Champagne-Ardenne, the University College London, and the School of GeoSciences, University of Edinburgh for the good collaboration. We also benefit largely from our collaborations with the ACE Science Team, in particular the University of Toronto and Waterloo, the NASA Langley Research Center, and all our colleagues from the NDACC Infrared Working and UVVis Working Groups, in particular IMK-IFU, Garmisch-Partenkirchen, and IMK-FZK, Karlsruhe. We would also like to thank the Deutsche Wetterdienst, Observatorium Lindenberg, for the help in setting up the correction procedures for the relative humidity measurements with the radio soundings. P.F. Coheur and J. Vander Auwera are respectively Research Associate and Senior Research Associate with the F.R.R.-FNRS. The "Fonds de la Recherche Scientifique" (F.R.S.- FNRS, Belgium, contracts FRFC and IISN), and the "Action de Recherches Concertées of the "Communauté française de Belgique" are gratefully acknowledged. In addition, we thank the European Union for financial support via the QUASAAR (QUAntitative Spectroscopy for Atmospheric and Astrophysical Research), HYMN (Hydrogen, Methane and Nitrous Oxide: Trend variability, budgets and interactions with the biosphere), UFTIR (Time series of Upper Free Troposphere observations from a European ground-based FTIR network), SCOUT-O_3 (Stratospheric-Climate Links with Emphasis on the Upper Troposphere and Lower Stratosphere) and GEOMON (Global Earth Observation and Monitoring of the Atmosphere) projects. The CINDI campaign was supported by ESA through the CEOS Intercalibration of Ground-Based Spectrometers and Lidars project, and on-site by dedicated teams from the Royal Dutch Meteorological Institute (KNMI). Finally the MAXDOAS aerosol measurements performed in Beijing were locally supported by the Institute of Atmospheric Physics of the Chinese Academy of Science. We thank the International Foundation High Altitude Research Stations Jungfraujoch and Gornergrat (HFSJG, Bern) for supporting the facilities needed to perform the observations. We acknowledge the collaboration with the team led by Dr. J-F. Müller (member of the AGACC Follow-Up Committee).

VII REFERENCES

Abbot, D. S., P. I. Palmer, R. V. Martin, K.V. Chance, D.J. Jacob, and A. Guenther, 2003, Seasonal and interannual variability of North American isoprene emissions as determined by formaldehyde column measurements from space, Geophys. Res. Lett., 30(17), 1886, doi:10.1029/2003GL017336.

Aikin, A., J. Herman, E. Maier and C. McQuillan, 1982, Atmospheric Chemistry of Ethane and Ethylene, J. Geophys. Res., 87(C4), 3105-3118.

Barret, B., D.Hurtmans, M. Carleer, M. De Mazière, E. Mahieu and P.-F. Coheur, 2005, Line narrowing effect on the retrieval of HF and HCl vertical profiles from ground-based FTIR measurements, J. Quant. Spectrosc. Radiat. Transfer, 95, 499-519.

Bergamaschi, P., M. Bräunlich, T. Marik and C. Brenninkmeijer, 2000, Measurements of the carbon and hydrogen isotopes of atmospheric methane at Izaña, Tenerife: Seasonal cycles and synoptic-scale variations, J. Geophys. Res., 105(D11), 14,531–14,546.

Casanova, S. E. B., K. P. Shine, T. Gardiner, M. Coleman and H. Pegrum, 2006, Assessment of the consistency of near-infrared water vapor line intensities using high-spectral-resolution ground-based Fourier transform measurements of solar radiation, J. Geophys. Res., 111, D11302, doi:10.1029/2005JD006583.

Cheymol, A., H. De Backer, 2007, Impact of the aerosol particle concentrations on UV index prediction, European Geosciences Union General Assembly.

Cheymol, A., H. De Backer, W. Josefsson and R. Stübi, 2006, Comparison and validation of the aerosol optical depth obtained with the Langley plot method in the UV-B from Brewer Ozone Spectrophotometer measurements, J. Geophys. Res., 111, D16202, doi:10.129/2006JD007131.

Clémer, K., M. Van Roozendael, C. Fayt, F. Hendrick, C. Hermans, G. Pinardi, R. Spurr, P. Wang, and M. De Mazière, 2010, Multiple wavelength retrieval of tropospheric aerosol optical properties from MAXDOAS measurements in Beijing, Atmos. Meas. Tech., 3, 863–878.

De Smedt, I., J.F. Müller, T. Stavrakou, R. Van der A, H. Eskes and M. Van Roozendael, 2008, Twelve years of global observation of formaldehyde in the troposphere using GOME and SCIAMACHY sensors, Atmos. Chem. Phys. Disc., Vol.8, pp. 7555-7608.

Dewitte S., presentation 02/05/2007, Analysis of the solar radiation at Ukkel from a climate change point of view, KMI-IRM.

Duchatelet, P., E. Mahieu, R. Ruhnke, W. feng, M. Chipperfield, P. Demoulin, P. Bernath, C.D. Boone, K.A. Walker, C. Servais and O. Flock, 2009, An approach to retrieve information on the carbonyl fluoride (COF_2) vertical distributions above Jungfraujoch by FTIR multi-spectrum multi-window fitting, *Atmos. Chem. Phys., 9,* 9027-9042.

Fischer, H., M. Behrens, M. Bock, U. Richter, J. Schmitt, L. Loulergue, J. Chappellaz, R. Spahni, T. Blunier, M. Leuenberger and T. F. Stocker, Nature 452, 864-867, 2008, Changing boreal methane sources and constant biomass burning during the last termination doi:10.1038/nature06825.

Frankenberg C., P. Bergamaschi, A. Butz, S. Houweling, J.F. Meirink, J. Notholt, A.K. Petersen, H. Schrijver, T. Warneke, I. Aben, 2008, Tropical methane emissions: A revised view from SCIAMACHY onboard ENVISAT, Geophys. Res. Letters, 35(L15811), doi:10.1029/2008GL034300.

Frankenberg C., Yoshimura K., Warneke T., Aben I., Butz A., Deutscher N., Griffith D., Hase F., Notholt J., Schneider M., Schrijver H., Röckmann T., 2009, Dynamic Processes Governing Lower-Tropospheric HDO/H_2O Ratios as Observed from Space and Ground, Science, DOI: 10.1126 19.

Friess U., P.S. Monks, J.J. Remedios, A. Rozanov, R. Sinreich, T. Wagner and U. Platt, 2006, MAXDOAS O_4 measurements: 1. A new technique to derive information on atmospheric aerosols: 2. Modeling studies, J. Geophys. Res. 111, D14203, doi:10.1029/2005JD006618.

Gardiner, T., A. Forbes, M. De Mazière, C. Vigouroux, E. Mahieu, P. Demoulin, V. Velazco, J. Notholt, T. Blumenstock, F. Hase, I. Kramer, R. Sussman, W. Stremme, J. Mellqvist, A. Strandberg, K. Ellingsen, and M. Gauss, 2008, Trend analysis of greenhouse gases over Europe measured by a network of ground-based remote FTIR instruments, Atmos. Chem. Phys., 8, 6719-6727.

Greenblatt G.D., J.J. Orlando, J.B. Burkholder and A.R. Ravishankara, 1990, Absorption measurements of oxygen between 330 and 1140 nm, J. Geophys. Res. 95, 18577-18582.

Heckel A., A. Richter, T. Tarsu, F. Wittrock, C. Hak, I. Pundt, W. Junkermann and J.P. Burrows, 2004, MAXDOAS measurements of formaldehyde in the Po-Valley, Atmos. Chem. Phys. Discuss. 4, 1151-1180.

Heckel A., A. Richter, T. Tarsu, F. Wittrock, C. Hak, I. Pundt, W. Junkermann and J.P. Burrows, 2005, MAXDOAS measurements of formaldehyde in the Po-Valley, Atmos. Chem. Phys., 5, 909-918.

Herbin, H., Hurtmans, D., Clerbaux, C., Clarisse, L., and Coheur, P.-F., 2009, $H_2{}^{16}O$ and HDO measurements with IASI/MetOp", Atmos. Chem. Phys., 9, 9433-9447

Holben B.N., T.F. Eck, I. Slutsker, D. Tanre, J.P. Buis, A. Setzer, E. Vermote, J.A. Reagan, Y.J. Kaufman, T. Nakajima, F. Lavenu, I. Jankowiak and A. Smimov, 1998, AERONET - A federated instrument network and data archive for aerosol characterization, Rem. Sens. Env. 66(l), 1-16.

Hönninger G., C. von Friedeburg and U. Platt, 2004, Multi axis differential absorption spectroscopy (MAXDOAS), Atmos. Chem. Phys., 4, 231-254.

Hurtmans D. et al., ASSFTS meeting, 2005; http://home.scarlet.be/dhurtma/ & dhurtma@ulb.ac.be

Irie H., Kanaya Y., Akimoto H., Iwabuchi H., Shimizu A., and Aoki K., 2008, First retrieval of tropospheric aerosol profiles using MAXDOAS and comparison with lidar and sky radiometer measurements, Atmos. Chem. Phys. 8, 341-350.

Irie H., Y. Kanaya, H. Akimoto, H. Iwabuchi, A. Shimizu and K. Aoki, 2009, Dual-wavelength aerosol vertical profile measurements by MAXDOAS ar Tsukuba, Japan, Atmos. Chem. Phys. 9, 2741-2749.

Jacquinet-Husson N. et al., 2008, The GEISA spectroscopic database: Current and future archive for Earth and planetary atmosphere studies, J. Quant. Spectrosc. Radiat. Transfer 109, 1043-1059.

Leiterer, U., H. Dier, D. Nagel, T. Naebert, D. Althausen, K. Franke, A. Kats and F. Wagner, 2005, Correction method for RS80-A Humicap Humidity Profiles and Their Validation by Lidar Backscattering Profiles in Tropical Cirrus Clouds, J. Atmos. Oceanic. Technol., 22, 18-29.

Li Q., D. J. Jacob, R. M. Yantosca, C. L. Heald, H. B. Singh, M. Koike, Y. Zhao, G. W. Sachse, D. G. Streets, 2003, A global three-dimensional model analysis of the

atmospheric budgets of HCN and CH_3CN: Constraints from aircraft and ground measurements, J. Geophys. Res., 108 (D21), 8827, doi:10.1029/2002JD003075.

Li X., T. Brauers, M. Shao, R.M. Garland, T. Wagner, T. Deutschmann and A. Wahner, 2008, MAXDOAS measurements in southern China: 1 automated aerosol profile retrieval using oxygen dimers absorptions, Atmos. Chem. Phys. Discuss. 8, 17661-17690.

Mandin J.-Y., V. Dana, C. Claveau, 2000, Line intensities in the υ5 band of acetylene 12C2H2, J. Quant. Spectrosc. Radiat. Transfer 67, 429-446.

Meier, A., G.C. Toon, C.P. Rinsland, A. Goldman and F. Hase, 2004, Spectroscopic Atlas of Atmospheric Microwindows in the middle Infra-Red, IRF Technical Report 048, ISSN 02841738 (Institut for Rymdfysik, Kiruna, Sweden), Appendix E.

Meller, R., and Moortgat, G. K., 2000, Temperature dependence of the absorption cross sections of formaldehyde between 223 and 323 K in the wavelength range 225 - 375 nm, J. Geophys. Res., 105(D6), 7089-7102, 10.1029/1999JD901074.

Miller, J. B., K. A. Mack, R. Dissly, J. W. C. White, E. J. Dlugokencky, and P. P. Tans, 2002, Development of analytical methods and measurements of $^{13}C/^{12}C$ in atmospheric CH_4 from the NOAA Climate Monitoring and Diagnostics Laboratory Global Air Sampling Network, J. Geophys. Res., 107(D13), 4178, doi:10.1029/2001JD000630.

Miloshevich, L. M., A. Paukkunen, H. Vomel and S. J. Oltmans, 2004, Development and Validation of a Time-Lag Correction for Vaisala Radiosonde Humidity Measurements, J. Atmos. Oceanic.Technol., 21, 1305-1327.

Nassar, R., P.F. Bernath, C.D. Boone, S.D. McLeod, R. Skelton, K.A. Walker, C.P. Rinsland and P. Duchatelet, 2006, A global inventory of stratospheric fluorine in 2004 based on Atmospheric Chemistry Experiment Fourier Transform Spectrometer (ACE-FTS) measurements, J. Geophys. Res., 111, D22313, doi:10.1029/2006JD007395.

Perrin, A., D. Jacquemart, F. Kwabia Tchanab, and N. Lacome, 2009: Absolute line intensities measurements and calculations for the 5.7 and 3.6 μm bands of formaldehyde, J. Quant. Spectros. Radiat. Transfer, 110, 700–716.

Platt U., 1994, Differential optical absorption spectroscopy (DOAS), in Air Monitoring by Spectroscopic Techniques, vol. 127, pp. 27-83, John Wiley, Hoboken, N.Y.

Randel, W. J., F. Wu, H. Vömel, G. E. Nedoluha and P. Forster, 2006, Decreases in stratospheric water vapor after 2001: Links to changes in the tropical tropopause and the Brewer-Dobson circulation, J. Geophys. Res., 111, D12312.

Risi C., A. Landais, S. Bony, J. Jouzel, V. Masson-Delmotte, and F. Vimeux, 2010, Understanding the ^{17}O excess glacial-interglacial variations in Vostok precipitation, J. Geophys. Res., 115, D10112, doi:10.1029/2008JD011535 16.

Rodgers C.D., 2000, Inverse Methods for Atmospheric Sounding: Theory and Practice, Ser. Atmos. Oceanic Planet. Phys., vol. 2, edited by F.W. Taylor, World Sci., Hackensack, N.Y.

Roscoe, H. K. et al. (50 authors), 2010, Intercomparison of slant column measurements of NO_2 and O_4 by MAXDOAS and zenith-sky UV and visible spectrometers, Atmos. Meas. Tech. Discuss., 3, 3383-3423, 2010, doi:10.5194/AMTD-3-3383-2010.

Rothman et al., 2005, The HITRAN 2004 molecular spectroscopic database, J. Quant. Spect. Rad. Trans., 96, 139–204.

Santer, B. D., M. F. Wehner, T. M. L. Wigley, R. Sausen, G. A. Meehl, K. E. Taylor, C. Ammann, J. Arblaster, W. M. Washington, J. S. Boyle and W. Brüggemann, 2003,

Contributions of Anthropogenic and Natural Forcing to Recent Tropopause Height Changes, Science, 301 (5632), 479-483.

Schneider, M. and F. Hase, 2009a, Reviewing the development of a ground-based FTIR water vapour profile analysis, Atmos. Meas. Tech. Discuss., 2, 1221–1246.

Schneider, M., M. Romero, F. Hase, T. Blumenstock, E. Cuevas, and R. Ramos, 2009b, Quality assessment of Izaña's upper-air water vapour measurement techniques: FTIR, Cimel, MFRSR, GPS, and Vaisala RS92, Atmos. Meas. Tech. Discuss., 2, 1625–1662.

Sherwood S. C., R. Roca, T. M. Weckwerth, and N. G. Andronova, 2010, Tropospheric water vapor, convection, and climate", Rev. Geophys., 48, RG2001, doi:10.1029/2009RG000301

Sinreich R., U. Friess, T. Wagner and U. Platt, 2005, Multi axis differential absorption spectroscopy (MAXDOAS) of gas and aerosol distributions, Faraday Discuss. 130, 153-164.

Soden, B. J., D. L. Jackson, V. Ramaswamy, M. D. Schwarzkopf and X. Huang, 2005, The Radiative Signature of Upper Tropospheric Moistening. Science, 310 (5749), 841-844

SPARC Assessment of Upper Tropospheric and Stratospheric Water Vapour, WCRP-113, December 2000; WMO/TD- No. 1043; SPARC Report No.2.

Spivakovsky, C. M., J.A. Logan, S.A. Montzka, Y.J. Balkanski, M. Foreman-Fowler, D.B.A. Jones, L.W. Horowitz, A. C. Fusco, C.A.M. Brenninkmeijer, Prather, S.C. Wofsy, M.B. McElroy, 2000, Three-dimensional climatological distribution of tropospheric OH: Update and evaluation, J. Geophys. Res.,105(D7), 8931–8980.

Spurr, R., 2008, LIDORT and VLIDORT: Linearized pseudo-spherical scalar and vector discrete ordinate radiative transfer models for use in remote sensing retrieval problems. Light Scattering Reviews, Volume 3, ed. A. Kokhanovsky, Springer.

Stavrakou, T., J.F. Müller, I. De Smedt, M. Van Roozendael, G.R. van der Werf, L. Giglio, and A. Guenther, 2009a, Evaluating the performance of pyrogenic and biogenic emission inventories against one decade of space-based formaldehyde columns, Atmos. Chem. Phys., 9, 1037–1060.

Stavrakou, T., J.F. Müller, I. De Smedt, M. Van Roozendael, G.R. van der Werf, L. Giglio, and A. Guenther, 2009b, Global emissions of non-methane hydrocarbons deduced from SCIAMACHY formaldehyde columns through 2003-2006, Atmos. Chem. Phys., 9, 3663-3679.

Stohl, A., C. Forster, A. Frank, P. Seibert and G. Wotawa, 2005, Technical note: The Lagrangian particle dispersion model FLEXPART version 6.2, Atmos. Chem. Phys., 5, 2461-2474.

Suortti et al., 2008, Tropospheric comparisons of Vaisala radiosondes and balloon-borne frost-point and Lyman-alpha hygrometers during the LAUTLOS-WAVVAP experiment, J. Atmos. Oceanic. Technol., 25, 149-166.

Van Roozendael, M., C. Fayt, J.C. Lambert, I. Pundt, T. Wagner, A. Richter, and K. Chance, 1999, Development of a bromine oxide product from GOME, in Proc. ESAMS'99, WPP-161, p. 543-547.

Wagner T., B. Dix, v.C. Friedeburg, U. Friess, S. Sanghavi, R. Sinreich, and U. Platt, 2004, MAXDOAS O_4 measurements: A new technique to derive information on atmospheric aerosols – Principles and information content, J. Geophys. Res. 109, D22205, doi:10.1029/2004JD004904.

Wagner T., T. Deutschmann, U. Platt, 2009, Determination of aerosol properties from MAXDOAS observations of the Ring effect, Atmos. Meas. Tech. Discuss., 2, 725-779.

Wittrock F., H. Oetjen, A. Richter, S. Fietkau, T. Medeke, A. Rozanov and J.P. Burrows, 2004, MAXDOAS measurements of atmospheric trace gases in Ny-Alesund – Radiative transfer studies and their application, Atmos. Chem. Phys. 4, 955-966.

WMO, 2007 (World Meteorological Organization), Scientific Assessment Report of Ozone Depletion: 2006, Global Ozone Research and Monitoring Project – Report No. 50, 572 pp., Geneva, Switzerland.

Worden, J., et al., 2006, Tropospheric Emission Spectrometer observations of the tropospheric HDO/H_2O ratio: Estimation approach and characterization, J. Geophys. Res., 111, D16309, doi:10.1029/2005JD006606.

Worden J., Noone D., Bowman K., 2007, "Importance of rain evaporation and continental convection in the tropical water cycle, Nature, 445, 528-532 18.

Zahn A., Franz P., Bechtel C., Grooss J.-U., and Röckmann T.,2006, "Modelling the budget of middle atmospheric water vapour isotopes", Atmos. Chem. Phys., 6, 2073-2090

Zieger, P., E. Weingartner, J. Henzing, M. Moerman, G. de Leeuw, J. Mikkila, K. Clémer, M. Van Roozendael, S. Yilmaz, U. Frieß, H. Irie, T. Wagner, R. Shaiganfar, S. Beirle, A. Apituley, K. Wilson, and U. Baltensperger, 2010, Comparison of ambient aerosol extinction coefficients obtained from in-situ, MAXDOAS and LIDAR measurements, Atmos. Chem. Phys. Discuss., 10, 29683-29734.

VIII LIST OF ACRONYMS

ACCENT	Atmospheric Composition Change – the European NeTwork of excellence
ACE_FTS	Canadian Atmospheric Chemistry Experiment - Fourier Transform Spectrometer
AERONET	AErosol RObotic NETwork
AOD	Aerosol Optical Depth
AGACC	Advanced exploitation of Ground-based measurements for Atmospheric Chemistry and Climate applications
AK	Averaging kernel
BA	boreal Asia
BIRA-IASB	Belgisch Instituut voor Ruimte-Aëronomie - Institut d'Aéronomie Spatiale de Belgique
CEOS	Committee on Earth Observation Satellites
CESAR	Cabaux Experimental Site for Atmospheric Research
CFC	Chloro Fluoro Carbons
CO	Carbon monoxide
CH_4	Methane
CIMEL	CIMEL Sun photometer
CINDI	Cabauw Intercomparison Campaign of Nitrogen Dioxide measuring Instruments
COST	Cooperation in Science and Technology (EC Programme)
CTM	Chemistry-transport model
DFS	Degrees of Freedom of Signal
DOFS	Degrees Of Freedom for Signal
DOAS	Differential Optical Absorption Spectroscopy
DSCDs	Differential slant column densities
ENVISAT	ESA's Environmental Satellite, launched in 2002
FLEXPART	Atmospheric particle dispersion model (http://transport.nilu.no/flexpart)
FTIR	Fourier Transform Infra-Red
GCOS	Global Climate Observing System
GEISA	Gestion et Etude des Informations Spectroscopiques Atmosphériques
GOME	Global Ozone Monitoring Experiment
GEOmon	Global Earth Observation and Monitoring (Project, EC/FP6)
GPS	Global Positioning System
HCFC	Hydrogen Chloro Fluoro Carbons
HCHO	Formaldehyde (also appears as H_2CO)
HCN	Hydrogen cyanide
HDO	semiheavy water or deuterium protium oxide
HITRAN	High-resolution transmission molecular absorption database
IASI	Infrared Atmospheric Sounding Interferometer
IMAGES	Tropospheric chemistry transport model developed at BIRA-IASB
IPCC	Intergovernmental Panel on Climate Change
IR	Infrared
ISSI	International Space Science Institute
ISSJ	International Scientific Station of the Jungfraujoch
IUPAC	International Union of Pure and Applied Chemistry
IWV	Integrated Water Vapour
KMI-IRM	Koninklijk Meteorologisch Instituut – Institut Royal de Météorologie

KNMI	Koninklijk Nederlands Meteorologisch Instituut
LIDAR	Light Detection and Ranging
LIDORT	Linearized discrete ordinate radiative transfer
LOS	Line of sight
LUT	Look up table
MCT	Mercury - Cadmium - Telluride
MAXDOAS	Multi-Axis Differential Optical Absorption Spectrometry
MARVEL	Measured Active Rotational-Vibrational Energy Levels
NAF	Northern Africa
NDACC	Network for the Detection of Atmospheric Composition Change
NMHCs	Nonmethane hydrocarbons
NMVOCS	Non-methane volatile organic compounds
NOx	Nitrogen Oxides
OH	Hydroxyl radical
OEM	Optimal estimation method
PBL	Planetary boundary layer
PTU	Pressure, temperature, relative humidity
RMS	Root-mean-square
RTM	Radiative Transfer Model
SAM	South America
SAF	South Afrrica
SE AS	Southeast Asia
SCIAMACHY	SCanning Imaging Absorption spetroMeter for Atmospheric CHartographY
SCOUT-O3	Stratospheric-Climate Links with Emphasis on the Upper Troposphere and Lower Stratosphere
SCQP-ULB	Service de Chimie Quantique et Photophysique, Université Libre de Bruxelles
SFIT-2	A spectral inversion (retrieval) algorithm used in the NDACC IRWG community
SZA	Solar zenith angle
SPARC	Stratospheric Processes and their Role in Climate
TPW	Total Precipitable Water
TUV	Tropospheric Ultraviolet and Visible Radiation Model
UT	Upper Troposphere
UTH	Upper Tropospheric Humidity
UTLS	Upper Troposphere/Lower Stratosphere
VMR	Volume mixing ratio
VOC	Volatile Organic Compound
UV-Vis	Ultraviolet – Visible
WAVACS	Water Vapour in the Climate System
WMO	World Meteorological Organization
WOUDC	The World Ozone and Ultraviolet Radiation Data Centre